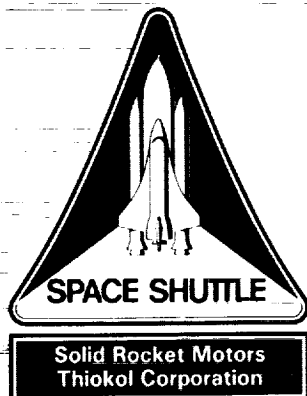


TWR-17592 (Rev B)



Space Shuttle Production Verification Motor 1 (PV-1) Static Fire Final Test Report

Volume I (Revision B)

August 1989

Prepared for

National Aeronautics and Space Administration
George C. Marshall Space Flight Center
Marshall Space Flight Center, Alabama 35812

Contract No. NAS8-30490
DR No. 5-3
WBS No. HQ302-10-10
ECS No. 1005

Thiokol CORPORATION
SPACE OPERATIONS

P.O. Box 707, Brigham City, UT 84302-0707 (801) 863-3511

Publications No. 89265

(NASA-CR-183784) SPACE SHUTTLE PRODUCTION
VERIFICATION MOTOR 1 (PV-1) STATIC FIRE
Final Test Report (Morton Thiokol) 142 p

CSCL 21H

N90-15991

Unclas
0243007

63/20



PV-1 Static Test, 18 August 1988

ORIGINAL PAGE
BLACK AND WHITE PHOTOGRAPH

Space Shuttle Production Verification Motor 1
(PV-1)
Final Test Report

Volume 1

Prepared by:

Diane Garecht
Test Planning and Reporting
Systems Engineer

Approved by:

A. J. Hawley
Requirements
Manager

W. Kelly 13 Sep 89
Project Engineer

S. Ham
Program Manager

R. Anderson 9/15/89
Systems Safety

Stephen M. West
Reliability

P. C. Tydeck 9-15-89
Data Management

ACTIVE PAGE RECORD

PAGE NO.	REVISION	PAGE NO.	REVISION	PAGE NO.	REVISION	PAGE NO.	REVISION
1-35	Basic						
36-37	A						
38-93	Basic						
64	B						
94	A						
95-96	Basic						
97	A						
98-127	Basic						

REVISION B
 89265-12.1

DOC NO. TWR-17592	VOL	ii
SEC	PAGE	

REVISION DESCRIPTION

REV LTR	DATE	DESCRIPTION
Basic	Oct 1988	
A	May 1989	<p>Revision A changes have been incorporated into the basic document to make it complete.</p> <p>Section 2, TEST OBJECTIVES</p> <p>ADDED: BL-1 The insulation shall ensure that system performance and structural integrity is maintained during the assembly process and operation. (3.2.1.8.1.1.c)</p> <p>Section 4, CEI SPECIFICATIONS</p> <p>ADDED: BL-1 Col 1, <u>Qualification Objectives (CEI paragraph number)</u></p> <p>The insulation shall ensure that system performance and structural integrity is maintained during the assembly process and operations. (3.2.1.8.1.1.c)</p> <p>Col 2, <u>Pass/Fail Criteria</u></p> <p>System performance and structural integrity during the assembly process and operation shall not be compromised due to insulation.</p> <p>Col 3, <u>Results (Reference Section)</u></p> <p>The insulation ensured that system performance and structural integrity was maintained during the assembly process and operation. For a complete insulation performance discussion, see TWR-17592, Volume III, Revision A.</p> <p>Paragraph 5.1, INTRODUCTION</p> <p>ADDED: Additional instrumentation discussion can be found in TWR-17592, Volume XII.</p>

REVISION DESCRIPTION

REV LTR	DATE	DESCRIPTION
Basic	Oct 1988	
B	Aug 1989	<p>Revision B changes have been incorporated into the basic document to make it complete. Revisions are marked in the text by a vertical bar in the right-hand margin.</p> <p>Section 3, Executive Summary</p> <p>ADDED TO: 3.1.4.11 Nozzle Composite Structures Performance</p> <p>Several strain plots in the nose inlet housing region exhibited strain aberrations at about the 14-sec time slice. most noticeable are the axial components at Location 5, and the hoop and axial components at Location 7, near the aft end of the nose inlet housing. Other gages demonstrating responses of a lower magnitude at this time slice hoop longwire gages at Locations J6 and J7 (Joint No. 2 proximity gages), J9 and J10 (Joint No. 3), and Location 9. An investigation of the cause of this event is currently being conducted. Despite these unexpected changes in strain magnitude, peak strains remained relatively low (less than 2,000 μin./in.), indicating metal part margins of safety were well above zero.</p>

ABSTRACT

All inspection and instrumentation data indicate that the PV-1 static test firing conducted 18 Aug 1988 was successful. With the exception of the intentionally flawed joints and static test modifications, PV-1 was flight configuration. Fail-safe flaws guaranteeing pressure to test the sealing capability of primary O-rings were included in the aft field joint, case-to-nozzle joint, and nozzle internal Joint 5. In this condition the only pass/fail criteria was to prevent leakage of internal combustion gases from the joint. The center field joint was flawed, guaranteeing pressure to the capture feature O-ring. The igniter-to-case joint had two intentional blowholes in the putty to allow pressure to the edge separation flaw. The test was conducted at ambient conditions, with the exception of the field joints and case/nozzle joints which were maintained at a minimum of 75°F.

Ballistics performance values were within specification requirements. The PV-1 motor exhibited chamber pressure oscillations similar to previously tested Space Shuttle redesigned solid rocket motors, particularly QM-7. The first longitudinal mode oscillations experienced by PV-1 were the strongest ever measured in a Space Shuttle motor. Investigation into this observation is being conducted. Joint insulation performed as designed with no evidence of gas flow within unflawed forward field joints. The intentionally flawed center and aft case field joint insulation performance was excellent. There was no evidence of hot gas past the center field joint capture feature O-ring, the case-to-nozzle joint primary O-ring, or the aft field joint primary O-ring. O-ring seals and barriers with assured pressure at the flaws showed erosion and heat effect, but all sealed against passage of hot gases with the exception of the aft field joint capture feature O-ring. There was no evidence of erosion, heat effect, or blowby on any O-ring seals or barriers at the unflawed joints. Nozzle performance was nominal with typical erosion. Post-test examination revealed that the forward nose ring was of the old high performance motor design configuration with the 150-deg ply angle. An investigation is underway to determine how the old design forward nose ring was mistakenly placed in an RSRM nose inlet assembly, although this

had no bearing on test performance and no problems were encountered. All nozzle components remained intact for post-test evaluation. Field joint heaters maintained the temperature at the controlling resistance temperature detector within the specified requirements during operation. The thrust vector control system operated correctly. The water deluge system, CO₂ quench, and other test equipment performed as planned during all required test operations.

CONTENTS

<u>Section</u>	<u>Page</u>
1 INTRODUCTION.	1
1.1 TEST ARRANGEMENT AND FACILITIES	1
1.2 TEST ITEM DESCRIPTION	1
1.2.1 Propellant/Liner/Inhibitor.	5
1.2.2 Insulation.	5
1.2.3 Nozzle/TVC.	8
1.2.4 Case/Seals.	11
1.2.5 Ignition System	21
1.2.6 JPS/Weatherseal/Systems Tunnel.	21
2 OBJECTIVES.	32
3 EXECUTIVE SUMMARY	38
3.1 SUMMARY	38
3.1.1 Case Performance.	38
3.1.2 Case Internal Insulation Performance.	38
3.1.3 Seals Component/Leak Check Performance.	43
3.1.4 Nozzle Assembly Performance	45
3.1.5 Igniter Performance	65
3.1.6 JPS/Factory Joint Weatherseal Performance	65
3.1.7 Systems Tunnel.	68
3.1.8 Instrumentation	68
3.1.9 Ground Support Equipment.	68
3.1.10 Loads and Environments.	68
3.1.11 Ballistics/Mass Properties Performance.	68
3.1.12 Aero/Thermal.	72
3.1.13 Dynamics.	77
3.2 RECOMMENDATIONS	87
3.2.1 Slag Prediction	87
3.2.2 Chamber Pressure Oscillation.	87
3.2.3 Nozzle Composite Structure.	87
3.2.4 Motor Pressure Measurement (Aft Dome)	87
3.2.5 Nozzle Instrumentation.	87
3.2.6 TASS Finite Element Model Results	87
4 CEI SPECIFICATIONS.	88
5 INSTRUMENTATION	97
5.1 INTRODUCTION.	97
5.2 OBJECTIVES.	97

CONTENTS (Cont)

<u>Section</u>		<u>Page</u>
	5.3 CONCLUSIONS/RECOMMENDATIONS	104
	5.4 DISCUSSION.	104
6	PHOTOGRAPHY	111
	6.1 STILL PHOTOGRAPHY	111
	6.2 MOTION PICTURES	111
7	GROUND SUPPORT EQUIPMENT.	117
8	LOADS AND ENVIRONMENTS.	118
	8.1 INTRODUCTION.	118
	8.2 OBJECTIVES.	118
	8.3 CONCLUSIONS/RECOMMENDATIONS	118
	8.4 RESULTS/DISCUSSIONS	118
9	APPLICABLE DOCUMENTS.	127

FIGURES

<u>Figure</u>		<u>Page</u>
1.1-1	PV-1 Static Test Motor During Assembly at T-24 Test Bay.	2
1.1-2	PV-1 Aft Skirt Conditioning.	3
1.2-1	PV-1 Test Article Flaw Summary	4
1.2-2	Overall View of PV-1 Test Article.	6
1.2.1-1	RSRM Propellant Grain Design Configuration	7
1.2.3-1	RSRM Nozzle Assembly	9
1.2.3-2	Nozzle Internal Joint 5 Flaw	10
1.2.3-3	Thrust Vector Actuation (TVA) System	12
1.2.4-1	Static Test Motor Configuration.	13
1.2.4-2	RSRM Case-to-Case Factory Joint.	14
1.2.4-3	RSRM Case-to-Case Field Joint.	15
1.2.4-4	Center Field Joint Flaw (Clevis)	16
1.2.4-5	Aft Field Joint Flaw (Clevis).	17
1.2.4-6	Aft Field Joint Flaw (Tang).	18
1.2.4-7	Aft Field Joint O-ring Flaw.	19
1.2.4-8	Case-to-Nozzle Joint	20
1.2.4-9	Case-to-Nozzle Insulation Bondline Defect.	22
1.2.4-10	Case-to-Nozzle Joint Flaw.	23
1.2.4-11	Nozzle Boss Induced Edge Separation.	24
1.2.4-12	Igniter-to-Forward Dome Edge Separation Locations.	25
1.2.5-1	RSRM Ignition System	26
1.2.6-1	Simplified Joint Heater.	27
3.1.4.1-1	PV-1 Polysulfide Separations	46
3.1.4.2-1	PV-1 Throat Assembly Bondline Separations.	51
3.1.4.3-1	Nose Cap Aft End Popped-Up Charred Material (204 deg).	52
3.1.4.3-2	PV-1 Nose Inlet Assembly Bondline Separations.	53
3.1.4.4-1	Cowl Aft End and Outer Boot Ring Forward End Popped-Up Charred Material	54
3.1.4.4-2	PV-1 Cowl/Outer Boot Ring (0 deg).	56
3.1.4.4-3	PV-1 Cowl/Outer Boot Ring (100 deg).	57
3.1.4.4-4	PV-1 Cowl/Outer Boot Ring (180 deg).	58
3.1.4.4-5	PV-1 Cowl/Outer Boot Ring (280 deg).	59
3.1.4.8-1	PV-1 Joint Flow Surface Gap Openings	60
3.1.4.8.1-1	PV-1 Blowpath in Aft Exit Cone Field Joint (224 deg)	61
3.1.4.8.1-2	PV-1 Blowpath in Aft Exit Cone Field Joint (224 deg)	62
3.1.5-1	RSRM Ignition System	66
3.1.5-2	Safety and Arming Device Configuration	67
3.1.6.1-1	Temperature at Controlling RTDs of Joints 1, 2, and 3.	69
3.1.6.1-2	Expanded Plot of Temperatures at Controlling RTDs for Joints 1, 2, and 3	70
3.1.6.1-3	Minimum Differential Temperature of Joints 1, 2, and 3	71
3.1.11-1	PV-1 Predicted and Measured Pressure at 79°F	74
3.1.11-2	PV-1 Predicted and Measured Thrust at 79°F	75

FIGURES (Cont)

<u>Figure</u>		<u>Page</u>
3.1.11-3	Waterfall Plot of PV-1 Dynamic Pressure, P016.	76
3.1.13.1-1	A401 Time Response	78
3.1.13.1-2	A402 Time Response	79
3.1.13.1-3	A403 Time Response	80
3.1.13.1-4	PV-1-A401 PSD Compared With NASA Criteria.	81
3.1.13.1-5	PV-1-A402 PSD Compared With NASA Criteria.	82
3.1.13.1-6	PV-1-A403 PSD Compared With NASA Criteria.	83
3.1.13.1-7	Auto-Spectrum Waterfall Plot for A401.	84
3.1.13.1-8	Auto-Spectrum Waterfall Plot for A402.	85
3.1.13.1-9	Auto-Spectrum Waterfall Plot for A403.	86
5.1-1	PV-1 Case Instrumentation.	98
5.1-2	PV-1 Head End Pressure Transducer Locations.	99
5.1-3	PV-1 Joint Growth.	100
5.1-4	PV-1 Case-to-Nozzle Joint Instrumentation.	101
5.1-5	PV-1 Nozzle Instrumentation.	102
5.1-6	PV-1 Aft Exit Cone Instrumentation	103
5.4-1	Instrumentation at Flawed Field Joints	107
5.4-2	Instrumentation at Flawed Nozzle-to-Case Joint	108
5.4-3	Nozzle Internal Joint 5.	109
6.2-1	Photography Coverage	114
6.2-2	Photography Coverage	115
6.2-3	Photography and Video Coverage	116
8.4-1	Tangential Line Loads Versus Time.	119
8.4-2	Axial Line Loads Versus Time	121
8.4-3	Strain Gage Locations.	122
8.4-4	Booster Local Coordinate System.	123
8.4-5	TVC Actuator Bracket	124
8.4-6	Actuator Bracket Stress Versus Time.	125
8.4-7	Actuator Bracket Stress Versus Time.	126

TABLES

<u>Table</u>	<u>Page</u>
1.2.6-1 PV-1 Differences From First Flight.	29
3.1.1.1-1 Field Joint Radial Growth Comparisons to PV-1	39
3.1.1.1-2 Fixed Housing Aft Dome Stress	40
3.1.4.1-1 PV-1 Polysulfide Groove Fill Post-Test Radial Width Measurements.	47
3.1.4.1-2 PV-1 Aft Exit Cone Forward End Phenolic Separations	48
3.1.4.1-3 PV-1 Forward Exit Cone Bondline Separations	50
3.1.11-1 PV-1 Performance Summary With CPW1-3600 CEI Specification Limits.	73
5.3-1 Nonrecoverable Channels, Prefire.	105
5.3-2 Instrumentation Anomalies	105
5.4-1 Instrumentation Summary	110
6.2-1 Photography and Video Coverage.	112
6.2-2 Photography and Video Coverage.	113

ACRONYMS

AP ammonium perchlorate
ATVC ascent thrust vector control
CCP carbon-cloth phenolic
CP cylindrical perforate
CTPB carboxyl-terminated polybutadiene
DR discrepancy report
EPDM ethylene propylene diene monomer
ETA external tank attach
GCP glass-cloth phenolic
GEI ground environmental instrumentation
GSE ground support equipment
HPM high performance motor
HPU hydraulic power unit
ID inside diameter
 I_{sp} specific impulse
JPS joint protective system
NBR nitrile butadiene rubber
MAP manual/automatic panel
OBR outer boot ring
OD outside diameter
OPT operational pressure transducer
PBAN polybutadiene acrylonitrile/acrylic acid copolymer
PMBT propellant mean bulk temperature
PV-1 production verification motor 1
RSRM redesigned solid rocket motor
RTD resistance temperature detector
RTV room temperature vulcanizing
S&A safety and arming device
SCN specification change notice
SRB solid rocket booster
SRM solid rocket motor
TVC thrust vector control
1-L first longitudinal

INTRODUCTION

The redesigned solid rocket motor (RSRM), used in pairs, is the primary Space Shuttle propulsive element, providing impulse and thrust vector control (TVC) from solid rocket motor (SRM) ignition to solid rocket booster (SRB) separation. The Space Shuttle Production Verification Motor (PV-1) test was a full-scale RSRM static firing. This test report includes a discussion of PV-1 performance and of test results compliance with the RSRM development and certification test program. A major focus of this report is placed on the test objectives, anomalies, and motor performance.

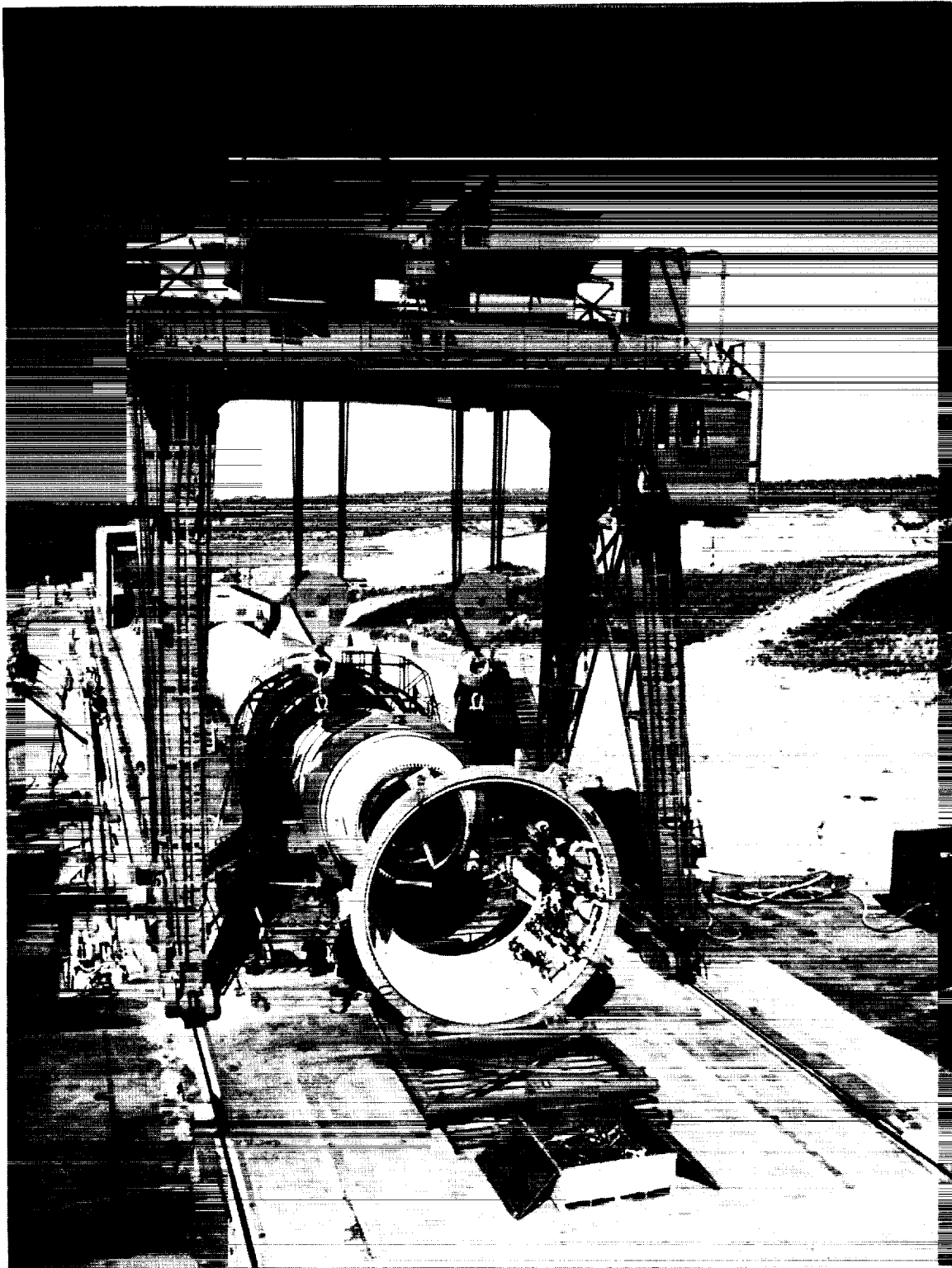
PV-1 was successfully fired on 18 Aug 1988 at the Morton Thiokol, Utah-based operations, test bay T-24. Two incidents delayed the PV-1 firing date. The first incident was the overpressurization of the TVC hydraulic system in the aft skirt. The QM-6 aft skirt was used to replace the damaged skirt. The second incident was where the leak check high pressure line was connected to the center field joint capture feature O-ring to primary O-ring cavity causing the capture feature O-ring to be extruded into the J-insulation area. Recovery required the disassembly of the motor to the center field joint for repairs. The test was conducted in accordance with the requirements of CTP-0055, "Space Shuttle Process Verification Motor (PV-1) Static Fire Test Plan." Postfire inspection procedures followed TWR-16473, Volumes I through IX.

1.1 TEST ARRANGEMENT AND FACILITIES

The PV-1 static test arrangement was in accordance with Drawings 2U65151 and 7U76254 and is shown in Figure 1.1-1. Test bay T-24 is equipped with a water deluge system and a CO₂ quench. The aft skirt (Figure 1.1-2) and the igniter area were conditioned by separate external heating sources.

1.2 TEST ITEM DESCRIPTION

The PV-1 static test article was configured to best approximate the RSRM flight motors, with the exception of the intentional flaws (Figure 1.2-1).



N104483-1

Figure 1.1-1. PV-1 Static Test Motor During Assembly at T-24 Test Bay

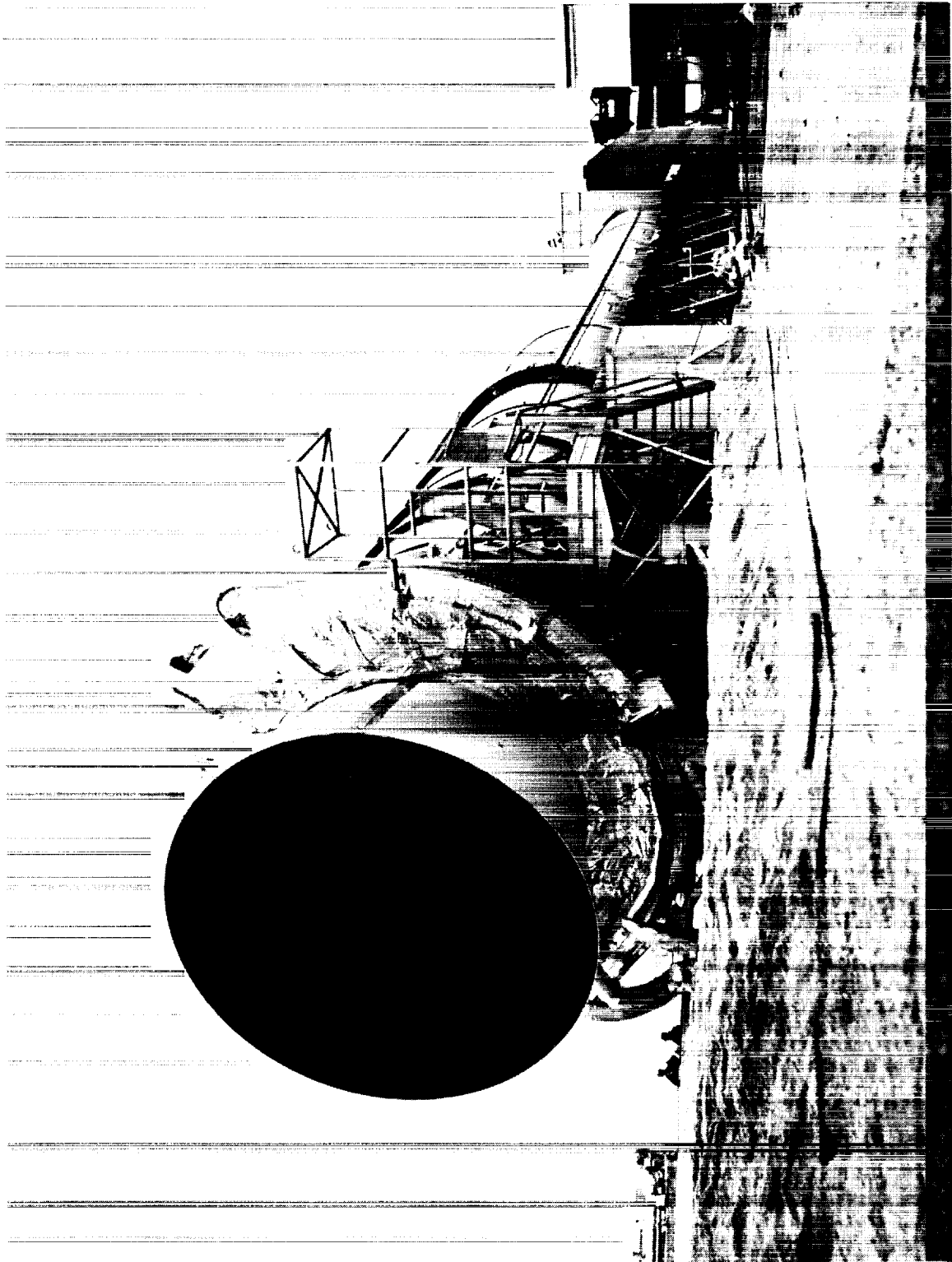
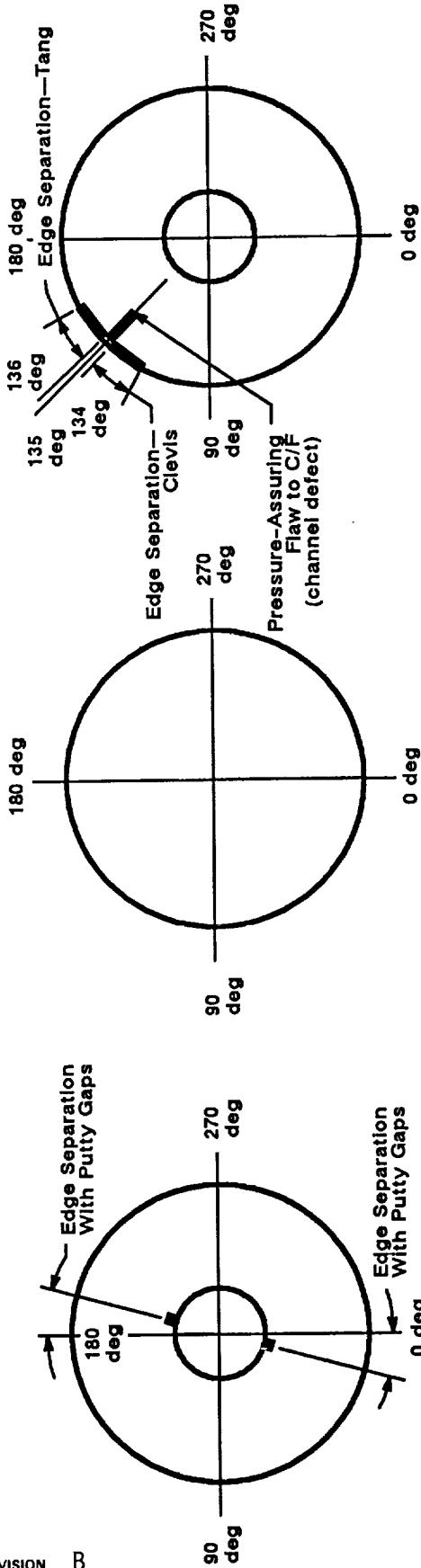


Figure 1.1-2. PV-1 Aft Skirt Conditioning

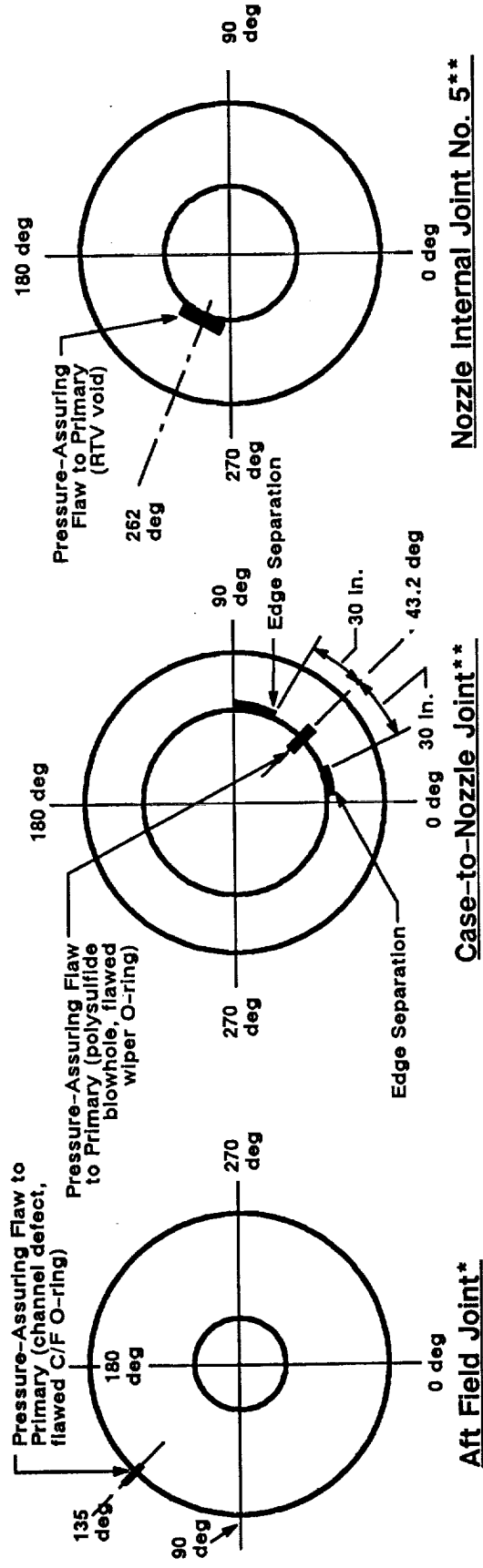
REVISION B



Center Field Joint*

Forward Field Joint*

Igniter/Case Joint*



Nozzle Internal Joint No. 5**

Case-to-Case Nozzle Joint**

Aft Field Joint*

* Forward looking aft
** Aft looking forward

A018655a

Figure 1.2-1. PV-1 Test Article Flaw Summary

The static test RSRM consisted of a lined, insulated, segmented rocket motor case loaded with solid propellant; ignition system complete with electro-mechanical safety and arming device (S&A), initiators, and loaded igniter; and a movable nozzle with flexible bearing and exit cone. A 360-deg external tank attach (ETA) ring (primary structure only) and an SRB aft skirt were attached with TVC systems and actuators, electrical and instrumentation items, and a thermal curtain assembly. The motor was instrumented to provide data to satisfy the test objectives. An overall view of the PV-1 test article is shown in Figure 1.2-2.

1.2.1 Propellant

The RSRM propellant, TP-H1148, is a composite-type solid propellant, formulated of polybutadiene acrylonitrile/acrylic acid copolymer (PBAN) binder, epoxy curing agent, ammonium perchlorate (AP) oxidizer, and aluminum powder fuel. A small amount of burning rate catalyst (iron oxide) is added to achieve targeted propellant burn rate.

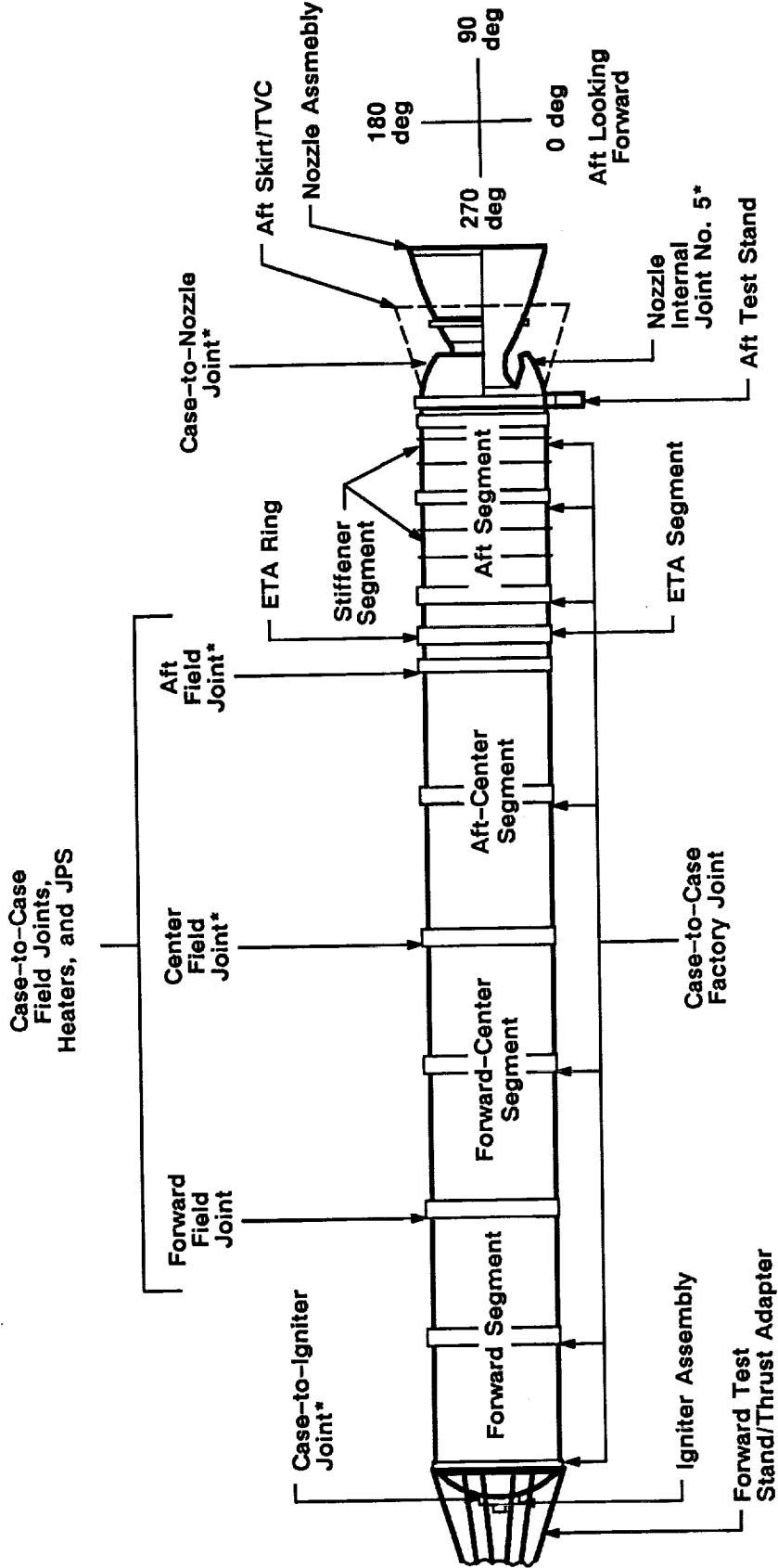
The forward segment propellant grain design consists of an 11-point star with a smooth bore-to-fin cavity transition region that tapers into a cylindrical perforated (CP) configuration. The two center segments are double-tapered CP configurations, and an aft segment is a triple-tapered CP configuration with a cutout for the partially submerged nozzle (Figure 1.2.1-1). The aft segment nozzle cutback region is formed using net cast molding.

1.2.2 Insulation

The internal insulation configuration for the RSRM is designed to provide thermal protection to the case during motor operation and subsequent heat soak, provide stress relief for the propellant grain, and provide a chemically compatible stratum to which the liner/propellant is bonded.

The internal insulation system includes case acreage insulation, joint insulation, joint bondlines, propellant stress relief flaps, forward-facing full web nitrile butadiene rubber (NBR) inhibitors, and aft-facing partial web castable inhibitors.

The materials to be used in the RSRM internal insulation system are the same as those used in the high performance motor (HPM) configuration, with



*Intentional Flaws

Figure 1.2-2. Overall View of PV-1 Test Article

A018816a

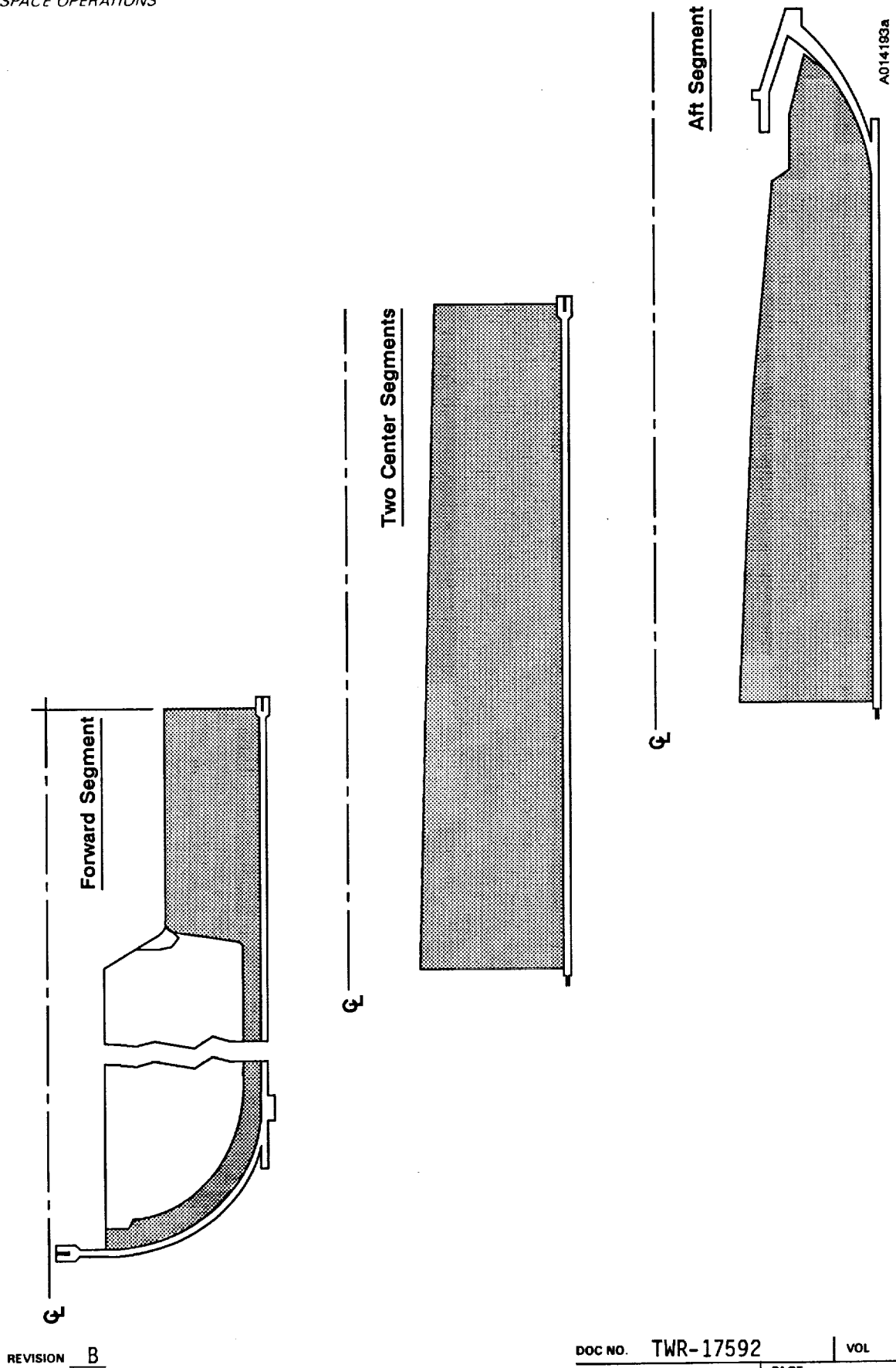


Figure 1.2.1-1. RSRM Propellant Grain Design Configuration

the exception of the joint adhesives. Asbestos silica-filled NBR, STW4-2621, is the material used for the primary case sidewall insulation, factory joints, field joints, case-to-nozzle joint, stress relief flaps, and the forward-facing inhibitors. A portion of the material used in the case sidewall layup in the aft end of the center segments beneath the stress relief flap and in the aft dome consists of carbon fiber-filled ethylene propylene diene monomer rubber (CF/EPDM), STW4-2868.

The bonding material selected for bonding the primary case insulation to the D6AC steel case is a two-part primer/adhesive system. The selected system is Chemlok® 205 primer and Chemlok adhesive. Chemlok is used where CF/EPDM is bonded to the NBR in the aft dome and in the center segments beneath the propellant stress relief flaps.

The adhesive used in the assembled J-insulation field joint configuration is a liquid pressure-sensitive adhesive conforming to STW5-3479. This material is a pressure-sensitive adhesive dispersed in methylchloroform solvent. The adhesive used in the case-to-nozzle joint is a two-part polysulfide adhesive (STW4-3311).

The liner material is an asbestos-filled carboxyl-terminated polybutadiene (CTPB) polymer which bonds the propellant to the case insulation in the SRM.

The inhibitor is the same as the HPM with castable inhibitors on the aft end of the forward and center segments. The aft facing inhibitor material is a CTPB polymer. NBR inhibitors are used on the forward face of the center and aft segments. The external insulation includes vulcanized silica-filled EPDM insulation over the factory joints.

1.2.3 Nozzle/TVC

The nozzle assembly is a partially submerged convergent/divergent movable design with an aft pivot point flexible bearing (Figure 1.2.3-1). The bond-line area in the flex bearing/fixed housing nozzle internal Joint 5 was intentionally flawed (Figure 1.2.3-2) to allow pressure to reach the primary O-ring. The aft skirt assembly which was attached to the aft segment contains the TVC system comprised of two SRB actuators and two hydraulic power units (HPU).

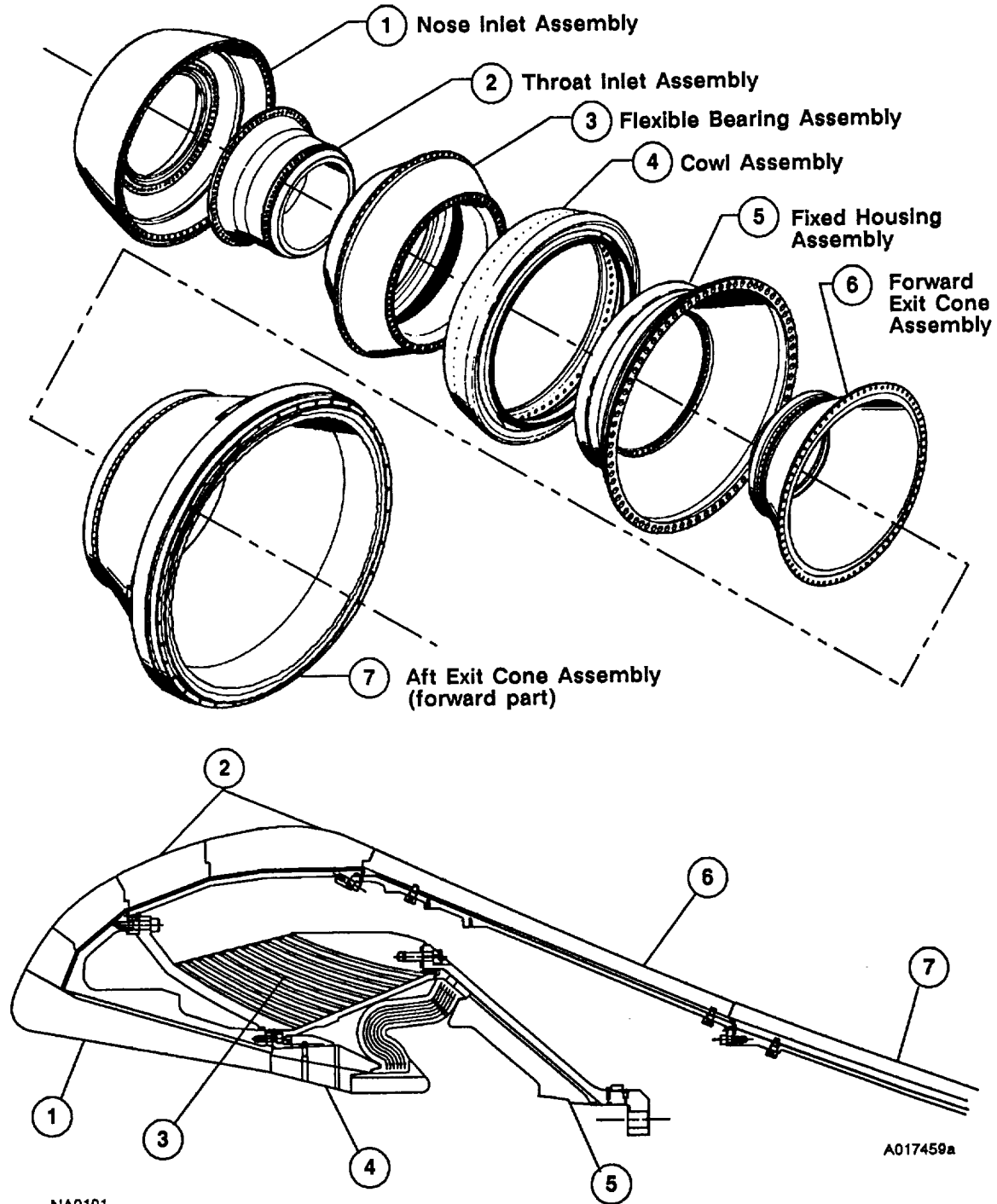
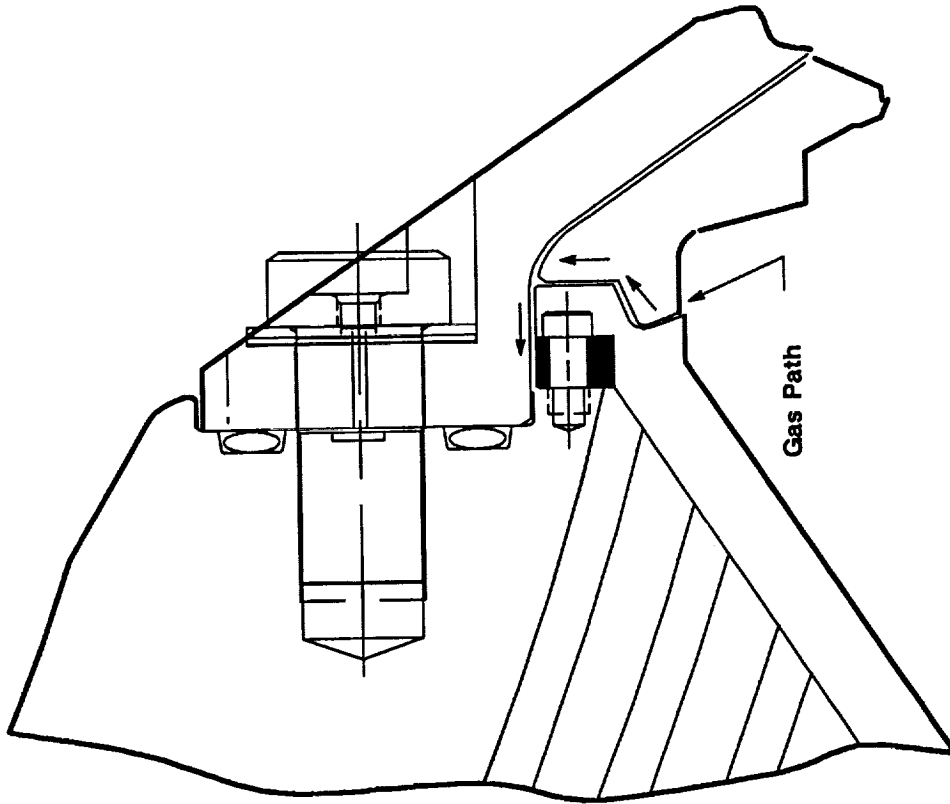


Figure 1.2.3-1. RSRM Nozzle Assembly



To assure pressure to the primary O-ring, a portion of the RTV filler (9 to 11 in. circumferentially, centered at 262 deg) was intentionally left out during joint assembly to provide a direct, unobstructed path to the primary O-ring.

Figure 1.2.3-2. Nozzle Internal Joint 5 Flaw

A015975a

The HPU Ground Test Controller, HPU manual/automatic panel (MAP), and the ascent thrust vector control (ATVC) units served as the control units for the TVC subsystem. A block diagram of the TVC subsystem and controllers are shown in Figure 1.2.3-3.

There was no linear shaped charge on PV-1.

1.2.4 Case/Seals

The case consists of 11 individual segments: the forward dome, 6 cylinder segments, the ETA segment, 2 stiffener segments, and the aft dome. The 11 segments are preassembled into four subassemblies before propellant casting. These four subassemblies are the forward segment assembly, the forward center assembly, the aft center segment assembly, and the aft segment assembly. These individual casting segments are joined by means of capture feature tang and clevis field joints, which in turn are held together by pins. The assembled case was approximately 116 ft in length and 12 ft in diameter (Figure 1.2.4-1).

Factory joints were configured with RSRM case segments and RSRM insulation configuration (Figure 1.2.4-2). Teflon[®] tape was added to all factory joints to prevent the NBR from bonding to the case providing a stress relief. A vulcanized weatherseal was installed at the factory joints.

The three field joints were configured with interference fit, capture feature joint hardware, and bonded RSRM (flight configuration) J-joint insulation configuration (Figure 1.2.4-3). The clevis-to-capture feature void (V_2) was filled with fluorocarbon joint filler. The center field joint had a pressure-assuring flaw to the capture feature O-ring (channel defect in clevis insulation; V_2 filler oriented with gap in line with flaw at 135 deg) as shown in Figure 1.2.4-4. The aft field joint also had a pressure-assuring flaw to the primary O-ring (channel defect in clevis and tang insulation; flawed capture feature O-ring; V_2 filler oriented with gap in line with flaw at 135 deg) as shown in Figures 1.2.4-5 through 1.2.4-7. The case-to-nozzle joint incorporated an RSRM fixed housing with 100 (0.875-in. dia) radial bolts and an RSRM interference fit bonded insulation configuration (Figure 1.2.4-8). The case-to-nozzle joint had a pressure-assuring flaw to the primary O-ring (polysulfide blowhole flaw and flawed wiper O-ring) as shown

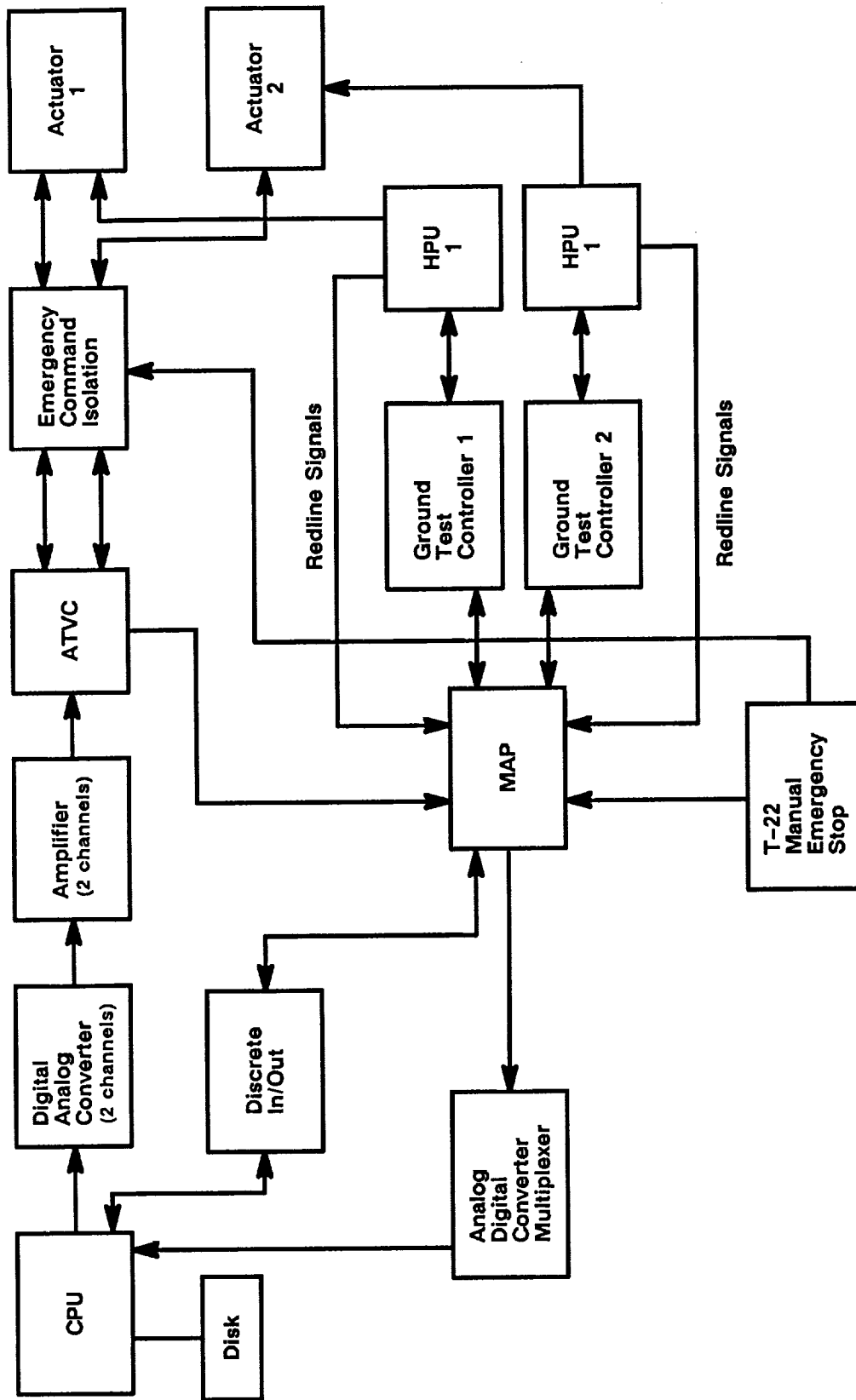


Figure 1.2.3-3. Thrust Vector Actuation System

A018701a

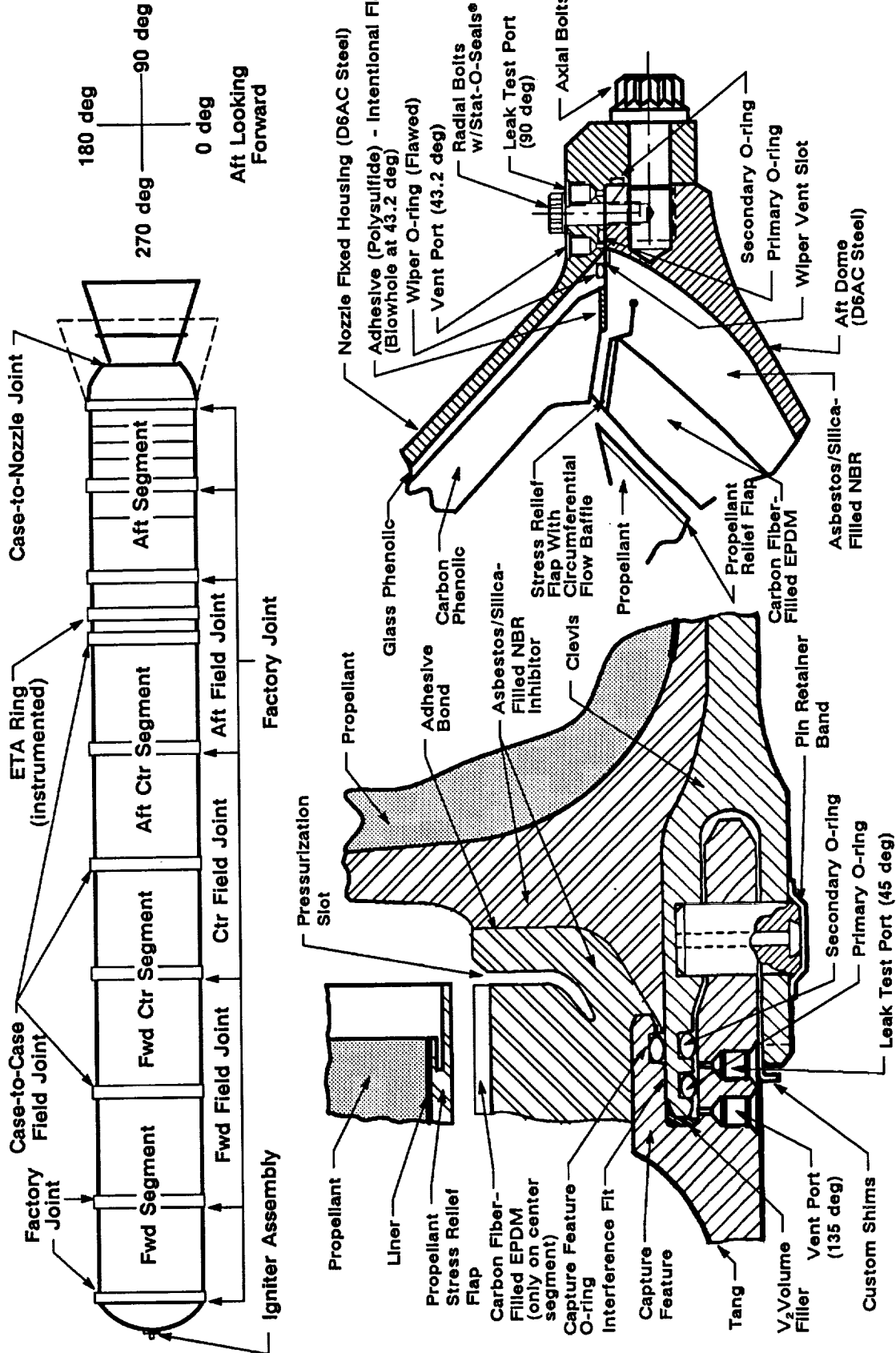
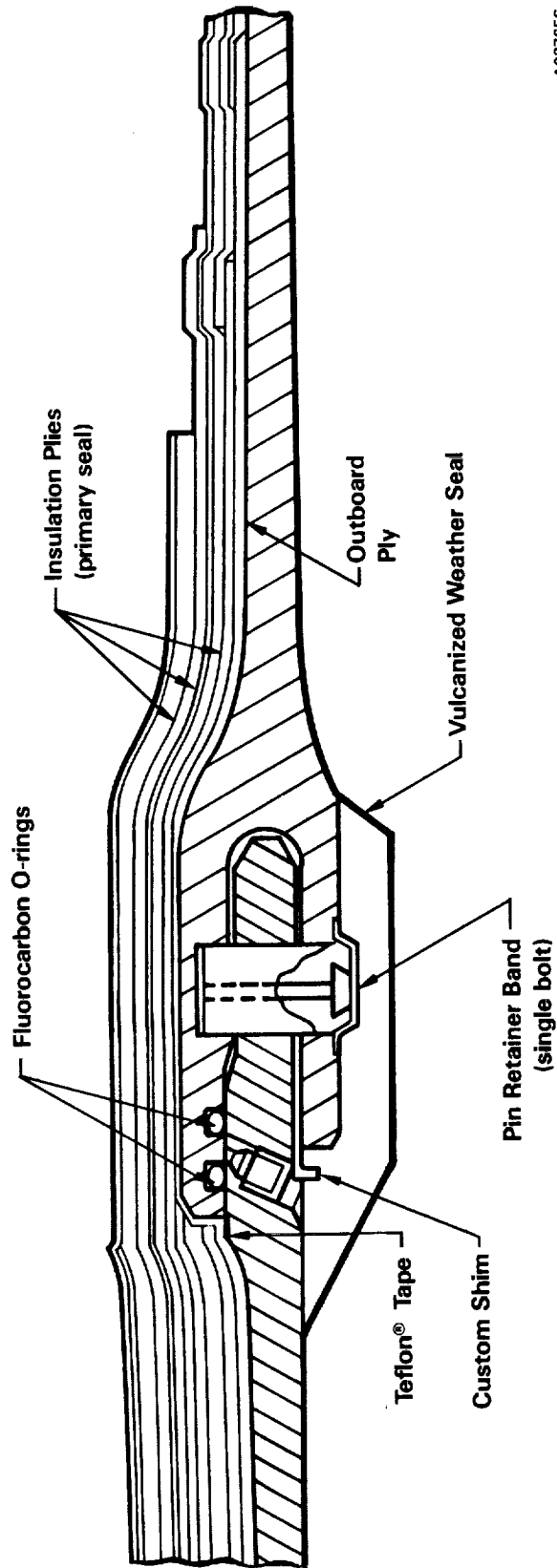


Figure 1.2.4-1. Static Test Motor Configuration

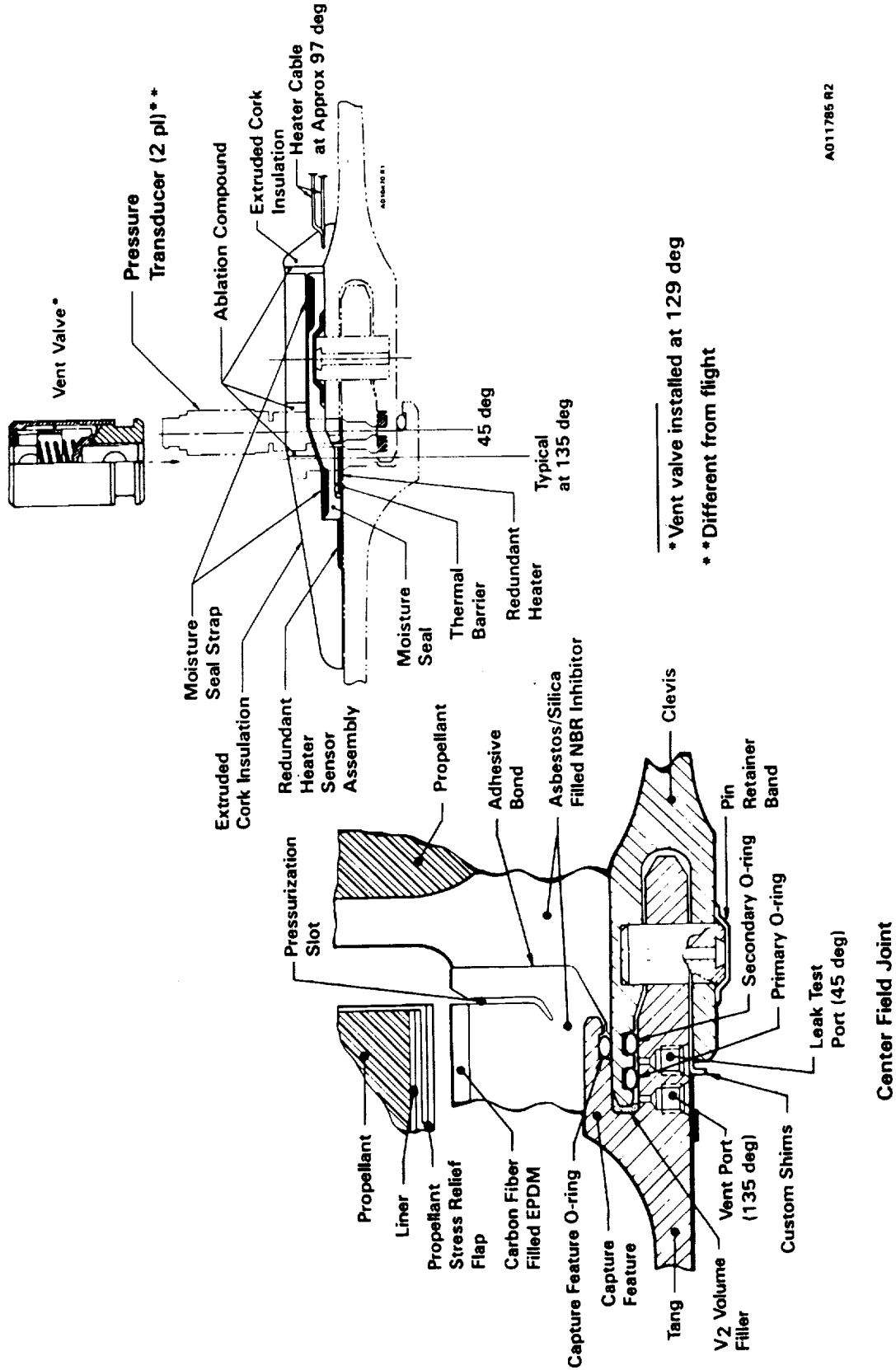
A018735a



A027656

Figure 1.2.4-2. RSRM Factory Joint

89265-14A



AO11785 R2

* Vent valve installed at 129 deg
** Different from flight

Figure 1.2.4-3. RSRM Aft Case-to-Case Field Joint

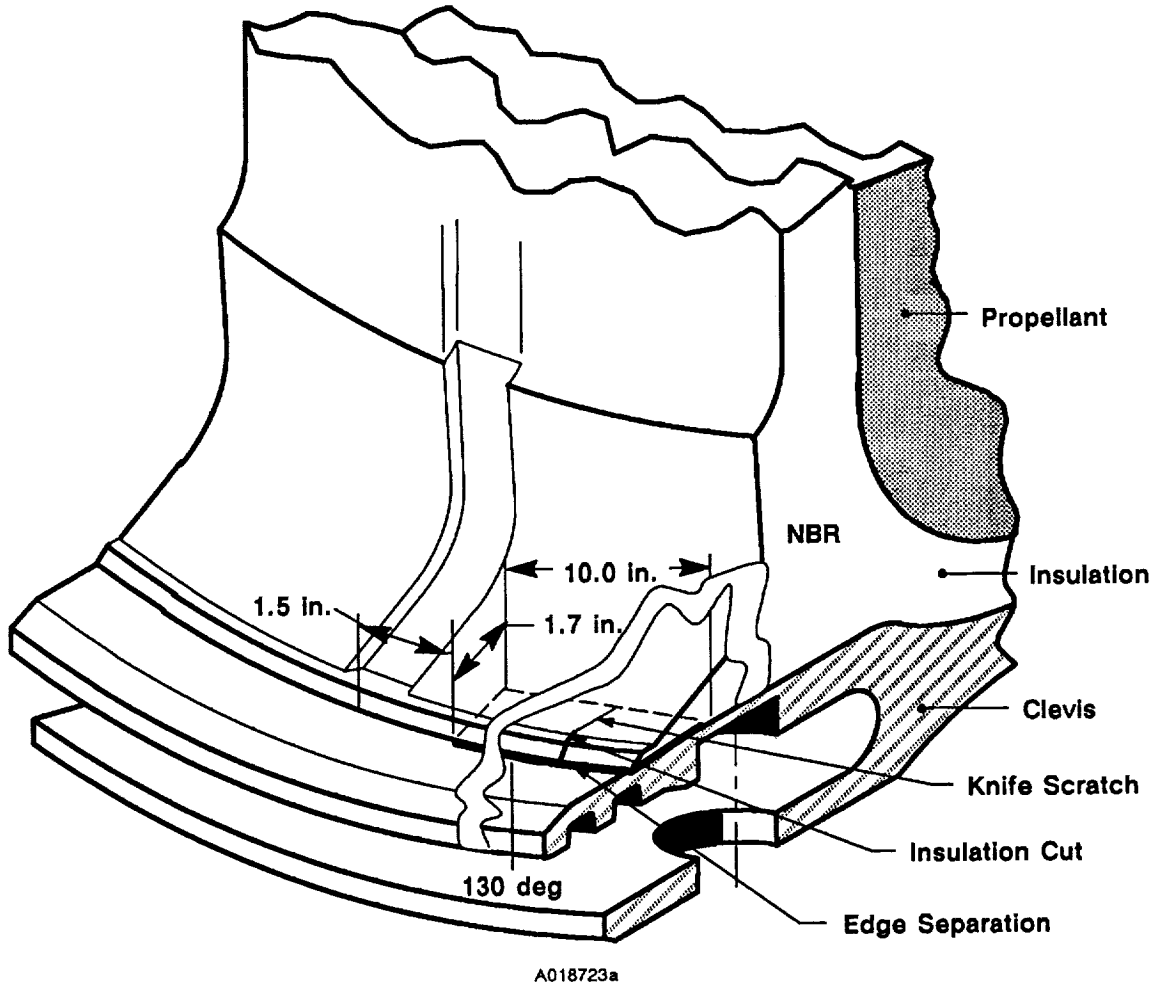


Figure 1.2.4-4. Center Field Joint Flaw (Clevis)

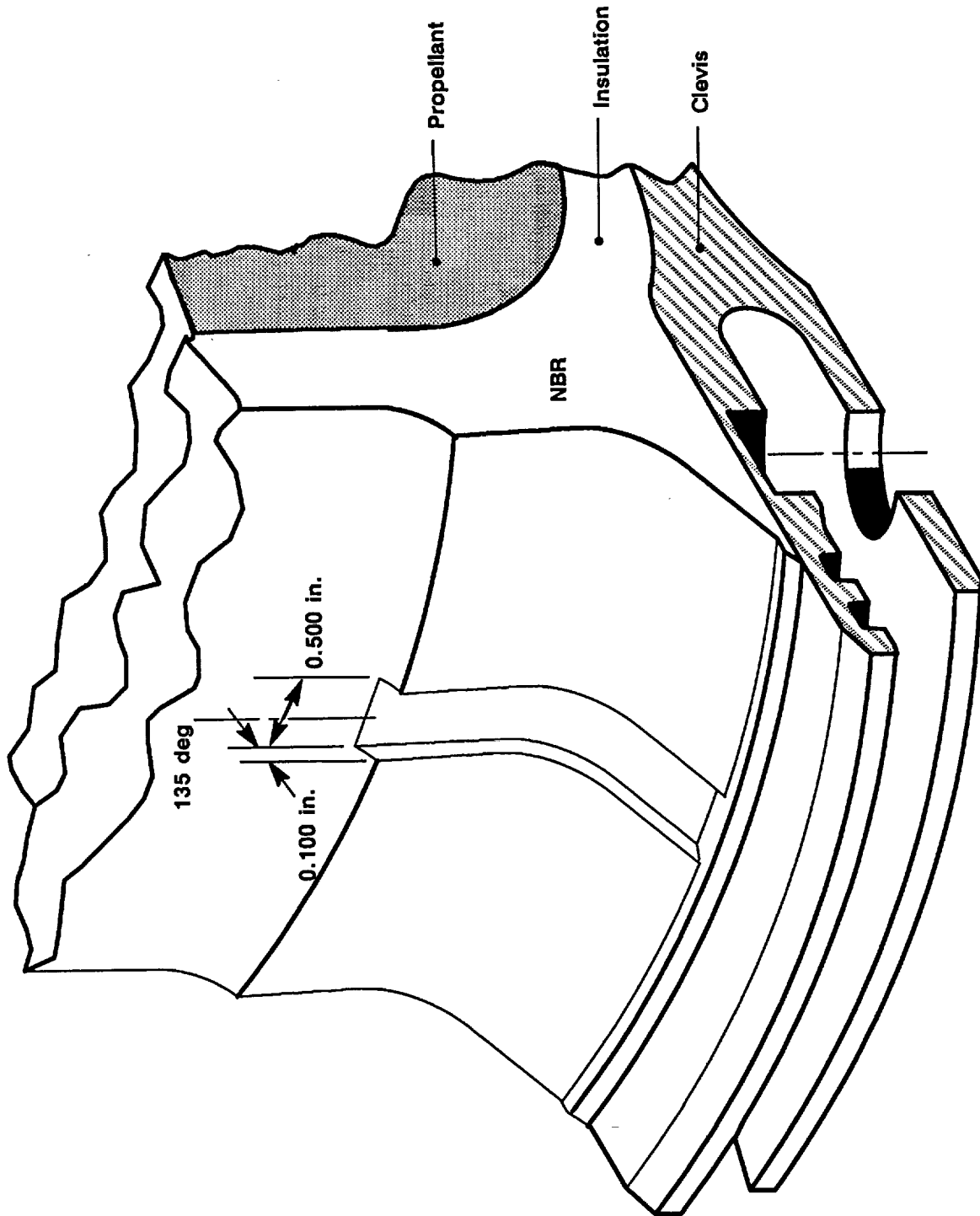


Figure 1.2.4-5. Aft Field Joint Flaw (Clevis)

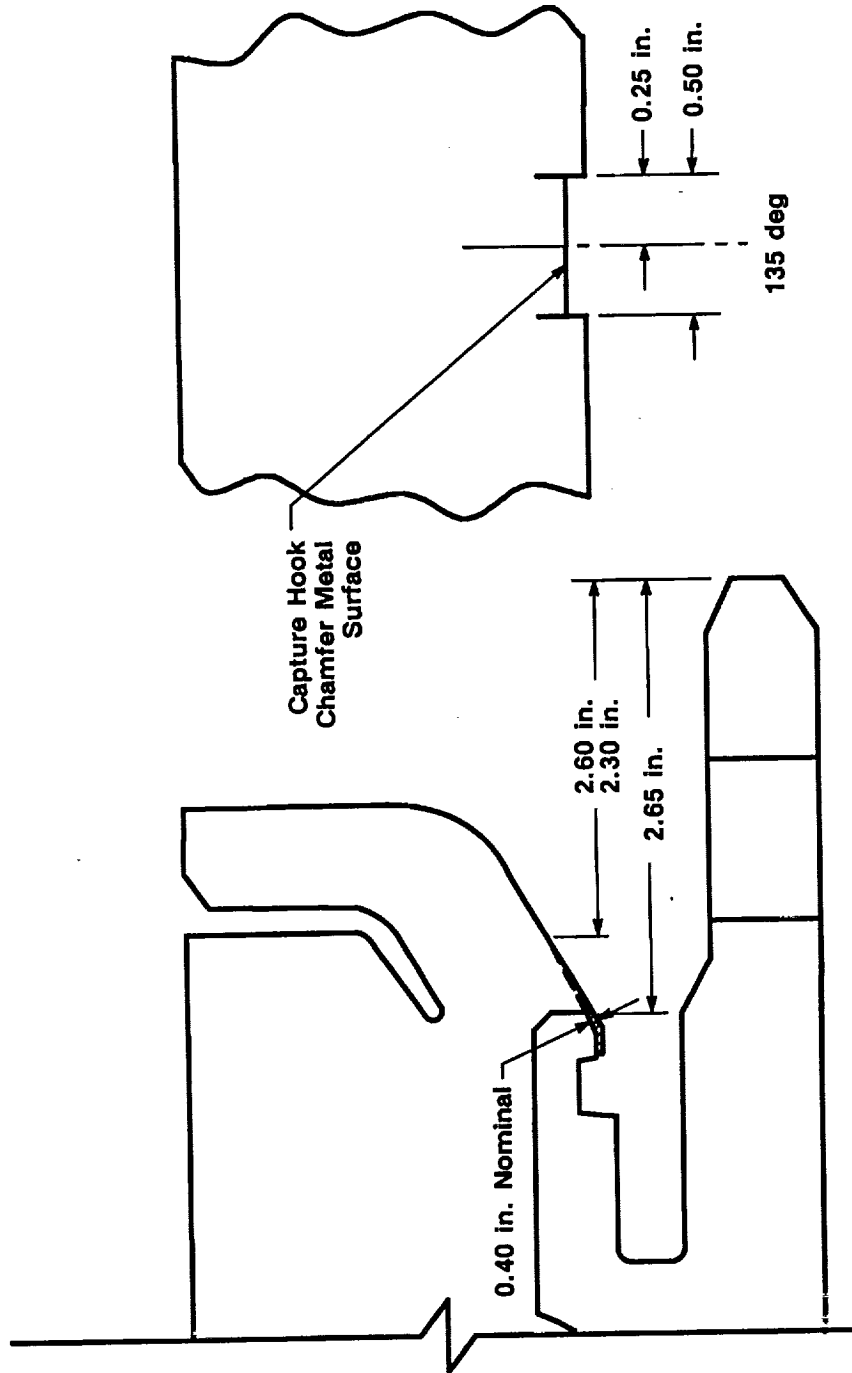


Figure 1.2.4-6. Aft Field Joint Flaw (Tang)

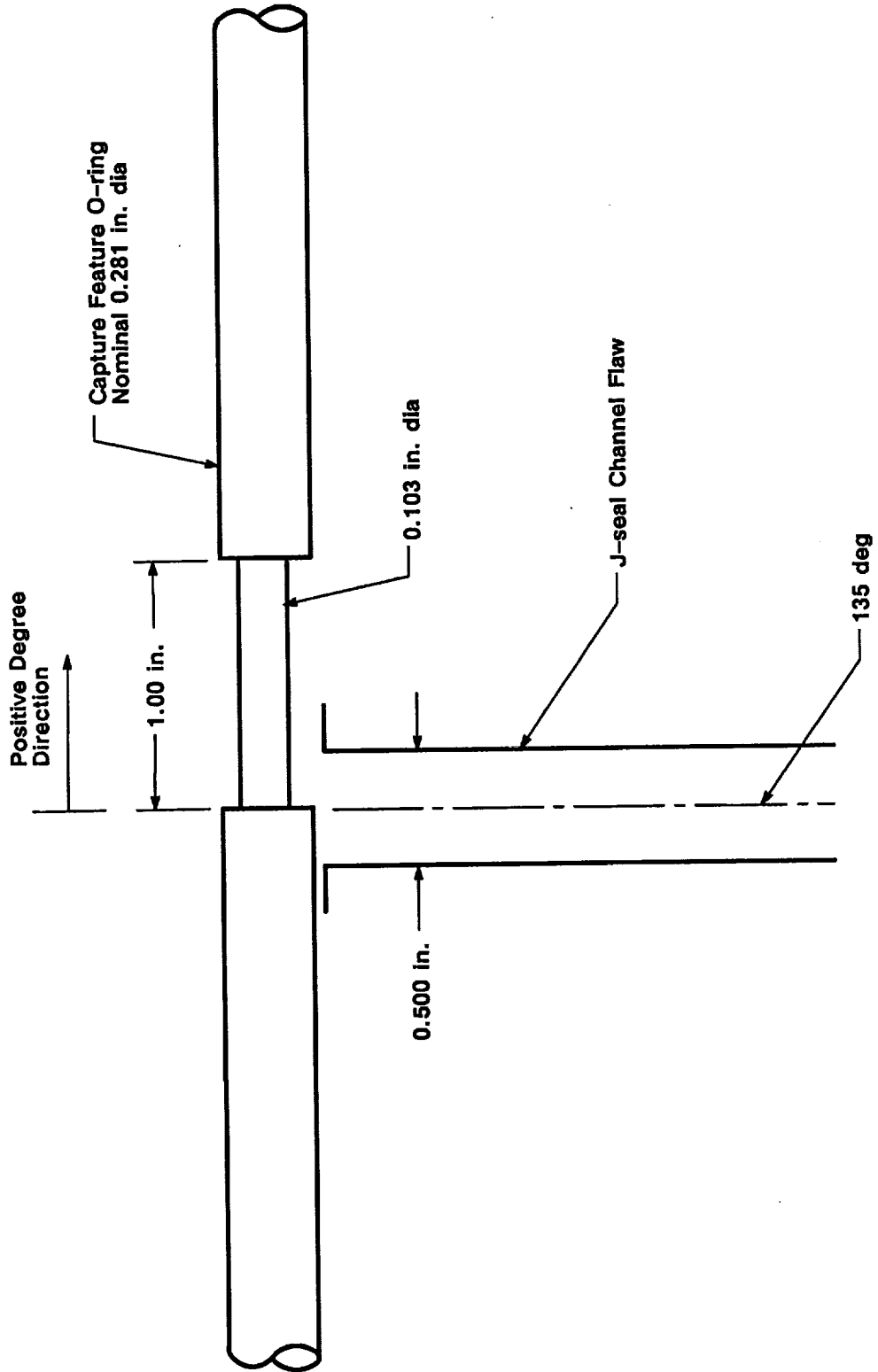


Figure 1.2.4-7. Aft Field Joint O-ring Flaw

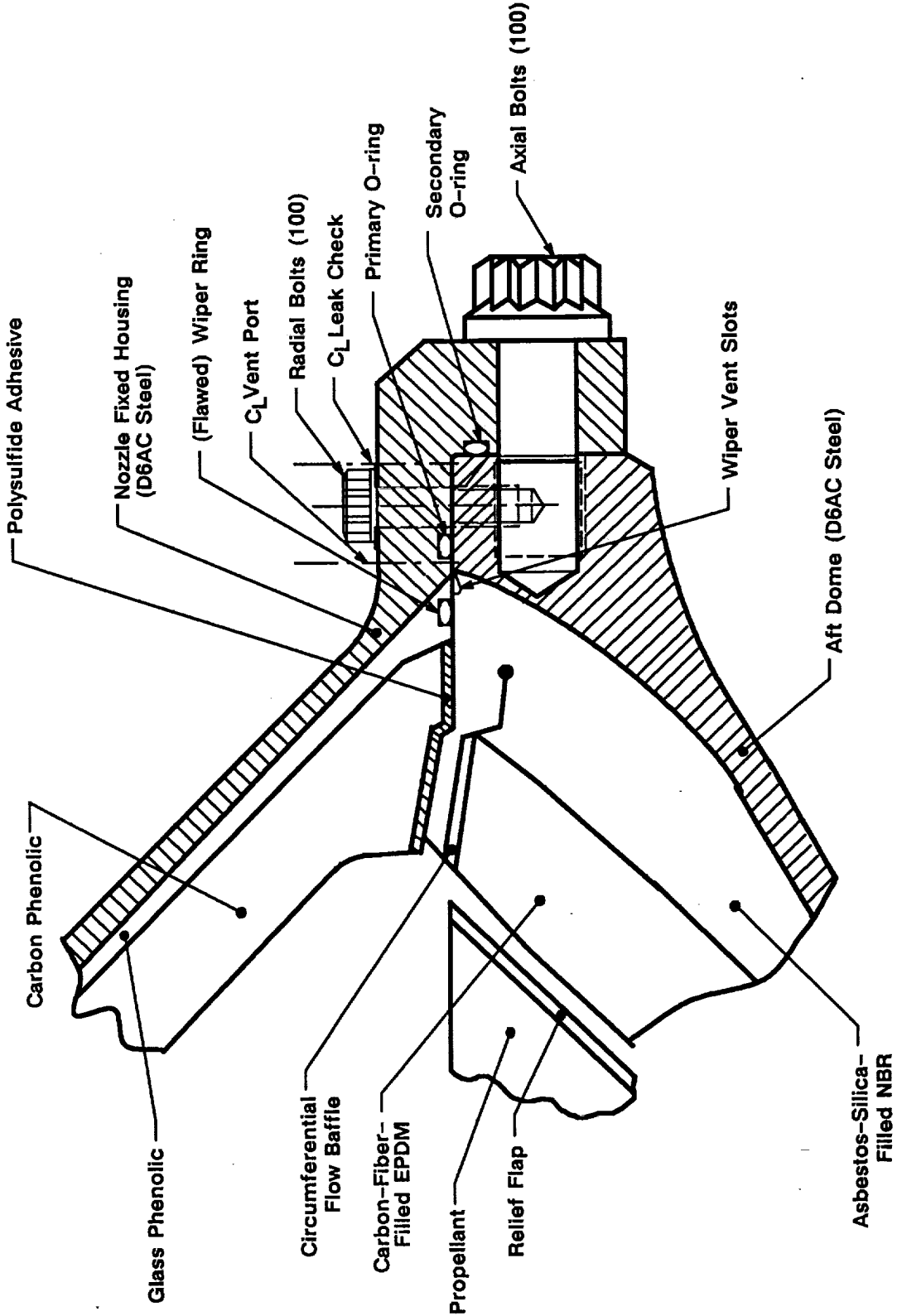


Figure 1.2.4-8. Case-to-Nozzle Joint

A018815a

in Figures 1.2.4-9 through 1.2.4-11. The igniter-to-forward dome joint had two artificial edge separations induced 180 deg apart in the forward dome insulation (Figure 1.2.4-12). A simplified joint protection system (JPS) was installed on all three field joints.

Fluorocarbon (STW4-3339) O-rings were employed for all primary and secondary seals/O-rings, the field joint capture feature, and the case-to-nozzle joint wiper O-rings. Case joints were assembled using long pins, 3-piece hat retainer band, and custom shims. Custom vent port plugs were installed in one joint. Corrosion protection consisted of full external paint and a thin film of grease (including O-rings, sealing surfaces, and pinholes).

1.2.5 Ignition System

The RSRM ignition system is a modified HPM igniter. It contains a single nozzle, steel chamber thickened at the nozzle end, external insulation, and tapered internal insulation, new liner material, vacuum putty from a new manufacturer, and solid propellant configured with a case-bonded 40-point star grain (Figure 1.2.5-1). The forward-mounted igniter is modified with a CO₂ quench port. A joint strip heater was installed on the igniter to ensure 100°F minimum at the gaskets for PV-1. An RSRM S&A device is installed on the igniter. Ultrasonically torqued bolts fastened the ignition system in place.

1.2.6 JPS/Weatherseal/Systems Tunnel

The simplified JPS installed on each field joint consisted of heaters and sensors only. The heaters consist of primary and redundant chemically etched foil circuits which are superimposed upon one another and laminated in Kapton® and fluoroethylene polymer Teflon. The heating surface is 1.25 in. wide and has a total thickness of approximately 0.062 inch. The underside of the heaters Kapton surface is coated with a pressure-sensitive adhesive. This adhesive provides bonding to the case during assembly. The lead wires extend from the heaters and are terminated in electrical connectors. Adjacent to the heater are two temperature sensor assemblies. Each assembly contains two resistance temperature detector (RTD) sensors. These were covered with a 0.25-in. thick strip of cork (Figure 1.2.6-1). The cork was

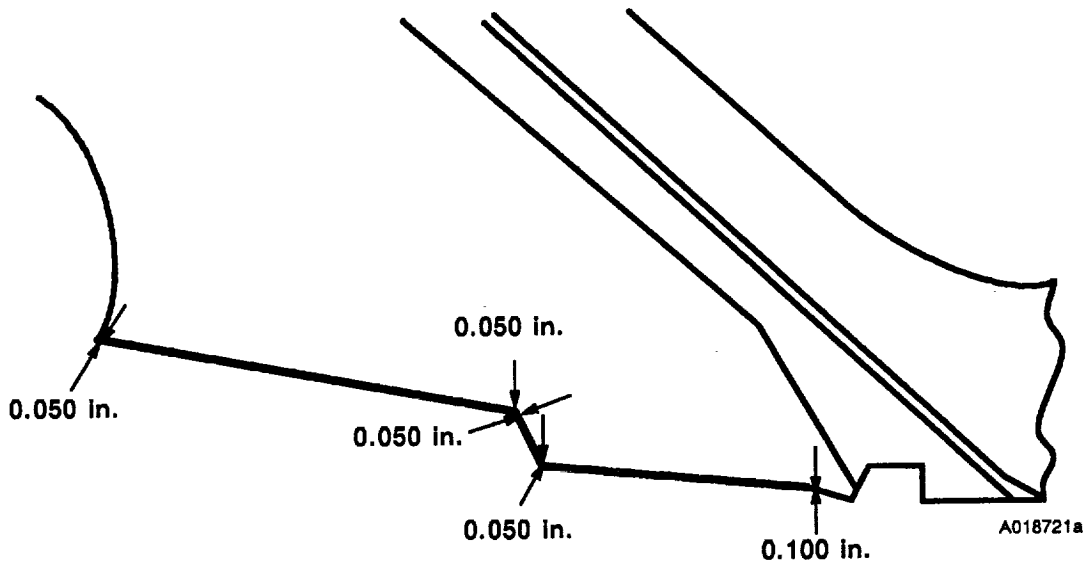
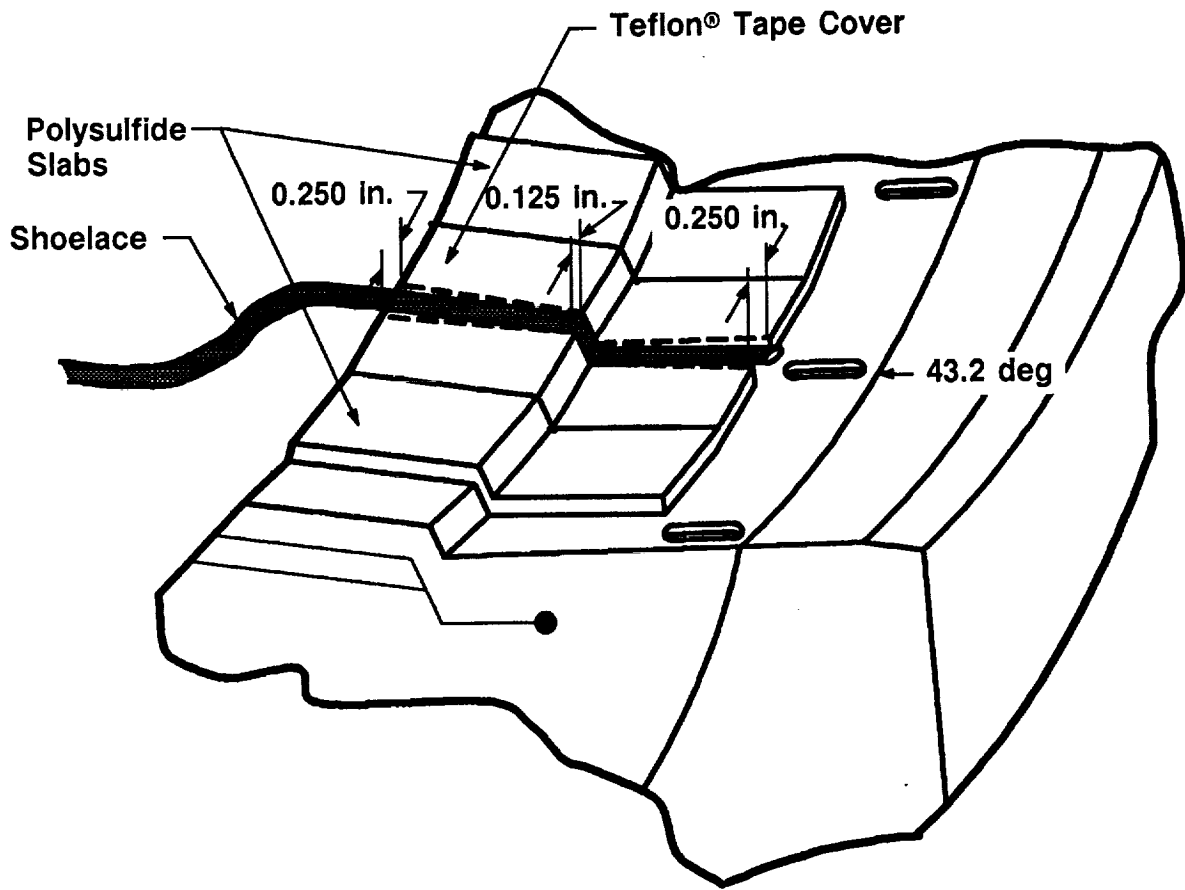


Figure 1.2.4-9. Case-to-Nozzle Insulation Bondline Defect

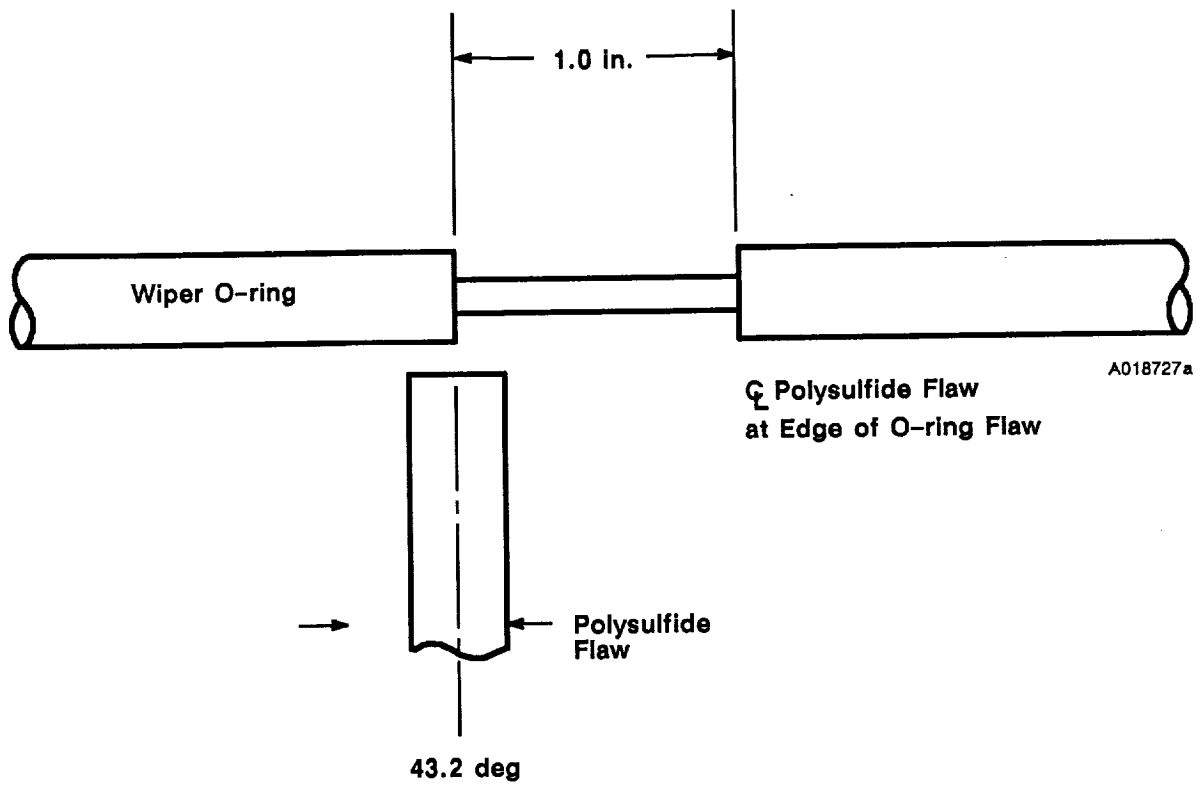


Figure 1.2.4-10. Case-to-Nozzle Joint Flaw

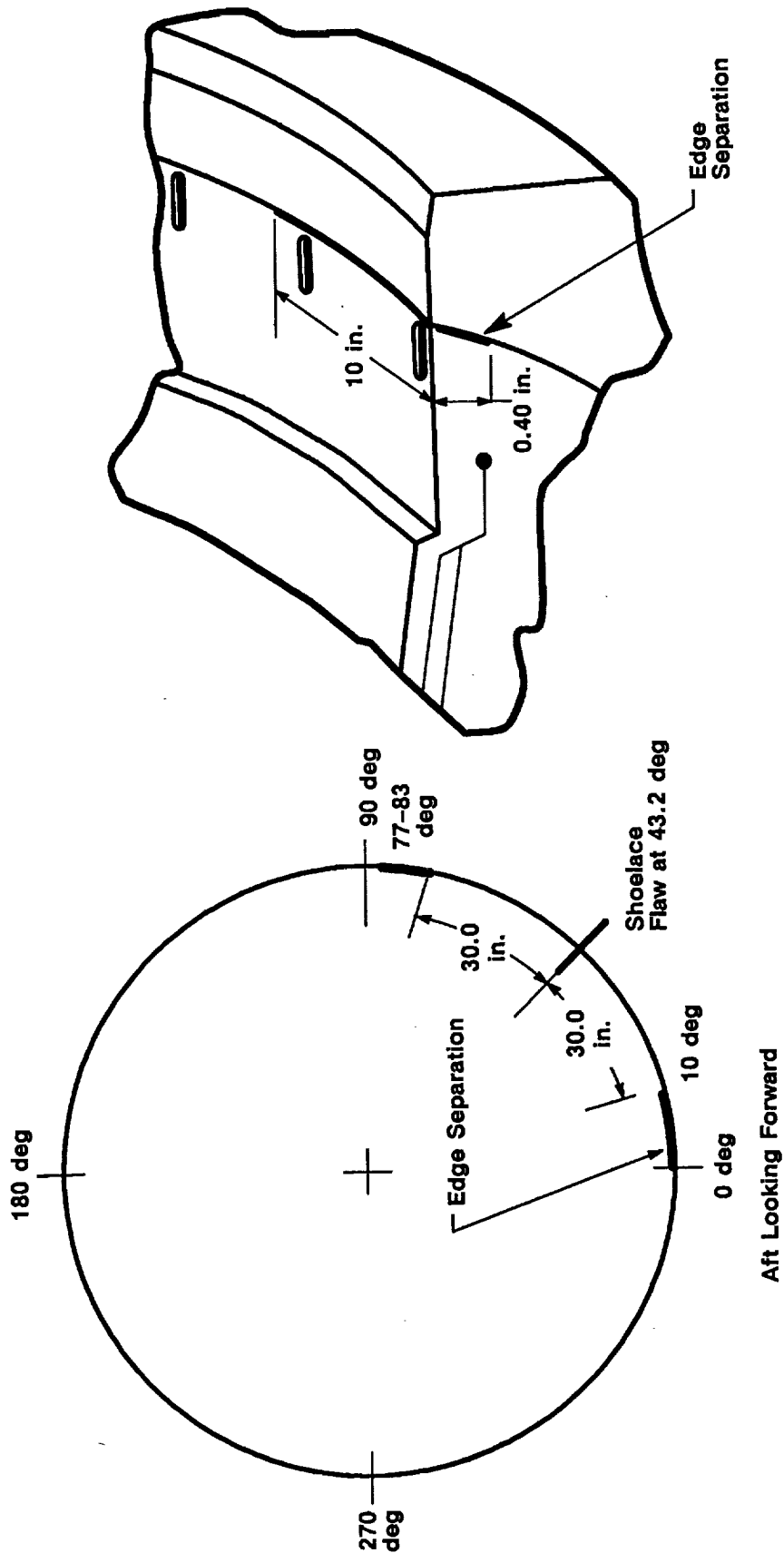


Figure 1.2.4-11. Nozzle Boss Induced Edge Separation

A015971a

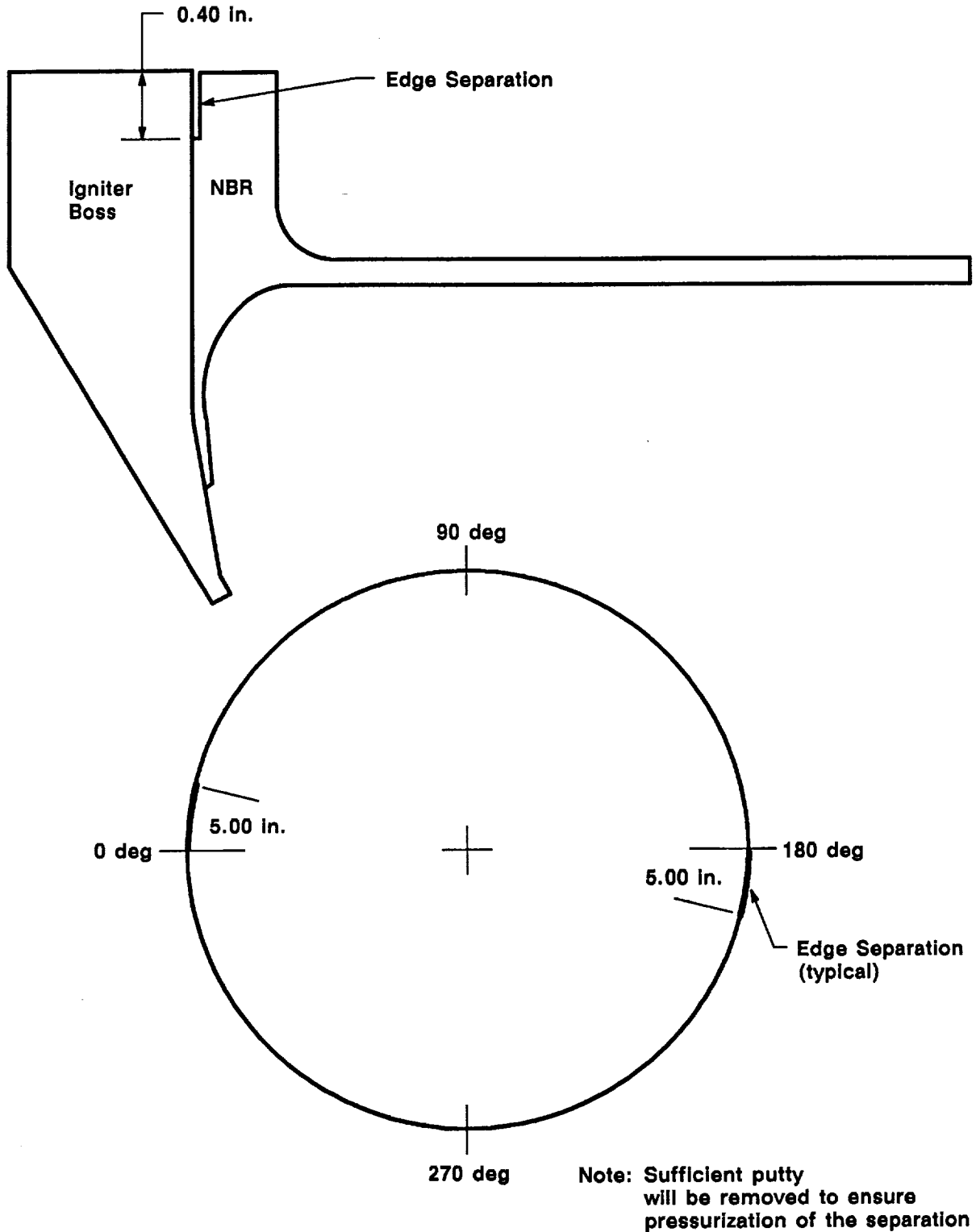


Figure 1.2.4-12. Igniter-to-Forward Dome Edge Separation Locations

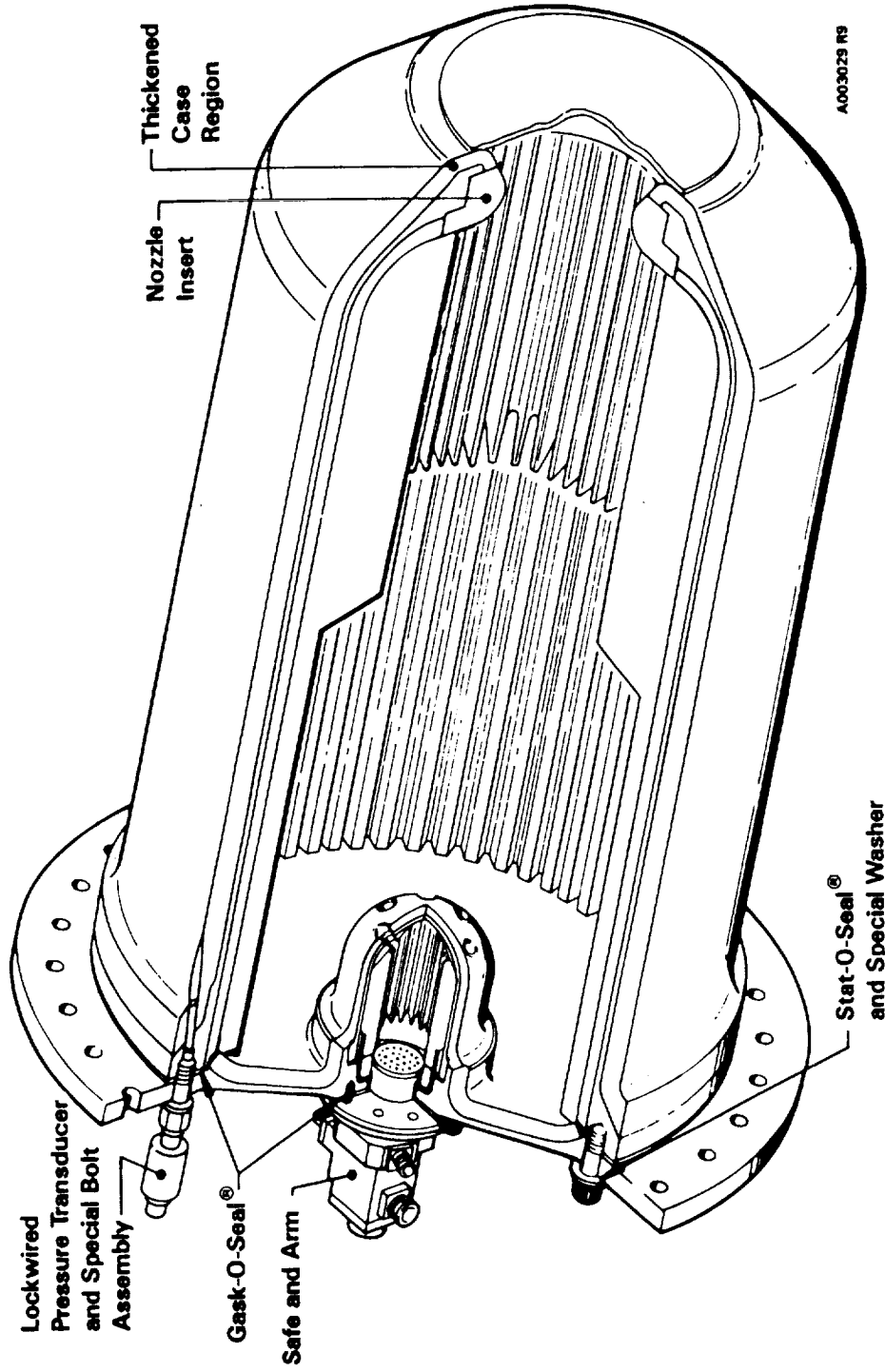


Figure 1.2.5-1. RSRM Ignition System

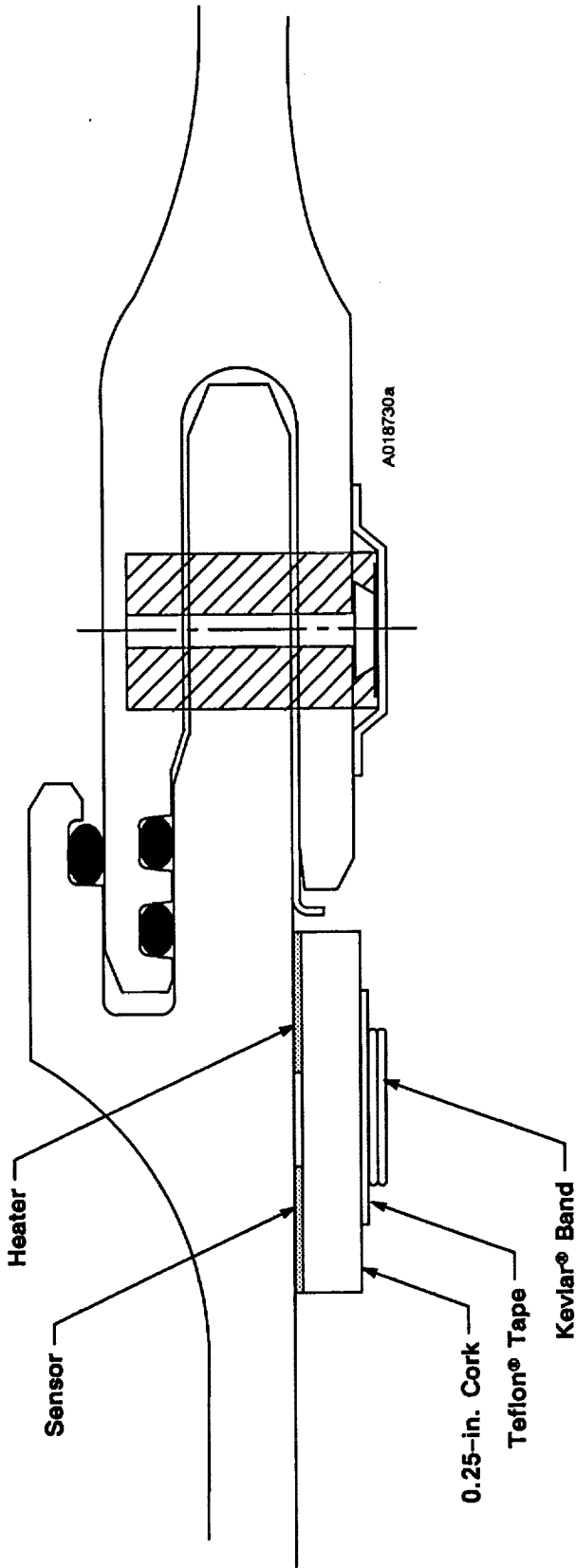


Figure 1.2.6-1. Simplified Joint Heater

held in place over the heaters and sensors by a single Kevlar band. The moisture seal and cork insulation were not installed on this motor. No systems tunnel was installed on PV-1.

The PV-1 drawing tree is included in Appendix A. PV-1 deviations from flight configuration are listed in Table 1.2.6-1.

Table 1.2.6-1. PV-1 Differences From First Flight

CHANGE	REASON	AUTHORIZATION	REMARKS
SNUBBER AND SNUBBER SUPPORT RING DELETED	THE SNUBBER AND SNUBBER RING ARE NOT CUSTOMARILY INSTALLED ON STATIC TEST MOTORS IN THE INTEREST OF SCHEDULE AND COST SAVINGS. THESE ITEMS ARE ALREADY QUALIFIED. THEY SERVE NO PURPOSE (NONFUNCTIONAL) ON STATIC TEST MOTORS, AND HAVE NO EFFECT ON NOZZLE / TVC PERFORMANCE.	PROGRAM MGMT MEMO E140/JJS-FY88-381	SNUBBER INSTALLATION ALSO LIMITS INSTRUMENTATION CABLE ROUTING FROM NOZZLE.
LSC DELETED	ENGINEERING WANTS TO PRESERVE NOZZLE AND EXIT COME FOR POST TEST EVALUATION. THEREFORE THEY DO NOT WANT TO DETONATE LSC IF INSTALLED. THE LSC IS A QUALIFIED COMPONENT. THE NOZZLE HAS THE SAME MATERIAL THICKNESS AS HPM NOZZLE. ALSO AN OFF LINE TVC DEMONSTRATION / QUALIFICATION TEST OF THE LSC SYSTEM HAS BEEN COMPLETED SUCCESSFULLY.	PROGRAM MGMT MEMO E140/JJS-FY88-381	
NOZZLE DUTY CYCLE	DIFFERENT THAN FLIGHT - TEST MORE SEVERE CONDITION (SAME DUTY CYCLE AS OM-6)	CEI SPEC REQUIREMENT	
INSTRUMENTED BOLTS IN NOZZLE TO CASE JOINT (STRAIN SERT)	PART OF THE STATIC TEST CONFIGURATION FOR STATIC TEST	STANDARD CONFIGURATION FOR STATIC TEST	NOT USED ON FLIGHT
REDUCED THREADS ON BOLTS CONNECTING FIXED HOUSING TO AFT END RING.	EVALUATE SEALING CAPABILITY OF NEW STAT-O-SEALS [®]	IMPROVED DESIGN AND APPROVED BY ENGINEERING AND NASA	THESE BOLTS WILL BE USED ON SECOND FLIGHT AND SUBS
FLAW IN NOZZLE JOINT NUMBER FIVE. RTV VOID PROVIDING A LEAK PATH TO THE PRIMARY O-RING.	EVALUATE SEALING CAPABILITY WITH ASSURED FLAW.	RPRB 17 DEC 87	

Table 1.2.6-1. PV-1 Differences From First Flight (Cont)

CHANGE	REASON	AUTHORIZATION	REMARKS
3 FLAWS: (NOZZLE TO CASE JOINT, CENTER FIELD JOINT AND AFT FIELD JOINT)	FTTM DESIGNATED AS A FLAW TEST MOTOR	NASA DIRECTIVE RPRB 17 DEC 87	PRESSURE ASSURED FLAW TO C/F O-RING AT CENTER FIELD JOINT. PRESSURE ASSURED FLAW TO PRIMARY O-RING AT AFT FIELD JOINT. PRESSURE ASSURED FLAW TO PRIMARY O-RING IN NOZZLE/CASE JOINT.
INSULATION EDGE SEPARATIONS IN CENTER FIELD JOINT, NOZZLE TO CASE JOINT, AND IGNITER TO CASE JOINT.	ENGINEERING ASSESSMENT TO DETERMINE TOLERANCES FOR EDGE SEPARATIONS.	RPRB 11 FEB 88	
TEST INSTRUMENTATION	TO RECORD PARAMETERS	PER DWG # 7U76264	MUCH DIFFERENT THAN DFI - REQUIRES OTHER CHANGES IN JOINT INSULATION ETC. - TO ACCOMMODATE STATIC TEST INSTRUMENTATION.
INSULATION - TPS AND SPLASH-DOWN PROTECTION SYSTEM HAVE BEEN DELETED.	STIFFENER RING / ETA RING AND THE AFT SKIRT ARE NOT CUSTOMARILY INSULATED FOR STATIC TEST. ALLOWS EASIER ACCESS FOR INSTRUMENTATION AND ASSEMBLY. THE TPS AND OTHER PROTECTION SYSTEMS ARE UNCHANGED AND ALL READY QUALIFIED.	COMMON PRACTICE THROUGHOUT PROGRAM. STANDARD STATIC TEST CONFIGURATION.	THESE SYSTEMS ARE UNDER INVESTIGATION. SOME QUESTION IF THEY CAN BE INSTALLED IN HORIZONTAL POSITION.
TEST ORIENTATION AND ASSY	ASSEMBLED AND TESTED HORIZONTALLY. USES DIFFERENT TOOLING / GSE.	STANDARD CONFIGURATION FOR STATIC TEST	DIFFERENCES: FIELD JOINT ASSEMBLED CLEVIS TO TANG - STATIC TEST NOZZLE ALIGNMENT SLAG BUILD UP - STATIC TEST MOTOR SAG - STATIC TEST
ETA RING	NOT FLIGHT INSULATED. INSTRUMENTED BUT NOT RECORDED		
AFT SKIRT	NO INSULATION - CONFIGURED FOR STATIC TEST. IN HORIZONTAL POSITION	STANDARD CONFIGURATION FOR TEST	ADDITIONAL INSTRUMENTATION INSTALLED FOR TVC SPECIAL TESTS
WATER DELUGE	COOL METAL HARDWARE TO ENSURE REUSABILITY	RPRB	DELUGE ADDED FOLLOWING DM-8 DESTRUCTION OF AFT SEGMENT
NO SYSTEMS TUNNEL	NASA REQUIREMENT HAS BEEN: PARTIAL SYSTEM TUNNEL ON 1 QUAL MOTOR FULL SYSTEM TUNNEL ON 1 QUAL MOTOR SELECTED OM-7 AND OM-8 FOR SYSTEM TUNNEL TESTING BECAUSE THEY ARE TO BE CONDITIONED.	NASA DIRECTIVE MEMO #SA42-103-87	

26 APR 88

A013032a

- A013032a.2 -

Table 1.2.6-1. PV-1 Differences From First Flight (Cont)

CHANGE	REASON	AUTHORIZATION	REMARKS
QUENCH PORT IGNITER ADAPTER - WITH CO2 PORT ADDED FOR STATIC TEST	TO ALLOW HEAD-END QUENCH - CO2 POSTFIRE - WITHOUT CO2 QUENCH WE COULD POTENTIALLY DAMAGE METAL HARDWARE. LOSE REUSABILITY OF CASE SEGMENTS AND INSULATION EROSION DATA	STANDARD CONFIGURATION FOR STATIC TEST 1U75166-02 CTP-0038	
IGNITER JOINT HEATERS	CERTIFY FOR THIRD FLIGHT	PENDING	NEW ITEM UNDERGOING EVALUATION TEST- ING
VENT PORT PLUG	ADJUSTABLE PLUG AT 135 DEG IN FORWARD FIELD JOINT	RPRB DIRECTION 10 FEB	
STIFFENER SEGMENTS HAVE SMALLER O-RING GLANDS AND MUST USE 7U O-RINGS	LOW INVENTORY OF LIGHTWEIGHT STIFF- ENERS	RPRB DIRECTION 16 DEC	
NO STIFFENER RINGS	HARDWARE DISCREPANCIES	DR DISPOSITION BY MRB	
NO SIDE LOADS APPLIED	CAPABILITY DOES NOT EXIST AT T-24 TEST FACILITY	DR DISPOSITION BY MRB	

REVISION _____

DOC NO. TWR-17592
SEC _____

PAGE _____ VOL _____

26 APR 88

A013632a

- A013632a.3 -

TEST OBJECTIVES

The PV-1 test objectives were derived from objectives in TWR-15723 to satisfy the requirements of Specification CPW1-3600, Addendum D, dated 3 Aug 1987.

Qualification Objectives (CEI Paragraph)

- A Certify the motor performance at ambient temperature. (3.2.1)
- B Certify the ignition interval. (3.2.1.1.1.1)
- C Certify the pressure rise rate. (3.2.1.1.1.2)
- D Determine the thrust-time curve for PV-1 and apply the data to the nominal thrust-time curve for certification of the RSRM design. (3.2.1.1.2.1)
- E Certify the performance tolerances and limits. (3.2.1.1.2.2)
- F Determine the impulse attained by PV-1 and apply the data to the nominal thrust-time curve for certification of the RSRM design. (3.2.1.1.2.4)
- G Certify that all RSRM seals, except the center and aft field joints and nozzle-to-case joints and igniter-to-case joints, but including adjustable vent port plug seals in the forward field joint, experience no erosion or blowby throughout the static test, if pressurized. (3.2.1.2)
- H Certify the sealing performance of the center and aft field joints and the nozzle-to-case and igniter-to-case joints. (3.2.1.2)
- I Certify the verifiability of the RSRM seals (except for the case-to-nozzle joint primary seal, the factory joint primary seal, the fixed housing-to-aft end ring primary seal, the igniter dual seal plugs (5 places), and the operational pressure transducer (OPT) primary and secondary seals). (3.2.1.2)
- J Certify that the forward field joint seals, if pressurized, accommodate static test motor structural deflections. (3.2.1.2.1.a)
- K Certify that the center and aft field joint and the nozzle-to-case joint accommodate static test motor structural deflections. (3.2.1.2.1.a)

- L Certify that the forward field joint seals, if pressurized, operate at ambient temperature. (3.2.1.2.1.b)
- M Certify that the center and aft field joint and nozzle-to-case joint operate at ambient temperature. (3.2.1.2.1.b)
- N Certify that the case field joint and case-to-nozzle joint seal verification does not degrade the performance or integrity of the sealing system. (3.2.1.2.1.c)
- O Certify that the bore seals for the forward and center field joint are verifiable in the proper direction. (3.2.1.2.1.d)
- P Certify that the case-to-nozzle joint O-ring temperature is maintained prior to static firing. (3.2.1.2.1.f)
- Q Certify that the factory joint insulation as a seal accommodates static test motor structural deflections and erosion. (3.2.1.2.2.a)
- R Certify that the factory joint insulation as a seal operates at ambient temperature. (3.2.1.2.2.b)
- S Certify that the insulation performs the seal function for the factory joint. (3.2.1.2.2.d)
- T Certify that the factory joint insulation is adequate to preclude leaks. (3.2.1.2.2.e.)
- U Certify that the flex bearing accommodates static test motor structural deflections. (3.2.1.2.3.a)
- V Certify that the flex bearing operates as a seal at ambient temperature. (3.2.1.2.3.b)
- W Certify that the flex bearing seal verification does not degrade the performance or integrity of the sealing system. (3.2.1.2.3.c)
- X Certify that the flex bearing maintains a positive gas seal between its internal components. (3.2.1.2.3.d)
- Y Certify that the ignition seals, if pressurized, except for the igniter-to-case joint, accommodate static test motor structural deflections. (3.2.1.2.4.a)
- Z Certify that the igniter-to-case joint accommodates static test motor structural deflection. (3.2.1.2.4.a)
- AA Certify that the ignition seals, if pressurized, except for the igniter-to-case joint, operate at ambient temperature. (3.2.1.2.4.b)

- AB Certify that the igniter-to-case joint operates at ambient temperature. (3.2.1.2.4.b)
- AC Certify that the ignition system seal verification does not degrade the performance or integrity of the sealing system. (3.2.1.2.4.c)
- AD Certify that the nozzle internal seals, except for Joint 5, and the aft exit cone field joint seals, if pressurized, can accommodate static test motor structural deflections. (3.2.1.2.5.a)
- AE Certify that the nozzle internal Joint 5 can accommodate static test motor structural deflections. (3.2.1.2.5.a)
- AF Certify that the nozzle internal seals, except Joint 5 and the aft exit cone field joint seals, if pressurized, operate at ambient temperature. (3.2.1.2.5.b)
- AG Certify that the nozzle internal Joint 5 operates at ambient temperature. (3.2.1.2.5.b)
- AH Certify that the nozzle internal seals and the aft exit cone field joint seals verification does not degrade the performance or integrity of the sealing system. (3.2.1.2.5.c)
- AI Certify that the bore seals for the nozzle are verifiable in the proper direction. (3.2.1.2.5.e)
- AJ Certify that the case is capable of containing the static test internal pressure. (3.2.1.3.a)
- AK Certify that the case ETA risers do not degrade the integrity of the case. (3.2.1.3.c)
- AL Certify by demonstrating horizontal assembly that the case segment mating joints have provisions to ensure proper segment orientation and alignment. (3.2.1.3.f)
- AM Certify that the nozzle assembly and exit cone design are compatible with the system performance requirements. (3.2.1.4, Morton Thiokol-imposed)
- AN Certify that the nozzle assembly is capable of vectoring through the planned duty cycle. (3.2.1.4.1)
- AO Certify the geometric nozzle alignment. (3.2.1.4.2)
- AP Certify the misalignment of the dynamic thrust vector with respect to the nozzle centerline. (3.2.1.4.3, 3.2.1.4.3.a)
- AQ Certify the radial offset between the dynamic thrust vector and the nozzle centerline. (3.2.1.4.3, 3.2.1.4.3.b)

- AR Certify the null offset angle at 0 psi nozzle stagnation pressure. (3.2.1.4.4.a)
- AS Certify the null offset angle at 615 psi nozzle stagnation pressure. (3.2.1.4.4.b)
- AT Certify the null offset angle at 915 psi nozzle stagnation pressure. (3.2.1.4.4.c)
- AU Certify the nozzle assembly TVC actuator attach points. (3.2.1.4.8)
- AV Certify the nozzle flame front liner design and fabrication. (3.2.1.4.13)
- AW Certify that the ignition system precludes hot gas leakage during and subsequent to motor ignition. (3.2.1.5.a)
- AX Certify by demonstration that the igniter and the S&A are separable from each other. (3.2.1.5.b)
- AY Certify the enable function of the S&A device. (3.2.1.5.1.a)
- AZ Certify the S&A change of position from safe to arm. (3.2.1.5.1.d)
- BA Certify that the S&A device will provide simplex remote position indication. (3.2.1.5.1.e)
- BB Certify the igniter design. (3.2.1.5.2)
- BC Certify that the RSRM design meets the electromagnetic compatibility requirements. (3.2.1.6.e)
- BD Certify the operation of the motor chamber pressure transducer and its installation. (3.2.1.6.2.1)
- BE Certify the installation and function of the ground environmental instrumentation. (3.2.1.6.2.3, Morton Thiokol-proposed SCN 3)
- BF Certify the installation and operation of the strain gages (steel) (aluminum) in the nozzle area. (3.2.1.6.2.3, Morton Thiokol-proposed SCN 3)
- BG Certify the installation and operation of the girth gages. (3.2.1.6.2.3, Morton Thiokol-proposed SCN 3)
- BH Certify the installation and operation of the temperature devices. (3.2.1.6.2.3, Morton Thiokol-proposed SCN 3)
- BI Certify the installation and operation of the igniter chamber pressure transducer. (3.2.1.6.2.4.a, Addendum G)

- BJ Certify the calibration of the motor chamber pressure transducer. (3.2.1.6.2.4.b, Addendum G, ICD 3-44005, 4.3.4)
- BK Certify the forward field joint insulation temperature control. (3.2.1.8.1.1.a)
- BL Certify the compatibility of the leak tests of seals of field joints, nozzle-to-case joint, and igniter-to-case joint with joints insulations. (3.2.1.8.1.1.b)
- BL-1 The insulation shall ensure that system performance and structural integrity is maintained during the assembly process and operation. (3.2.1.8.1.1.c)
- BM Certify that the forward field joint insulation provides seal protection. (3.2.1.8.1.1.d)
- BN Certify the ability of the insulation to protect the forward case joint from thermal degradation during an ambient temperature full-duration motor burn. (3.2.1.8.1.1.e)
- BO Certify by inspection that the forward field joint insulation will withstand slag accumulation during motor operation. (3.2.1.8.1.1.g)
- BP Certify that the ballistic performance is not affected by the field joint, case-to-nozzle joint, and igniter-to-case joint insulation. (3.2.1.8.1.1.i)
- BQ Certify that the igniter insulation provides adequate thermal protection for the main igniter chamber and adapter metal parts. (3.2.1.8.3)
- BR Certify the ability of the field joint heater assembly to maintain the temperature of the field joints. (3.2.1.11.a)
- BS Certify the inert weight by inspection. (3.2.2.2.1)
- BT Certify the propellant weight by inspection. (3.2.2.2.2)
- BU Deleted
- BV Provide data for certification of the reliability of the RSRM design. (3.2.3)
- BW Certify that the primary structure, thermal protection and pressure vessels meet design safety factors. (3.2.3.1)
- BX Certify that the RSRM segments are capable of horizontal assembly/disassembly. (3.2.5.1)

- BY Certify that the electrical bonding meets the requirements of MIL-B-5087B. (3.3.5.2)
- BZ Certify the installation of low pressure transducer fairings (nonmetallic) and the triaxial accelerometer assembly mounting block (metallic) on the forward dome. (3.3.6.1.1, MSFC-HDBK-505A)
- CA Certify the case insulation minimum design thermal safety factor. (3.3.6.1.2.2)
- CB Certify the thermal design safety factor for the case insulation adjacent to metal part field joints and extending over factory joints. (3.3.6.1.2.3)
- CC Certify the case insulation sandwich construction region (aft and center segment aft end) design safety factor. (3.3.6.1.2.4)
- CD Certify the insulation performance. (3.3.6.1.2.6)
- CE Certify the nozzle design safety factors. (3.3.6.1.2.7)
- CF Certify by demonstration that the RSRM design minimizes the need for new on-plant logistics facilities, and that existing facilities and facility equipment are used for the storage of spares and maintenance functions to the maximum possible extent. (3.4.3)
- CG Certify that the outer boot ring (OBR) shows: 1) no evidence of hot gas erosion inside the flex boot cavity except that produced by the ventholes, and 2) that OBR hoop continuity exists through the beginning of motor pressure to tailoff.
--Delamination and wedgeout of 35-deg wrap acceptable
--Need not comply with CEI spec 3.2.1.4.13.b dealing with general wedgeouts
- CH Certify the function of the igniter heater. (3.2.1.5.3., SCN 42)

Developmental Objectives

- A Acquire engineering data for model validation.
B Evaluate the use of the 3-in-1 gage for data collection.
C Evaluate the nozzle Joint 2 bonding process change.
D Measure joint gap opening in the nozzle internal joints.

EXECUTIVE SUMMARY

3.1 SUMMARY

All of the objectives that can be addressed to date have been met. All inspection and instrumentation data indicate that the PV-1 static test firing was successful. Data were gathered at instrumented locations during pretest, test, and post-test operations. Dimensional measurements were taken before and after static testing to document insulation performance. The information assembled from the test procedures has supplied valuable knowledge and understanding about the performance of the RSRM design components utilized in PV-1.

3.1.1 Case Performance

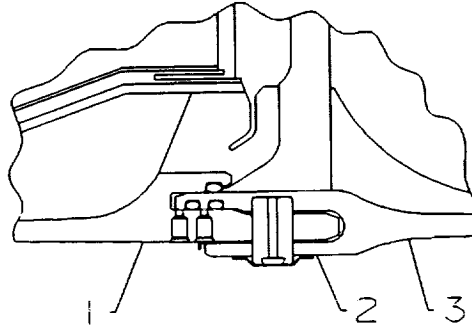
No anomalies associated with case or joint hardware occurred in the PV-1 static test. Assembly procedures proved adequate, and valuable motor structural response data were gathered during the test. Chamber pressure was contained, and joint gap openings were restrained well under the maximum allowable values. No local yielding was measured. TWR-17592, Volumes II and IV contain a complete discussion of case performance.

3.1.1.1 Field Joints. All results were as expected. The radial growth compared very closely to that on other static tests. The greatest value occurred on the center field joint, and had a value of 0.181 in. (Table 3.1.1.1-1). The gap opening for the center field joint was recorded as 0.008 in., which correlates closely with other tests. Biaxial strain gages were placed near the case-to-nozzle joint to measure local strains. The maximum calculated stress was found to be -47.0 ksi (Table 3.1.1.1-2).

3.1.2 Insulation Performance

3.1.2.1 External Evaluation. Post-test inspection revealed no anomalies related to the factory joint weather seal. There were no hotspots on the

Table 3.1.1.1-1. Field Joint Radial Growth Comparison to PV-1



Center Field Joint			Joint Pressure					848
LOCATION	GAGE	STRAIN		RADIAL GROWTH (Inches)				PRED
		PV-1	PV-1	QM-7	QM-6	DM-9	DM-8	
1	R304	BG	BG	ND	ND	0.161	0.167	0.158
2	S966*	2208	0.162	0.166	0.142	0.163	0.163	0.148
3	S635	2472	0.181	0.183	0.174	0.184	0.184	0.183

Aft Field Joint			Joint Pressure					838
LOCATION	GAGE	STRAIN		RADIAL GROWTH (Inches)				PRED.
		PV-1	PV-1	QM-7	QM-6	DM-9	DM-8	
1	R305	BG	BG	ND	0.158	0.160	0.166	0.152
2	S968*	2068	0.152	0.150	0.149	0.148	0.155	0.135
3	S686	2170	0.159	0.151	0.159	0.153	0.164	0.148

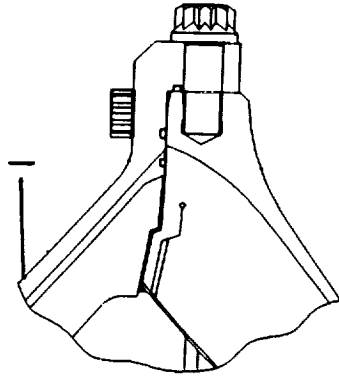
* PV-1, QM-7, QM-6, and DM-9 Locations are 1/3 Inch Aft of DM-8 Location.
 BG Bad Gage Before Test
 ND - No Data

ETA Ring

PV-1	360 degree
QM-7	360 degree
QM-6	360 degree
DM-9	360 degree
DM-8	270 degree
PRED	360 degree

Table 3.1.1.1-2. Fixed Housing Aft Dome Stress

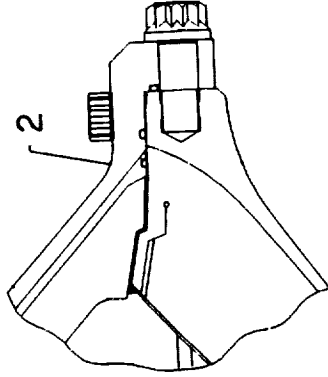
TEST NAME: PV-1 8-18-88
 JOINT: FIXED HOUSING, AFT DOME
 DESCRIPTION: NOZZLE / CASE BIAXIAL GAGES
 CORRECTED LOCAL PRESS: 819.1
 THE TIME RANGE IS 0.0 TO 180.0 SECONDS



LOCAT	ANGULAR LOCATION	HOOP GAGE	MERID GAGE	MAX CORRESPONDING		TEST DATA				ADJUSTED ANALYSIS			
				HOOP STRESS (KSI)	MERID STRESS (KSI)	HOOP STRAIN (UIN/IN)	MERID STRAIN (UIN/IN)	HOOP STRAIN (UIN/IN)	MERID STRAIN (UIN/IN)	%DIFF HOOP	%DIFF MERID		
1	0.0	R528	R527	-33.6	7.5	-1202	685	-979	627	-18.6	-8.6		
1	90.0	R530	R529	-30.7	8.9	-1116	626	-977	628	-12.4	0.3		
1	180.0	R532	R531	-32.6	9.1	-1176	665	-980	480	-16.7	-27.7		
1	270.0	R534	R533	-34.0	7.1	-1204	654	-979	628	-18.7	-4.0		
AVERAGE:				-32.7	8.2	-1175	657						

Table 3.1.1.1-2. Fixed Housing Aft Dome Stress (Cont)

TEST NAME: PV-1 8-18-88
 JOINT: FIXED HOUSING, AFT DOME
 DESCRIPTION: NOZZLE / CASE BIAXIAL GAGES
 CORRECTED LOCAL PRESS: 819.1
 THE TIME RANGE IS 0.0 TO 180.0 SECONDS



LOCAT	ANGULAR LOCATION	HOOP GAGE	MERID GAGE	MAX CORRESPONDING		TEST DATA		ADJUSTED ANALYSIS		%DIFF HOOP	%DIFF MERID
				STRESS (KSI)	HOOP STRESS (KSI)	HOOP STRAIN (UIN/IN)	MERID STRAIN (UIN/IN)	HOOP STRAIN (UIN/IN)	MERID STRAIN (UIN/IN)		
2	0.0	R520	R519	-38.1	26.5	1303	-1536	1206	-891	-7.5	-42.0
2	90.0	R522	R521	-35.2	33.8	1512	-1511	1210	-893	-19.9	-40.9
2	180.0	R524	R523	-31.1	31.4	1390	-1345	1206	-890	-13.2	-33.8
2	270.0	R526	R525	-47.0	25.8	1375	-1821	1209	-783	-12.1	-57.0
AVERAGE:				-37.9	29.4	1395	-1553				

external case. PV-1 slag weight was 1,497 lb. The external water deluge system operated correctly on PV-1, as did the CO₂ forward and aft end quench systems.

3.1.2.2 Case-to-Case Field Joints. Insulation performance in all three case-to-case field joints was excellent. In the unflawed forward case field joint, the joint bondline appeared to have made contact for the full circumference as evidenced by a postfire indication of adhesive contact. There was no evidence of circumferential flow or hot gas penetration (i.e., sooting and charring) into the joint beyond the nominal expected char and erosion. No damage to the capture feature, primary, or secondary O-rings was observed. The flawed center and aft case field joint insulation performance was excellent. No evidence of gas flow was identified within the joint bondline except as a result of the channel defects. The capture feature O-ring in the center field joint was eroded in the circumferential area surrounding the channel defect. The preliminary postfire condition of the intentional clevis and tang edge separations in the center field joint indicates that the separations had not grown from the installed prefire condition. The edges of the tang and clevis insulation were slightly charred and fragile. The flawed capture feature O-ring in the aft field joint was eroded through adjacent to the channel defect. No heat effect or erosion of the primary or secondary O-rings was identified in either of the flawed joints.

3.1.2.3 Case-to-Case Factory Joints. Disassembly and evaluation are not complete.

3.1.2.4 Case-to-Nozzle Joint. The case-to-nozzle joint had an intentional gas path to the wiper O-ring, allowing pressure to reach the flawed wiper O-ring. The pressure-assuring flaw through the polysulfide and the flawed wiper O-ring allowed chamber gas to reach the primary O-ring. Although the gas path was filled with char, no substantial erosion of the defect was evident. Two voids in the polysulfide forward of the step on each side of the precured polysulfide slabs which formed the gas path and two other voids within the polysulfide bondline were identified. None of the voids extended

across the entire bondline and none received hot gas. Two edge separations were installed at the aft dome insulation-to-case interface on each side of the intentional gas path. Preliminary results indicate the edge separations had not grown from the prefire condition.

3.1.2.5 Component Team Evaluation. The Insulation Component Program Team evaluation of observations will be presented in TWR-17592, Volume III. No critical, major, or minor anomalies were identified, but a potential anomaly that "remains observation" was identified (polysulfide voids).

TWR-17592, Volume III contains a detailed description of the insulation test results.

3.1.3 Seals Component/Leak Check Performance

3.1.3.1 Field Joints. There was no evidence of gas blowby past any non-flawed seal. The center field joint capture feature O-ring was eroded at the flaw location, with a 0.027-in. cross section remaining at the greatest eroded area, and still sealed. The aft field joint flawed capture feature O-ring was completely eroded through the cross section at the flaw location, but no soot was found past the interference fit, and no erosion or evidence of blowby was found to the primary O-ring. Pressure transducers confirm these findings.

3.1.3.2 Factory Joints. Disassembly and evaluation is not complete.

3.1.3.3 Case-to-Nozzle Joint. The flawed wiper O-ring was completely eroded through at the flaw location, with 0.006 in. of erosion measured on the primary O-ring at the flaw location with no evidence of soot or hot gas past the forward groove wall. Pressure transducers confirm these findings.

3.1.3.4 Igniter Joints. All gaskets (inner, outer, and S&A) performed with no signs of heat effect or sooting past the primary seals. All sealing surfaces were free of soot. The outer igniter gasket was in excellent condition on the forward dome and adapter sides of the putty flaw locations. The primary igniter gaskets revealed that no blowby or erosion had occurred. No corrosion or hardware damage was observed.

3.1.3.5 Exit Cone Field Joint (Joint 1). A blowhole was found on the exit cone field joint (Joint 1) through the room temperature vulcanizing (RTV) at 224 deg. Soot was found at 224 deg on the glass phenolic, but did not reach the primary O-ring. Inspection of the O-rings while in the grooves showed no damage, erosion, or heat effects. One scratch was found on the primary O-ring, and one scratch and one nick on the secondary O-ring. The nature of this damage indicates the cause to be installation disassembly clips. RTV was found up to the primary O-ring intermittently around the joint.

Heavy grease was found forward of the primary O-ring on the glass phenolic of the forward exit cone at 182 deg. The grease caused a terminating void in the RTV on the glass phenolic forward of the primary O-ring approximately 1.5 in. circumferentially by 0.1875 in. radially. A small streak of fluorescent green-colored grease was found on the steel of the forward exit cone next to the glass phenolic approximately 360 deg around the joint. A streak of black discolored grease was found on the steel on the forward exit cone across from the polysulfide on the aft exit cone intermittently 360 deg around the joint.

No corrosion was found.

3.1.3.6 Internal Nozzle Joints. Inspection of the forward end ring-to-nose inlet housing (Joint 2) revealed two major pressure paths through the RTV. Soot and sooted grease were present up to but not past the primary O-ring.

There were eight areas where pressure reached the primary seal at some point during the test firing on the forward exit cone-to-throat support housing (Joint 4). Some of the RTV voids were caused by grease being hydraulically forced up into the RTV bondline during joint assembly. It is believed that the other voids occurred at the time of the backfill operation.

No anomalies were found to the nose inlet housing-to-throat support housing (Joint 3). No damage was found during inspection of the primary and secondary O-rings out of the groove. Preliminary inspection of the sealing surface revealed no signs of damage. Excess grease was noted in the bottom of both O-ring grooves.

The intentional flaw on the fixed housing-to-aft end ring (Joint 5) allowed pressure to reach the primary O-ring. No evidence of soot or blowby past the primary O-ring was found. TWR-16416 documented evaluation of Joint 5. TWR-17592, Volume IV contains a complete discussion of seal performance.

3.1.3.7 Leak Test. Based on the success of current leak test procedures used on PV-1, QM-6, and QM-7, it is concluded that all leak tests currently performed on RSRM joints are certified for use on flight motors. TWR-17592, Volume IV contains a description of leak check procedure test results.

3.1.4 Nozzle Assembly Performance

3.1.4.1 Forward and Aft Exit Cones. PV-1 aft exit cone and forward exit cone liner erosion was nominal showing no major washing or pocketing. Minor surface ply lifting and minor wash areas were observed intermittently around the aft exit cone circumference, aft of the compliance ring. Maximum depth of the wash areas was 0.15 in. radially. Erosion forward of the compliance ring was smooth and uniform. Typical dimpled erosion (0.15-in. maximum radial depth) appeared on the forward 6 in. of the liner 360 deg circumferentially. The forward end of the liner appeared to be pulled away from the shell over a 1.5-ft arc centered at 160 deg. The aft exit cone liner was raised approximately 0.20 in. above the forward exit cone liner at this location.

The polysulfide groove fill on the aft exit cone forward end showed separations within the polysulfide. Locations and dimensions are presented in Figure 3.1.4.1-1. The maximum radial width of the separations was 0.10 inch. Post-test measurements of the polysulfide groove radial width showed that the groove was up to 0.11 in. wider than the nominal pretest size (Table 3.1.4.1-1), indicating that the liner pulled away from the shell during post-test cooldown. There were no subsurface voids.

The aft exit cone forward end showed glass-cloth phenolic (GCP)/carbon-cloth phenolic (CCP) separations intermittently around the circumference. The maximum separation was 0.22 inch. Table 3.1.4.1-2 lists the locations

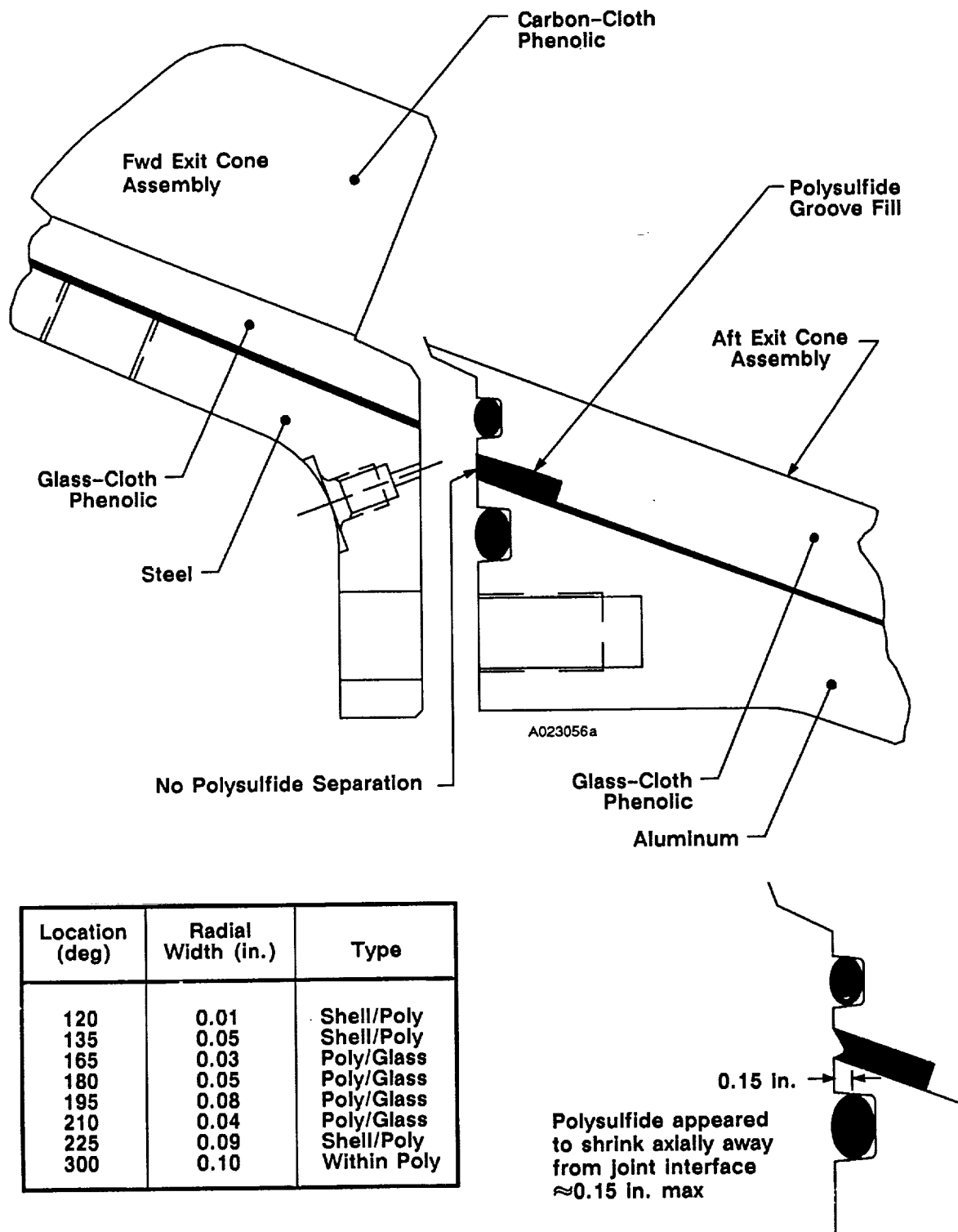
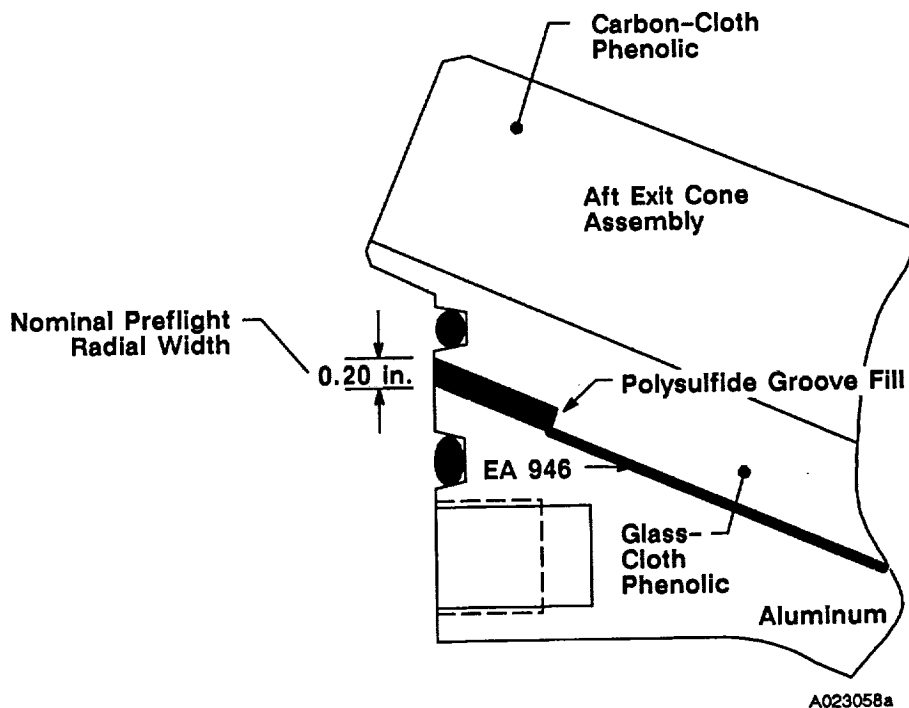
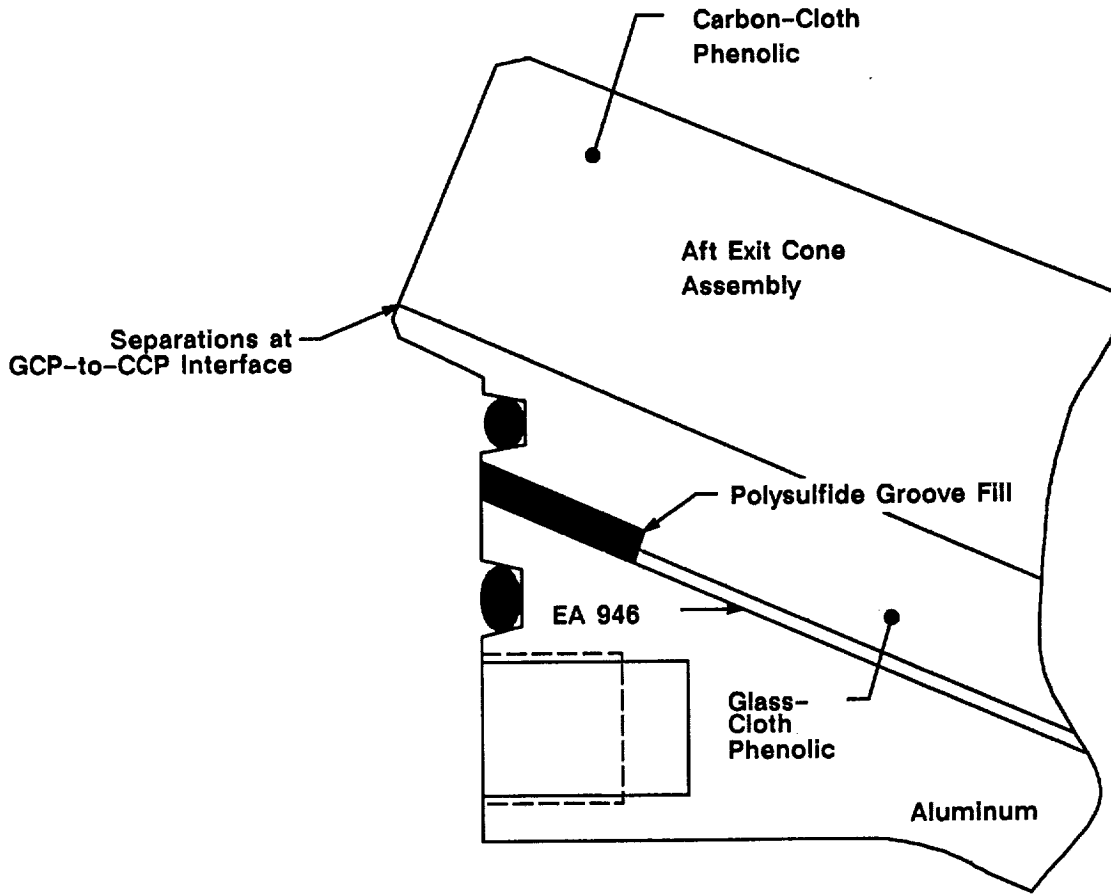


Figure 3.1.4.1-1. PV-1 Polysulfide Separations

Table 3.1.4.1-1. PV-1 Polysulfide Groove Fill Post-Test Radial Width Measurements

<u>Angular Location (deg)</u>	<u>Radial Width (in.)</u>
0	0.16
15	0.16
30	0.16
45	0.16
60	0.16
75	0.16
90	0.16
105	0.16
120	0.16
135	0.15
150	0.16
165	0.18
180	0.17
195	0.16
210	0.17
225	0.17
240	0.16
255	0.16
270	0.16
285	0.16
300	0.16
315	0.16
330	0.16
345	0.16





A018722a

Location (deg)	GCP/CCP Separation Radial Width (in.)
105	0.01
120	0.03
150	0.22
165	0.06
210	0.01
225	0.01
270	0.08
285	0.12

Table 3.1.4.1-2. PV-1 Aft Exit Cone Forward End Phenolic Separations

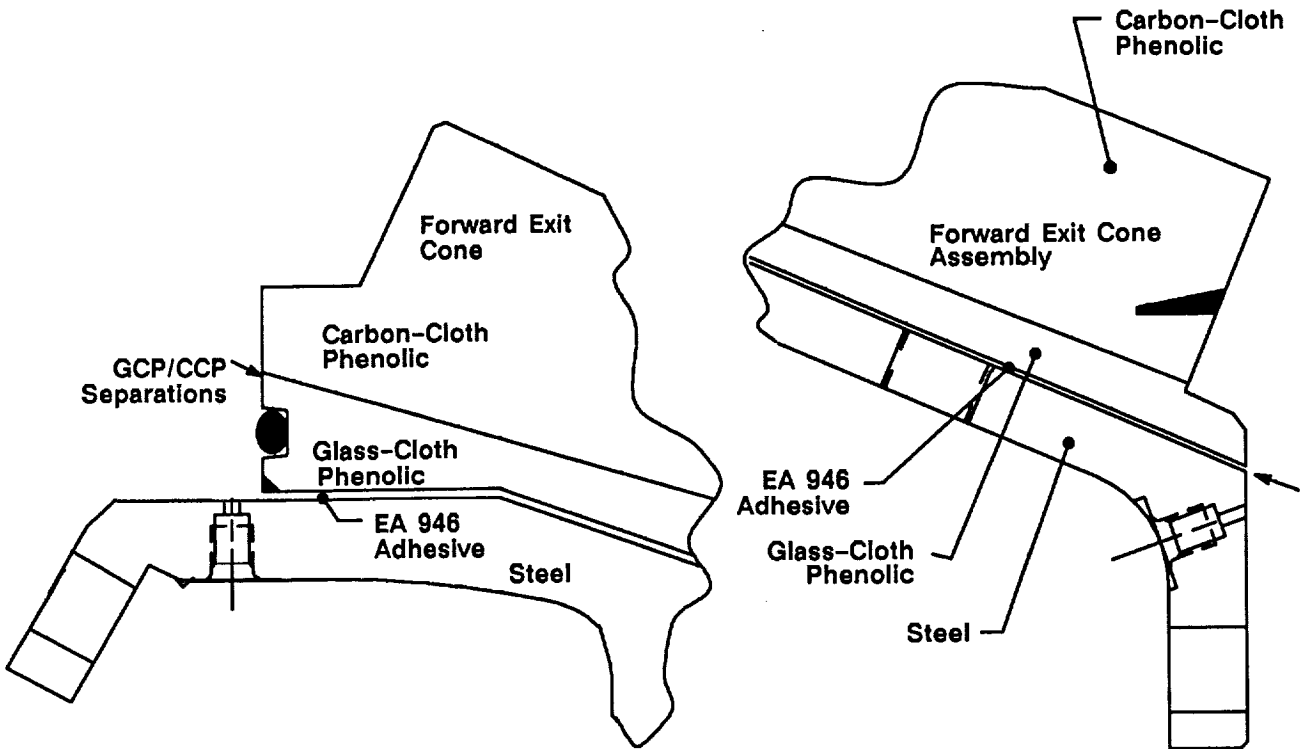
and dimensions of the separations. The forward exit cone aft end showed a bondline separation extending 360 deg circumferentially. The forward end of the forward exit cone showed bondline separations intermittently around the circumference which were a maximum of 0.07 in. wide radially. Table 3.1.4.1-3 lists the locations and dimensions of the separations. There were no signs of heat effect in or adjacent to any of the separations.

3.1.4.2 Throat Assembly. Erosion of the throat ring and throat inlet ring was smooth and uniform, typical of past motors. The aft end of the throat assembly showed intermittent bondline separations. The maximum radial width was 0.005 inch. Figure 3.1.4.2-1 lists the locations and dimensions of the separations.

3.1.4.3 Nose Inlet Assembly. All regions of the nose inlet assembly eroded smoothly, with no visible pockets or wash areas. The aft 2 in. of the nose cap showed popped-up charred CCP material intermittently around the part circumference (Figure 3.1.4.3-1). No wedgeouts were observed on the forward or aft ends of the nose cap. Bondline separations were observed on the nose cap aft end and also between the GCP and CCP intermittently around the circumference. Figure 3.1.4.3-2 lists the locations and dimensions of the separations.

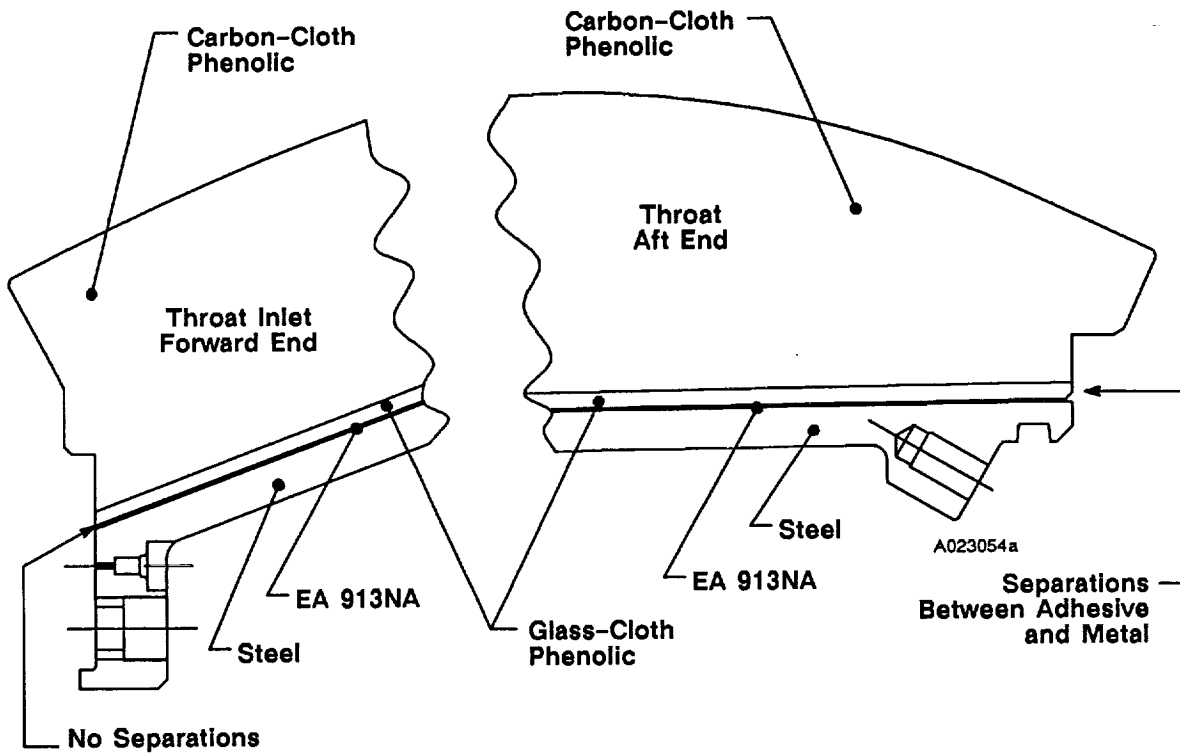
Post-test examination revealed that the forward nose ring was of the old HPM design configuration with the 150-deg ply angle. An investigation is underway to determine how the old design forward nose ring was mistakenly placed in an RSRM nose inlet assembly. The erosion of the forward nose ring and aft inlet ring was smooth and uniform. There were no wedgeouts or popped-up charred CCP material on either of the rings. A continuous bondline separation of 0.004 in. radial width was observed on the aft end of the -504 ring. This condition has been observed on previous post-test and postflight nozzles.

3.1.4.4 Cowl Ring. Erosion of the cowl ring was approximately 0.15 in. greater on the forward 4.5 in. of the ring. Popped-up charred CCP material was observed on the aft end of the cowl at 220 deg (Figure 3.1.4.4-1).



Forward End GCP/CCP Separations		Aft End Metal-to-Adhesive Bondline Separations		
Location (deg)	Radial Separation (in.)	Location (deg)	Radial Separation (in.)	Axial Length (in.)
0	0.05	0	0.05	>4
15	0.03	15	0.06	>4
30	0.05	30	0.07	>4
45	--	45	0.08	>4
60	0.05	60	0.08	>4
75	0.07	75	0.08	>4
90	0.03	90	0.07	>4
105	0.05	105	0.07	>4
120	0.03	120	0.07	>4
135	0.03	135	0.06	>4
150	0.04	150	0.06	>4
165	0.05	165	0.04	>4
180	0.05	180	0.04	>4
195	--	195	0.06	>4
210	0.02	210	0.06	>4
225	0.05	225	0.08	>4
240	0.02	240	0.08	>4
255	0.03	255	0.07	>4
270	--	270	0.04	>4
285	0.01	285	0.06	>4
300	--	300	0.07	>4
315	--	315	0.08	>4
330	0.02	330	0.06	>4
345	0.03	345	0.07	>4

Table 3.1.4.1-3. PV-1 Forward Exit Cone Bondline Separations



**Aft End
Metal-to-Adhesive
Bondline Separations**

Location (deg)	Radial Width (in.)
60	0.05
75	0.05
165	0.05
180	0.05
195	0.05

Figure 3.1.4.2-1. PV-1 Throat Assembly Bondline Separations

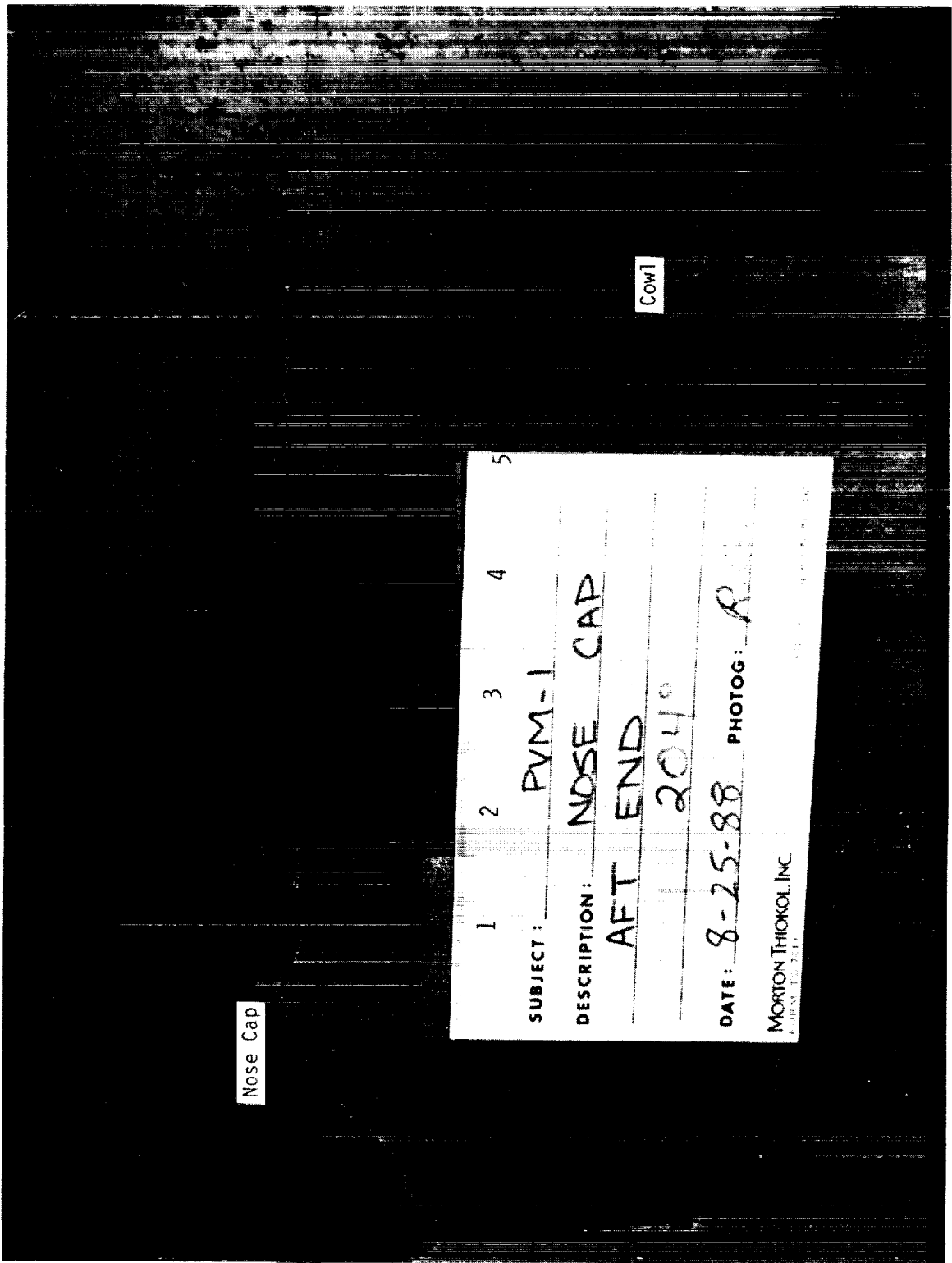
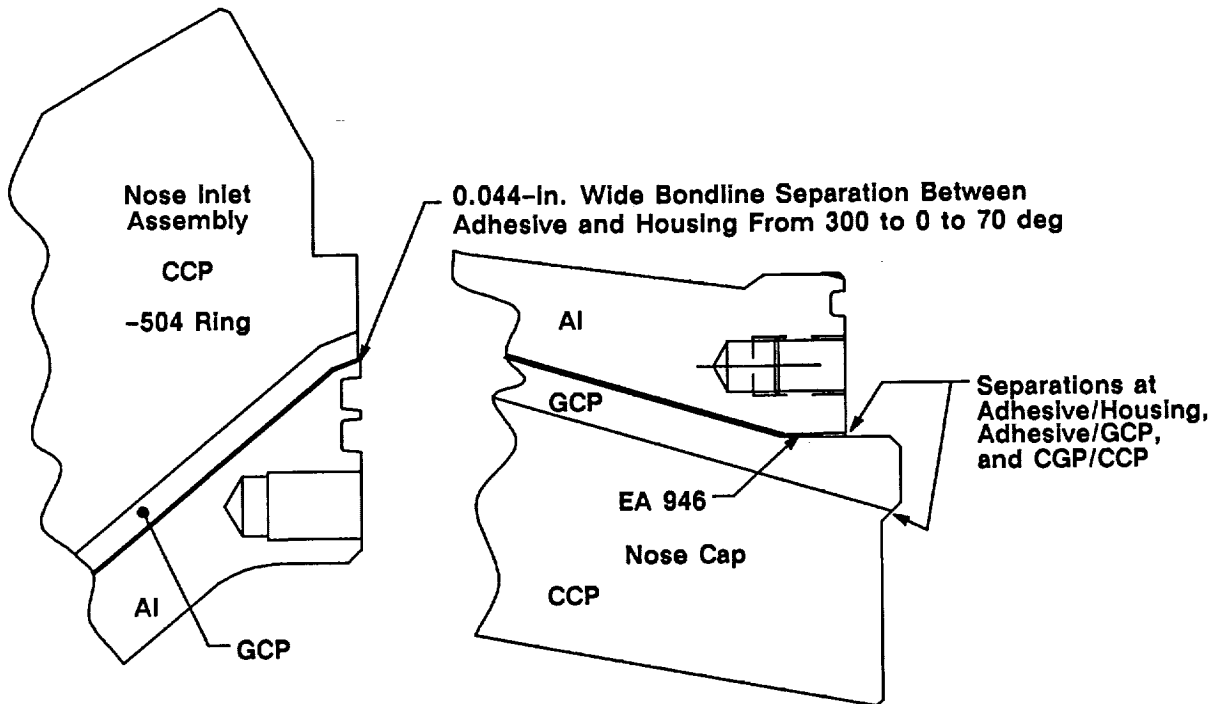


Figure 3.1.4.3-1. Nose Cap Aft End Popped-Up Charred Material (204 deg)

REVISION B ORIGINAL PAGE
BLACK AND WHITE PHOTOGRAPH

DOC NO. TWR-17592 | VOL
SEC | PAGE 52



Location (deg)	Nose Cap Aft End Radial Bondline Separation (in.)	Separation Type*
0	0.040	1
15	0.040	1
30	0.030	1
45	0.020	1
60	0.008	2
140	0.005	2
142	0.005	2
192-198	0.003	2
255	0.030	1
304	0.010	3
306-312	0.008	3

A023053a

- * Type 1 = GCP/CCP
- Type 2 = Adhesive/GCP
- Type 3 = Metal/Adhesive

Figure 3.1.4.3-2. PV-1 Nose Inlet Assembly Bondline Separations



Popped-Up Charred CCP

SUBJECT
DESCRIPTION
DATE
PHOTOG
MAY 1968

Figure 3.1.4.4-1. Cowl Aft End and Outer Boot Ring Forward End Popped-Up Charred Material

Cross-ply cracks isolated in charred CCP material extended axially through the ventholes. Unlike other motor nozzles, the shear pinholes extended only into the silica-cloth phenolic due to new assembly procedures. All cowl ventholes appeared plugged with slag (Figures 3.1.4.4-2 through 3.1.4.4-5). There were no bondline separations observed on the forward end of the cowl assembly.

3.1.4.5 Outer Boot Ring. The structural backup OBR was intact. Delaminations, attributed to two-sided heating and cooldown, were observed 360 deg circumferentially. Charred CCP material on the aft tip fractured and popped up over a majority of the circumference, but there was no missing material. Popped-up charred CCP material was also located on the forward 1.5 in. of the OBR at 216 deg. Both of these conditions have been observed on previous post-test and postflight nozzles and have been shown to occur after motor operation. The flow surface bondline gap between the OBR and cowl ring was 0.20 in., which is typical of past static test and flight nozzles. The cavity side of the flex boot showed no evidence of flow or erosion.

3.1.4.6 Fixed Housing Insulation. Erosion was smooth and uniform and appeared typical of previous motors. There were no bondline separations located on the aft or forward ends of the fixed housing assembly.

3.1.4.7 Nozzle Plug. There was no nozzle plug installed in the PV-1 nozzle.

3.1.4.8 Nozzle Internal Joints. Post-test subassembly flow surface gaps are shown in Figure 3.1.4.8-1.

3.1.4.8.1 Aft Exit Cone/Forward Exit Cone Field Joint. A blowpath approximately 0.15 in. wide circumferentially extended from the flow surface, through the RTV, to an unfilled void area located at 224 deg (Figures 3.1.4.8.1-1 and 3.1.4.8.1-2). The GCP of the aft and forward exit cone was lightly sooted at the blowpath location, but was not heat affected. Soot did not reach the primary O-ring. The primary O-ring saw pressure, but showed no signs of blowby, erosion, or heat effect. There was no metal damage observed.

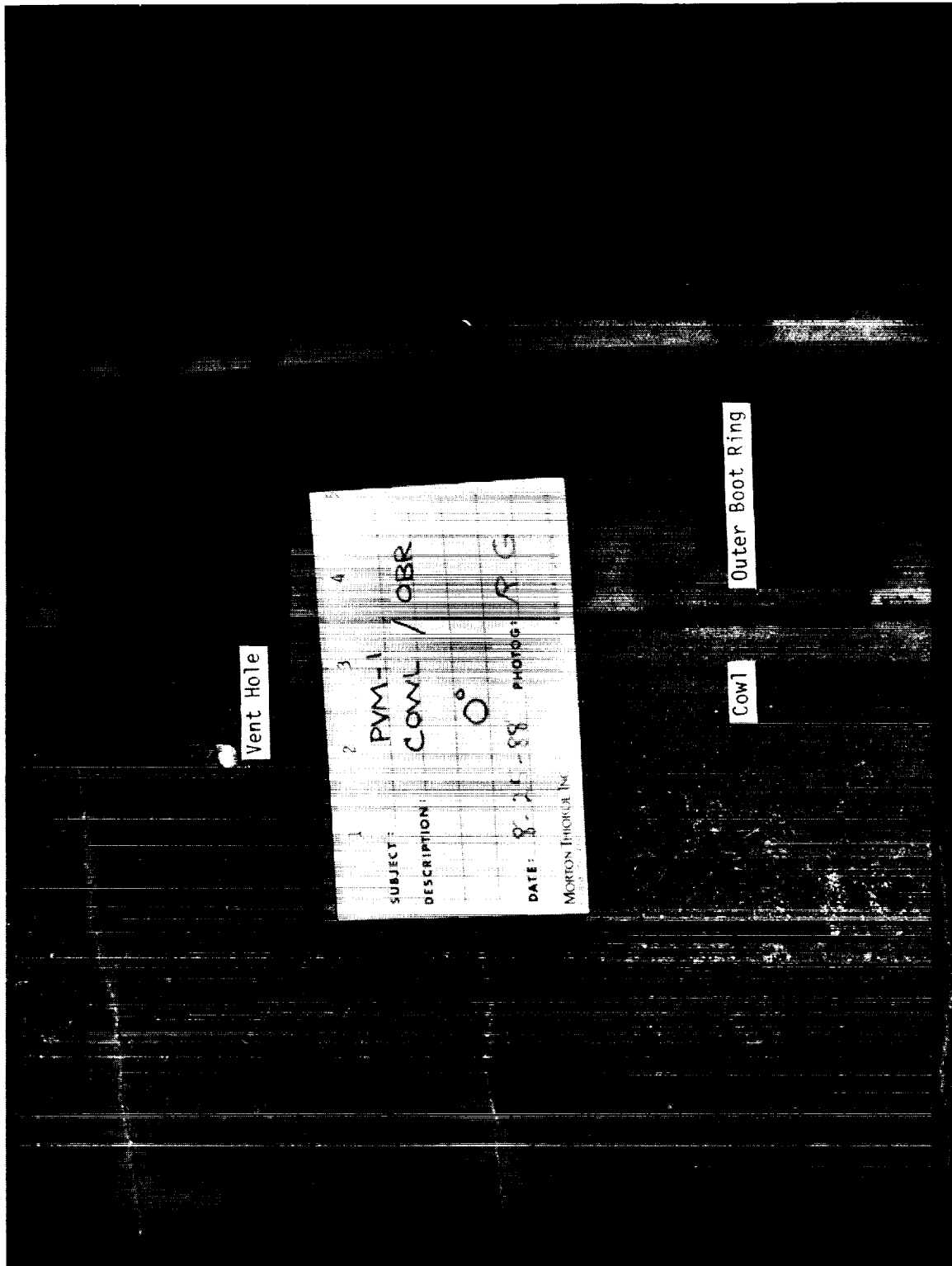


Figure 3.1.4.4-2. PV-1 Cowl/Outer Boot Ring (0 deg)

REVISION B

ORIGINAL PAGE
BLACK AND WHITE PHOTOGRAPH

DOC NO.	TWR-17592	VOL	
SEC		PAGE	56

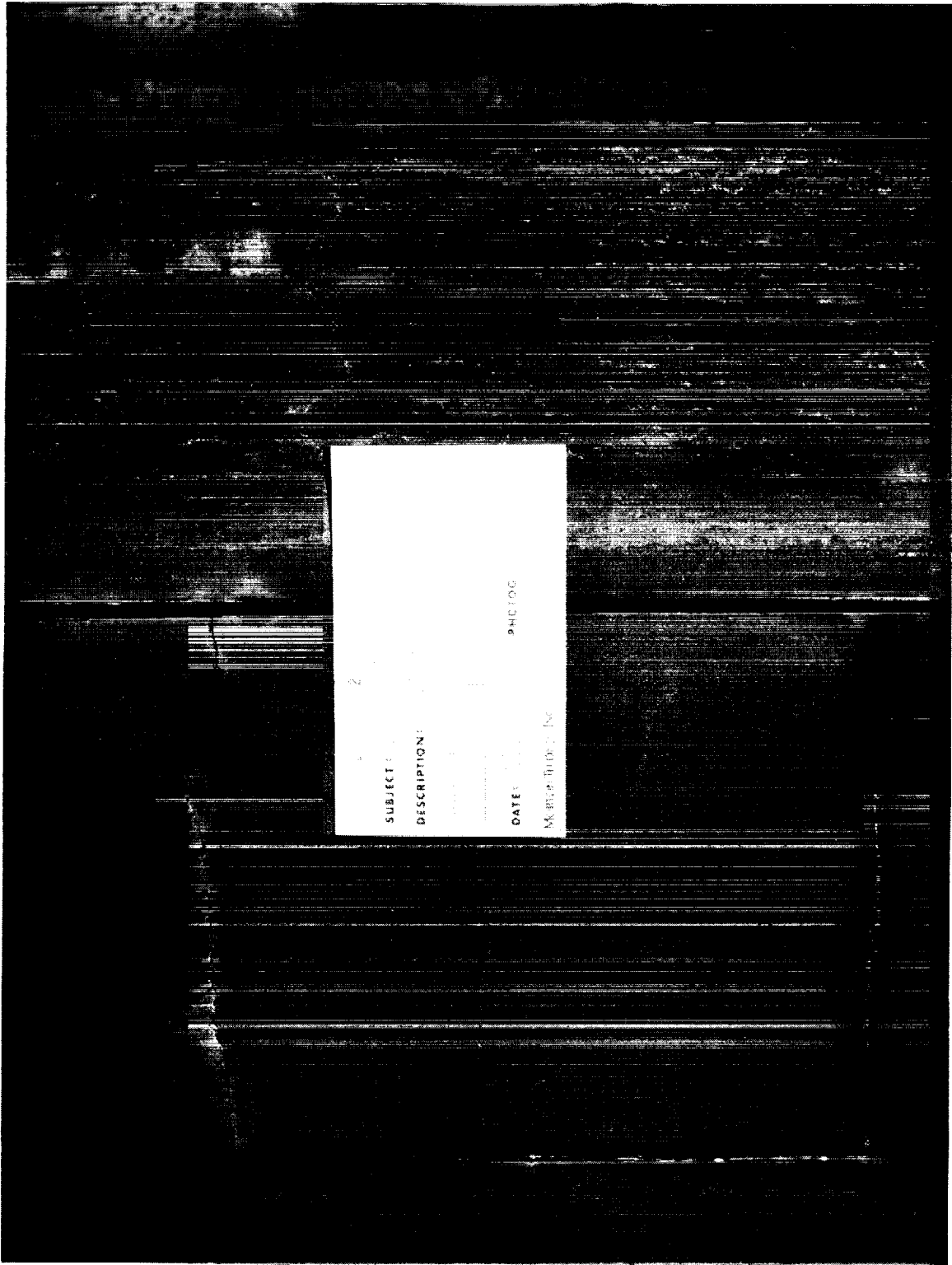


Figure 3.1.4.4-3. PV-1 Cowl/Outer Boot Ring (100 deg)

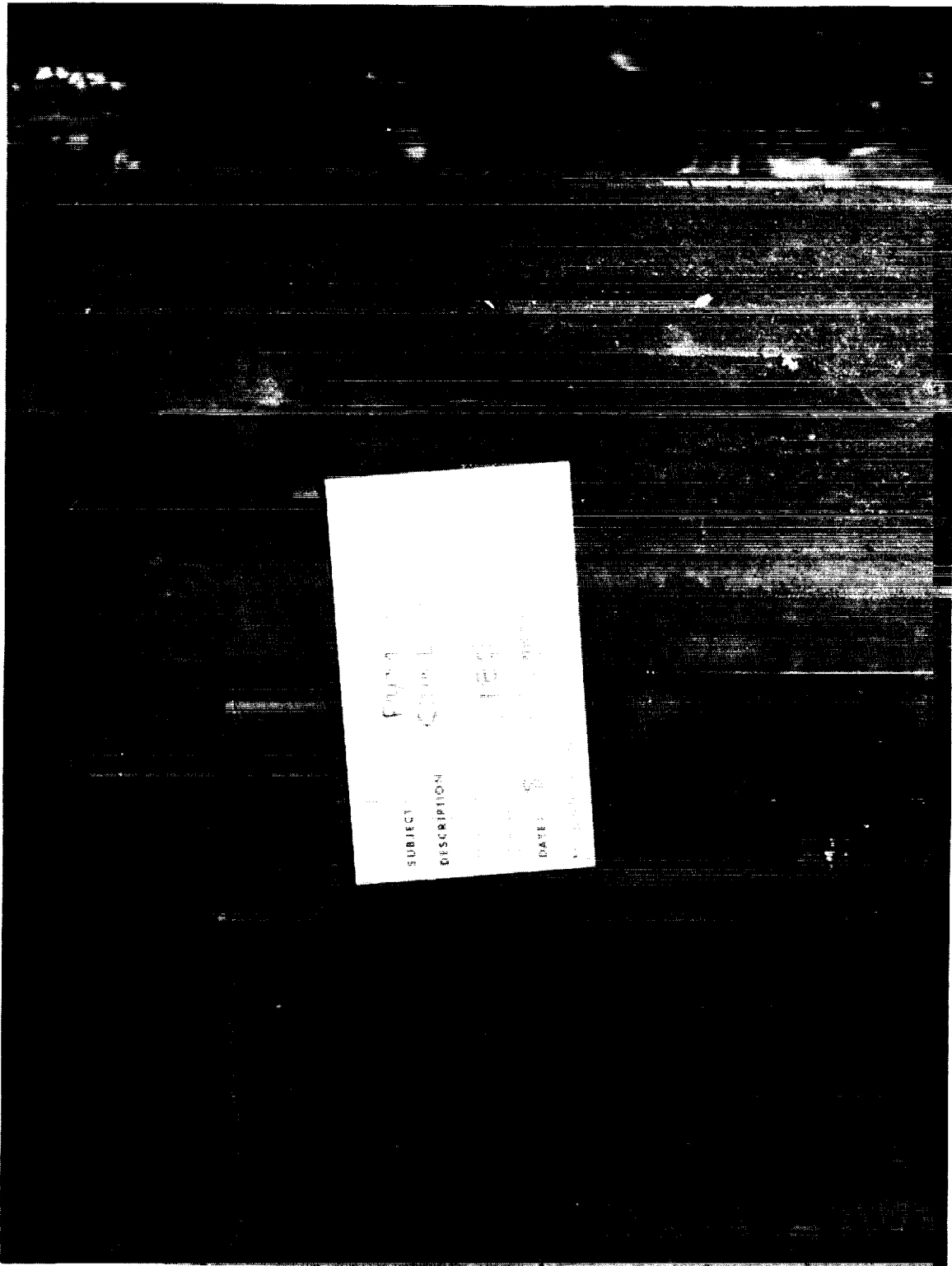


Figure 3.1.4.4-4. PV-1 Cowl/Outer Boot Ring (180 deg)

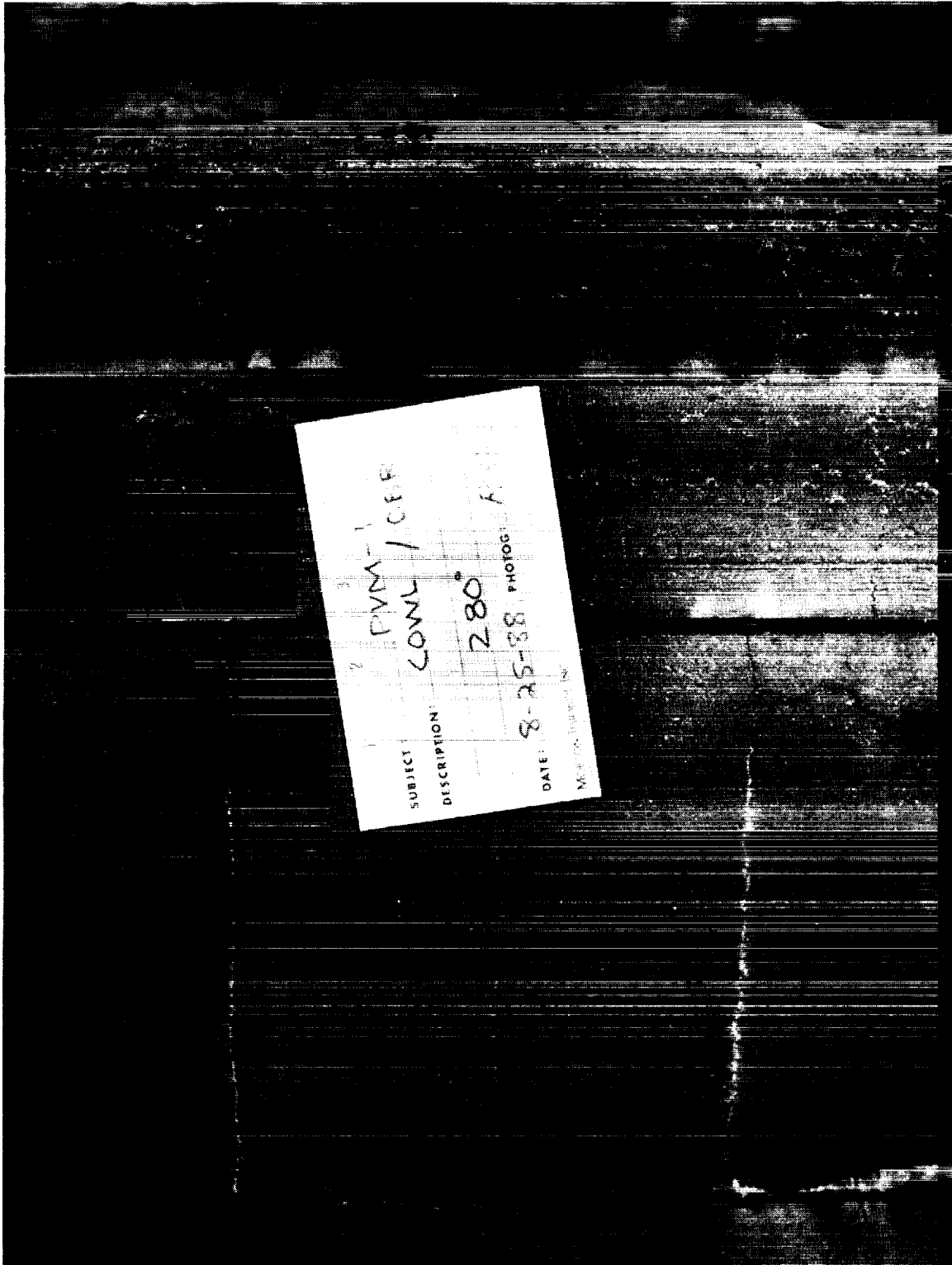


Figure 3.1.4.4-5. PV-1 Cowl/Outer Boot Ring (280 deg)

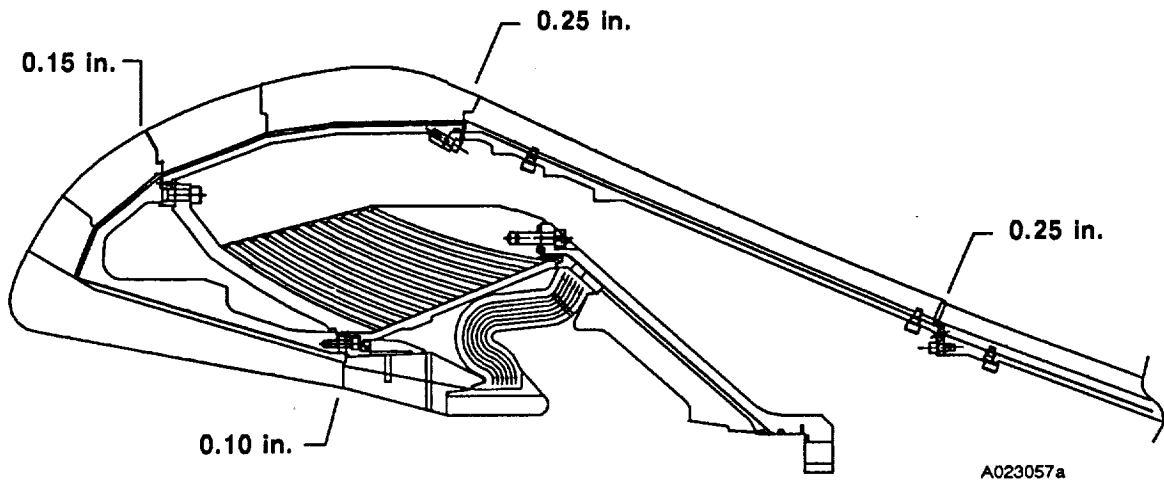


Figure 3.1.4.8-1. PV-1 Joint Flow Surface Gap Openings

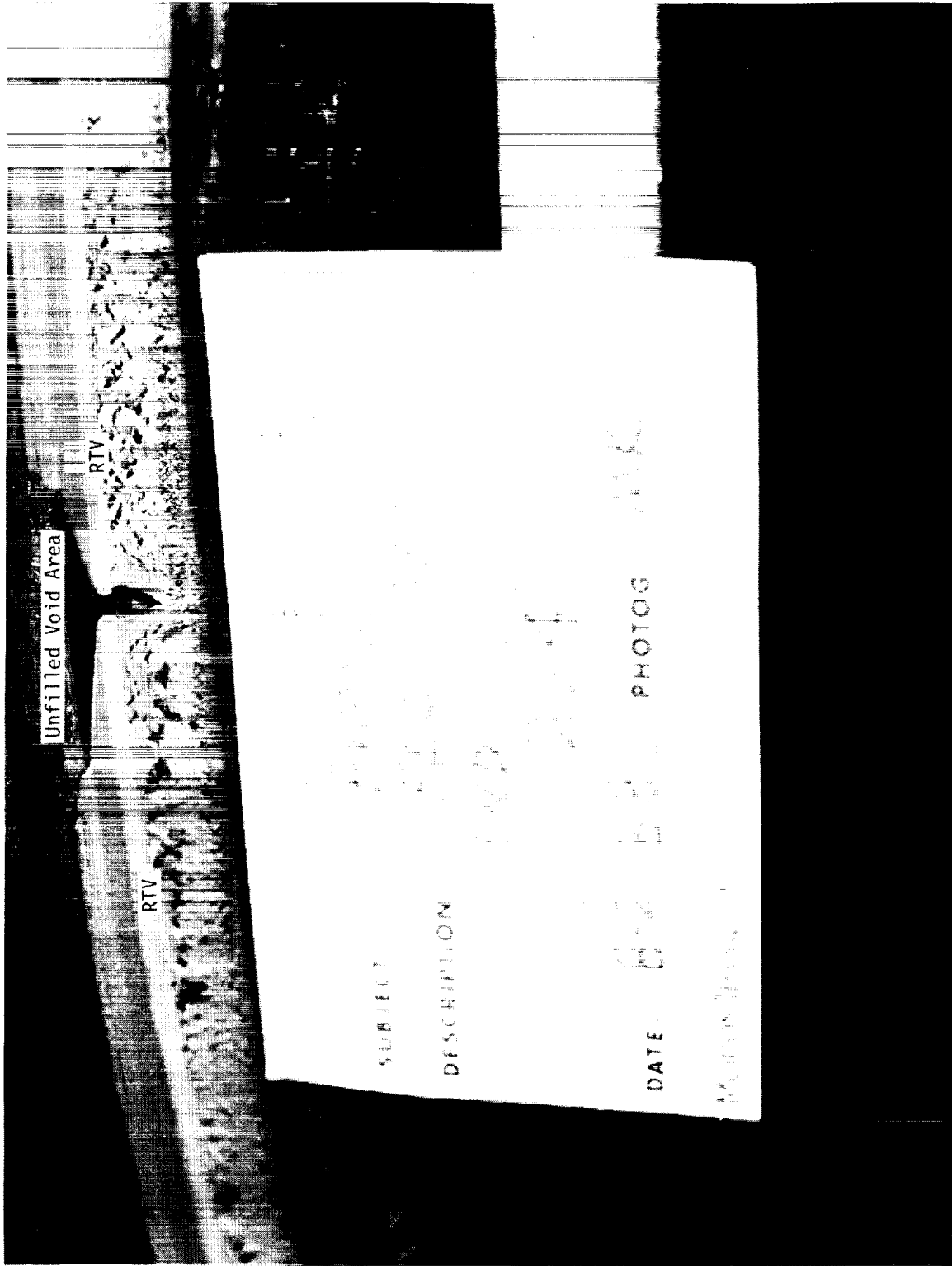


Figure 3.1.4.8.1-1. PV-1 Blowpath in Aft Exit Cone Field Joint (224 deg)

REVISION B

DOC NO. TWR-17592
SEC

VOL

PAGE

61

ORIGINAL PAGE
BLACK AND WHITE PHOTOGRAPH

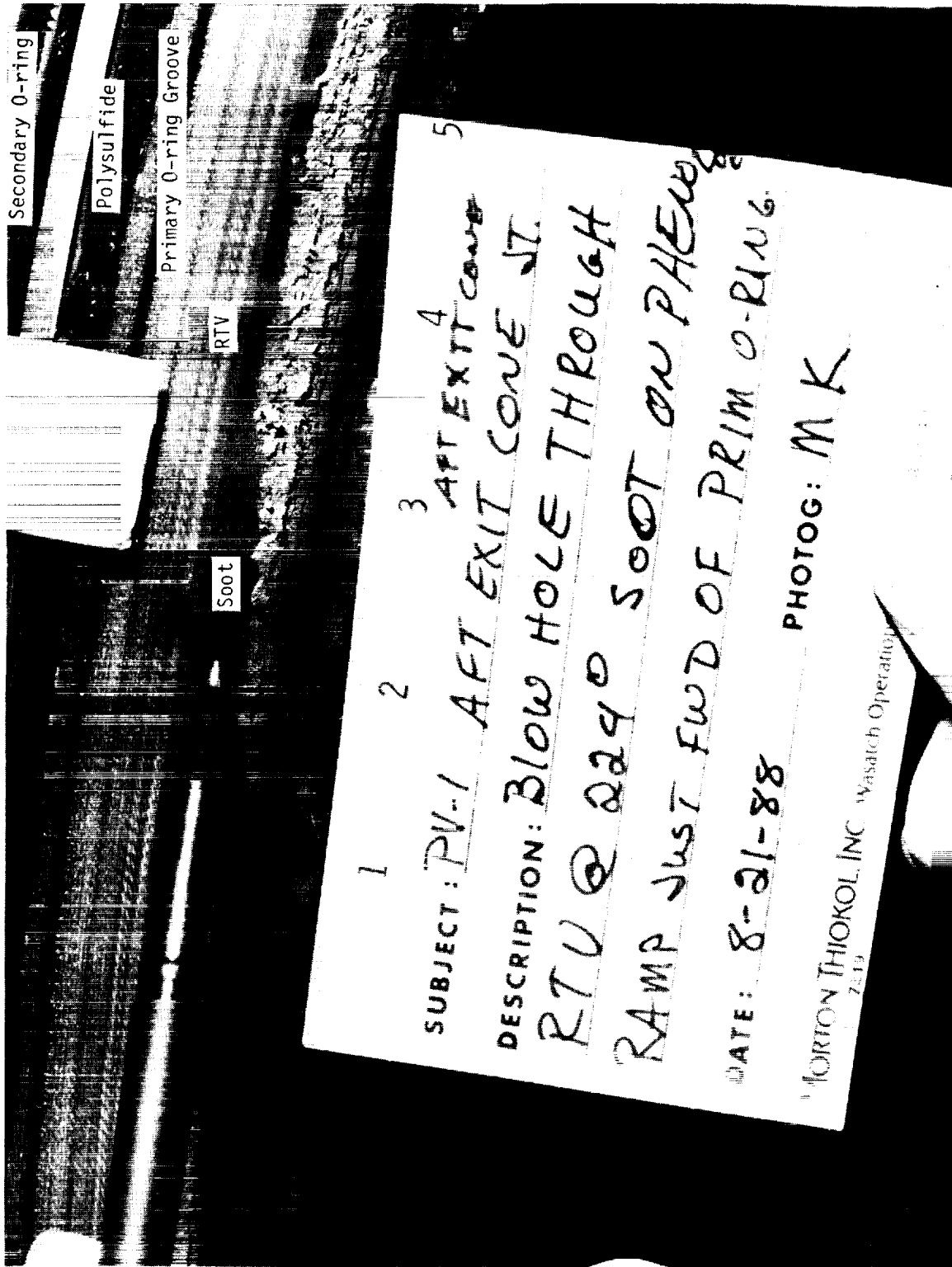


Figure 3.1.4.8.1-2. PV-1 Blowpath in Aft Exit Cone Field Joint (224 deg)

3.1.4.8.2 Throat Inlet/Forward Exit Cone Joint. The RTV backfill of the forward exit cone/throat nozzle joint did not extend below the joint char line at the 45-, 50-, 65-, 75-, 100-, 195-, 225-, and 262.5-deg locations. Soot was observed at these unfilled areas indicating pressure reached the primary O-ring, although it showed no evidence of blowby, erosion, or heat effect. There was no sign of heat-affected CCP or GCP below the joint char line and no metal damage observed in this joint.

3.1.4.8.3 Nose Inlet/Throat Joint. The backfilled RTV extended below the joint char line 360 deg circumferentially. RTV extended along the radial inside diameter (ID) bondline intermittently around the circumference and along the axial bondline. There were no voids or blowpaths observed in the RTV, and the joint was free of soot. There was no metal damage observed.

3.1.4.8.4 Nose Inlet/Bearing Forward End Ring/Cowl Joint. The PV-1 nozzle was the first to incorporate the RTV backfill on the nose inlet/bearing forward end ring/cowl joint. The RTV backfill appeared to extend below the joint char line 360 deg circumferentially and reached the GCP intermittently. Blowpaths, the largest one measuring 0.88 in. wide circumferentially, extended from the flame surface through the RTV to the unfilled void areas. The paint on the bearing forward end ring flange outside diameter (OD) surface was blistered, indicating heat effect. Soot also reached the nose inlet housing aft end axial boltholes over most of the circumference. The primary O-ring saw pressure, but showed no signs of blowby, erosion, or heat effect. The nose cap GCP and the cowl silica-cloth phenolic insulators in line with the largest blowpath were heat affected.

3.1.4.8.5 Fixed Housing/Bearing Aft End Ring Joint. RTV filled the radial portion of the fixed housing/bearing aft end ring joint circumferentially except at the intentional flaw location from 253 to 268 deg. Soot was observed on the radial portion and on the aft 0.25 in. of the axial portion of the bondline at the flaw location. Soot did not extend to the steel bearing aft end ring and primary O-ring. The primary O-ring saw pressure but showed no signs of blowby, erosion, or heat effect. The remainder of the joint circumference showed no blowpaths or soot. Small isolated voids were

observed within the radial portion of the bondline intermittently around the circumference. There was no metal damage observed in the joint.

3.1.4.9 Flex Bearing Performance. Evaluation is not complete.

3.1.4.10 Nozzle Thrust Vector Control Performance. The TVC system appears to have performed as planned and followed the specified duty cycle well.

3.1.4.11 Nozzle Composite Structures Performance. The structural integrity of the nozzle was verified; the instrumentation data demonstrated positive safety margins at all locations measured. In general, predicted strains correlated fairly well with measured values. Nozzle strains are generally low. Excluding the counterbore region at the forward end of the fixed housing, strain magnitudes are less than 2,000 $\mu\text{in./inch}$. Several strain plots in the nose inlet housing region exhibited strain aberrations at about the 14-sec time slice. Most noticeable are the axial components at Location 5, and the hoop and axial components at Location 7, near the aft end of the nose inlet housing. Other gages demonstrating responses of a lower magnitude at this time slice include hoop longwire gages at Locations J6 and J7 (Joint No. 2 proximity gages), J9 and J10 (Joint No. 3), and Location 9. An investigation of the cause of this event is currently being conducted. Despite these unexpected changes in strain magnitude, peak strains remained relatively low (less than 2,000 $\mu\text{in./in.}$), indicating metal part margins of safety were well above zero. Hoop strains tend to follow the pressure trace, and most strain predictions match test results well.

Strain and deflection measurements in all five internal nozzle joint regions supported analysis predictions that all sealing surfaces either closed or opened less than 2 mil. Note that this was the case of Joint 5 with a pressure-assuring flaw to the primary seal.

Bondline separation gages located in the forward and aft exit cone shear pinholes indicated no bond gap separations during static firing. TWR-17592, Volume V contains a detailed description of nozzle/flex bearing/ composite structures/TVC test results.

3.1.5 Igniter Performance

The RSRM ignition system is a forward end, internally mounted, solid rocket-type igniter which is 47.5 in. long and contains approximately 132 lb of TP-H1178 propellant (Figure 3.1.5-1). The PV-1 igniter had two intentional putty flaws located in the igniter adapter-to-forward dome joint. The flaws were located at 0 and 80 deg. Postfire inspection revealed no anomalies associated with the putty flaws. Postfire inspection of the S&A device (Figure 3.1.5-2) showed the system performed as predicted with no anomalies. A detailed description of the PV-1 igniter performance will be in TWR-17592, Volume VI.

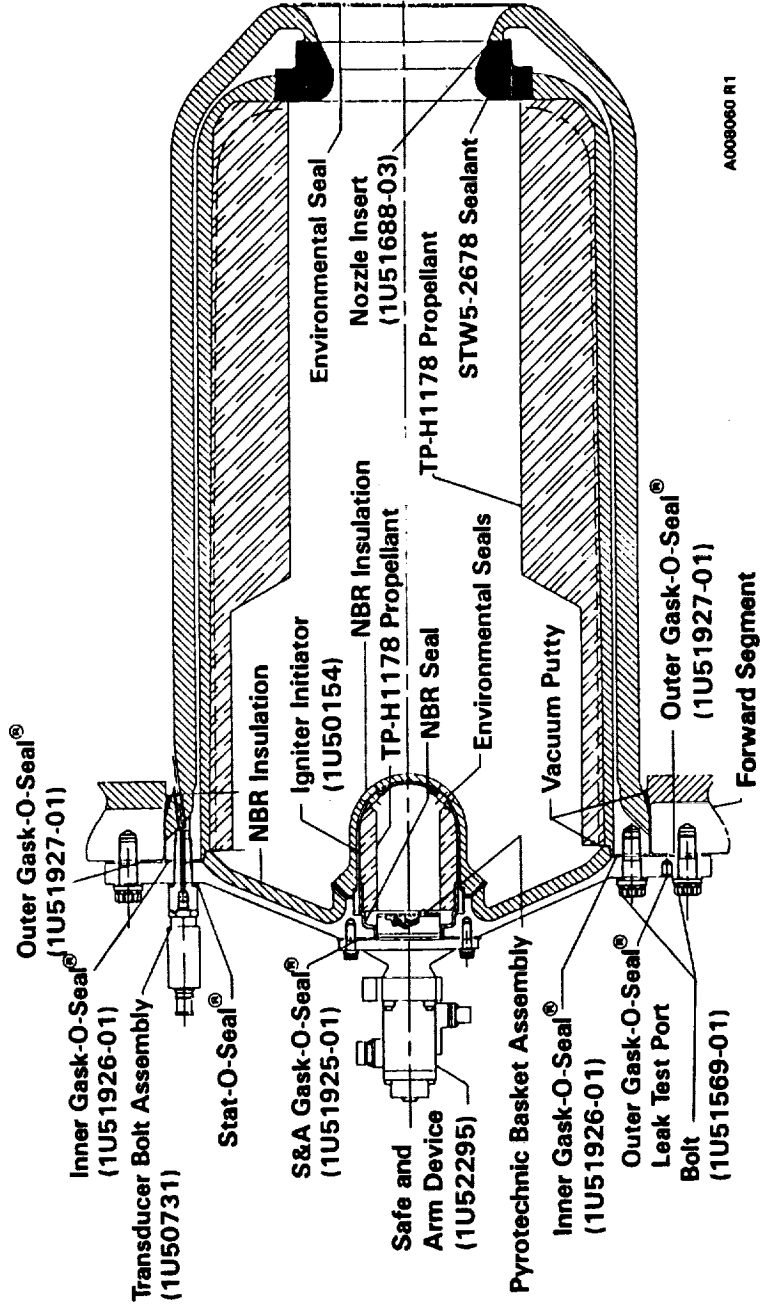
3.1.5.1 Igniter Heater Performance. The igniter heater, used to condition the igniter inner, outer, and S&A gasket rubber seals within temperature requirements, consists of a 430-W flexible strip heater which wraps around the igniter adapter flange. Thick cork (0.25-in.) is wrapped around the heater, and the heater and cork are secured in place with a steel T-bolt latch band clamp. The heater performed as required until building rollaway when one temperature sensor dropped from 128° to 115°F as a result of convective cooling.

One anomaly for the igniter heater was noted. The heater buckled off the surface of the igniter adapter in two places, which caused two hot spots on the heater and resulted in charred heater insulation in those areas. Testing of the heater subsequently showed no degradation of insulation resistance, dielectric withstanding voltage, or continuity.

3.1.6 JPS/Factory Joint Weatherseal Performance

3.1.6.1 JPS. The simplified field joint protection system for PV-1 consisted of heaters and sensors only. These were covered with a 0.25-in. thick strip of cork (Figure 1.2.6-1). The cork was held in place over the heaters and sensors by a single Kevlar bond. The moisture seal and cork insulation were not installed on this motor.

The heater performed as designed. There were no anomalies.



A008080 R1

Figure 3.1.5-1. RSRM Ignition System

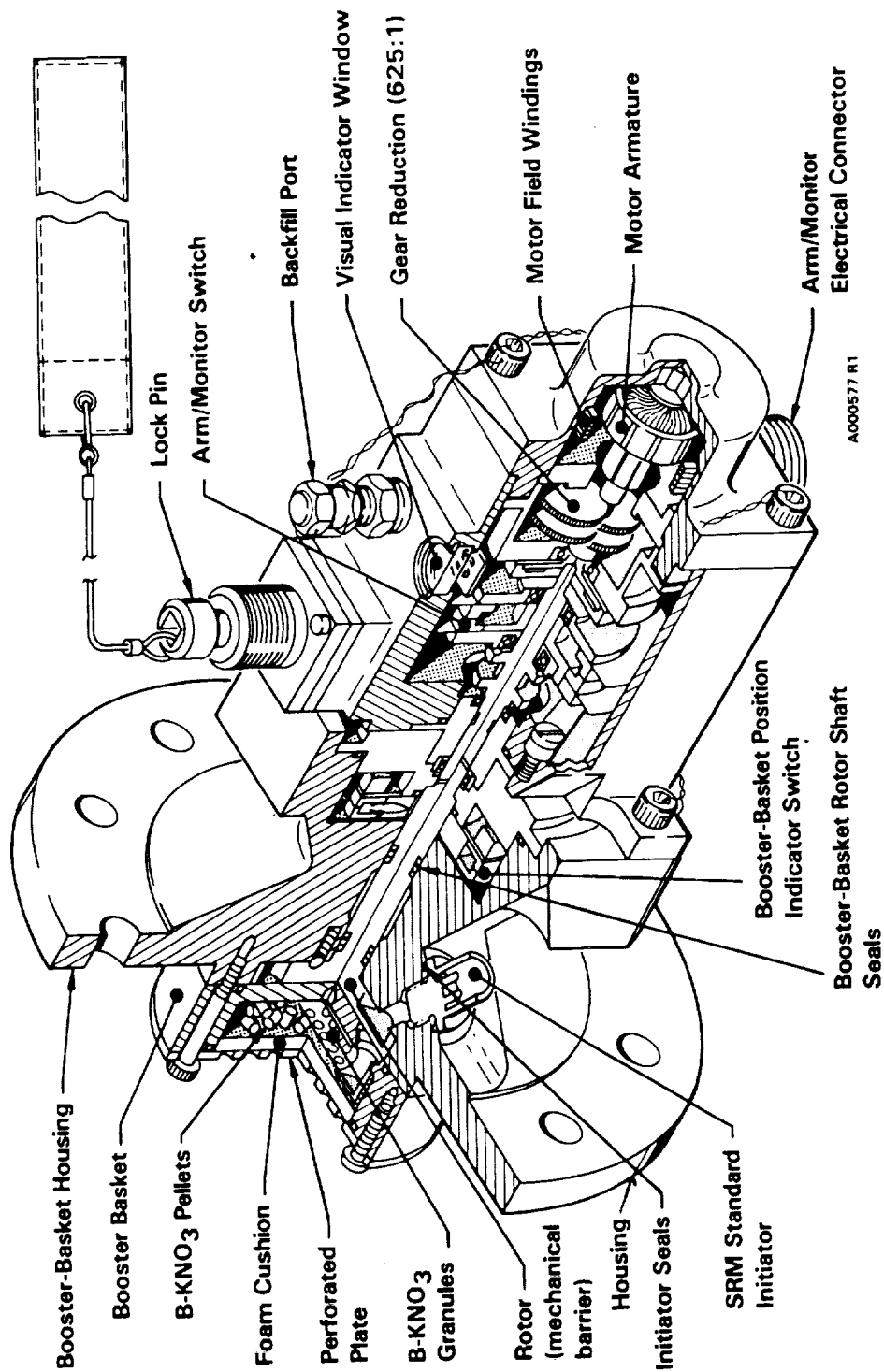


Figure 3.1.5-2. Safety and Arming Device Configuration

Field joint heaters maintained the temperature at the controlling resistance temperature detector at or above 100°F, and maintained this temperature with a maximum deviation of -0.1° and +0.4°F.

Figure 3.1.6.1-1 is a plot of the temperature at the controlling RTDs of the three joints. The drop in temperature at 1000 hr is due to heater power shut off during the dry run.

Figure 3.1.6.1-2 is an expanded plot of the controlling RTD temperature. The maximum deviation in temperature was -0.1° and +0.4°F.

Figure 3.1.6.1-3 is a plot of the minimum differential temperatures of the three joints. The maximum of 18.8°F occurred on the aft joint at 1240 hr, when the last data were recorded.

3.1.7 Systems Tunnel

There was no systems tunnel on PV-1 per the Redesign Program Review Board directive.

3.1.8 Instrumentation

All instrumentation-related test objectives were met. Instrumentation performed well with only a few exceptions. A detailed discussion is included in Section 5 of this volume.

3.1.9 Ground Support Equipment

All ground support equipment (GSE) used on PV-1 is discussed in the applicable component volume of TWR-17592.

3.1.10 Loads and Environments

The PV-1 static test was completed successfully with case line loads much lower than those experienced in the lift-off phase of flight, which is the highest load phase. The stresses experienced by the nozzle actuator bracket were calculated and found to be far lower than the yield stress of the bracket material.

3.1.11 Ballistics/Mass Properties Performance

The PV-1 ballistic performance was typical and within expected limits. The intentional flaws in the joints and the insulation had no noticeable affect

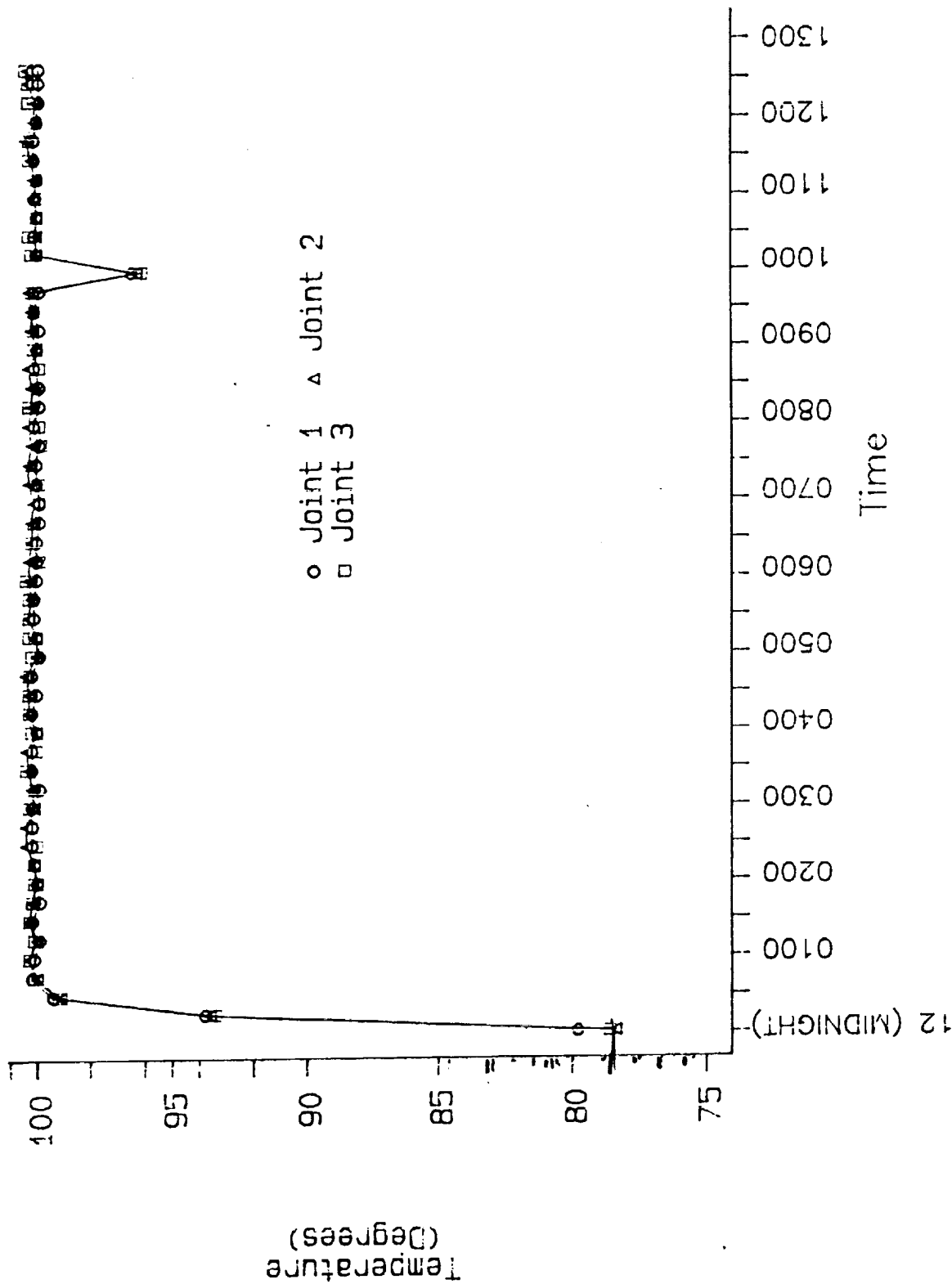


Figure 3.1.6.1-1. Temperature at Controlling RTDs of Joints 1, 2, and 3

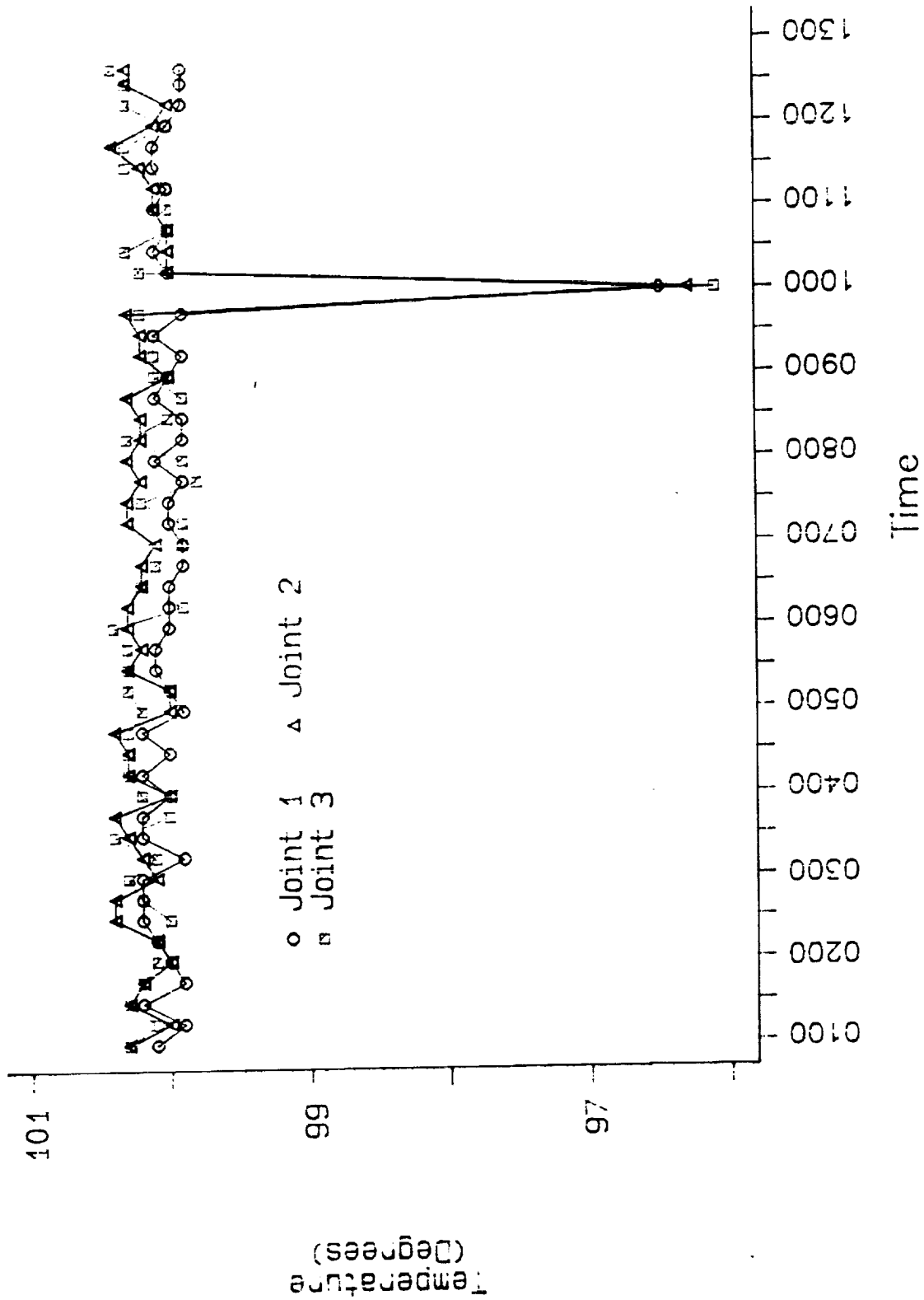


Figure 3.1.6.1-2. Expanded Plot of Temperatures at Controlling RTDs for Joints 1, 2, and 3

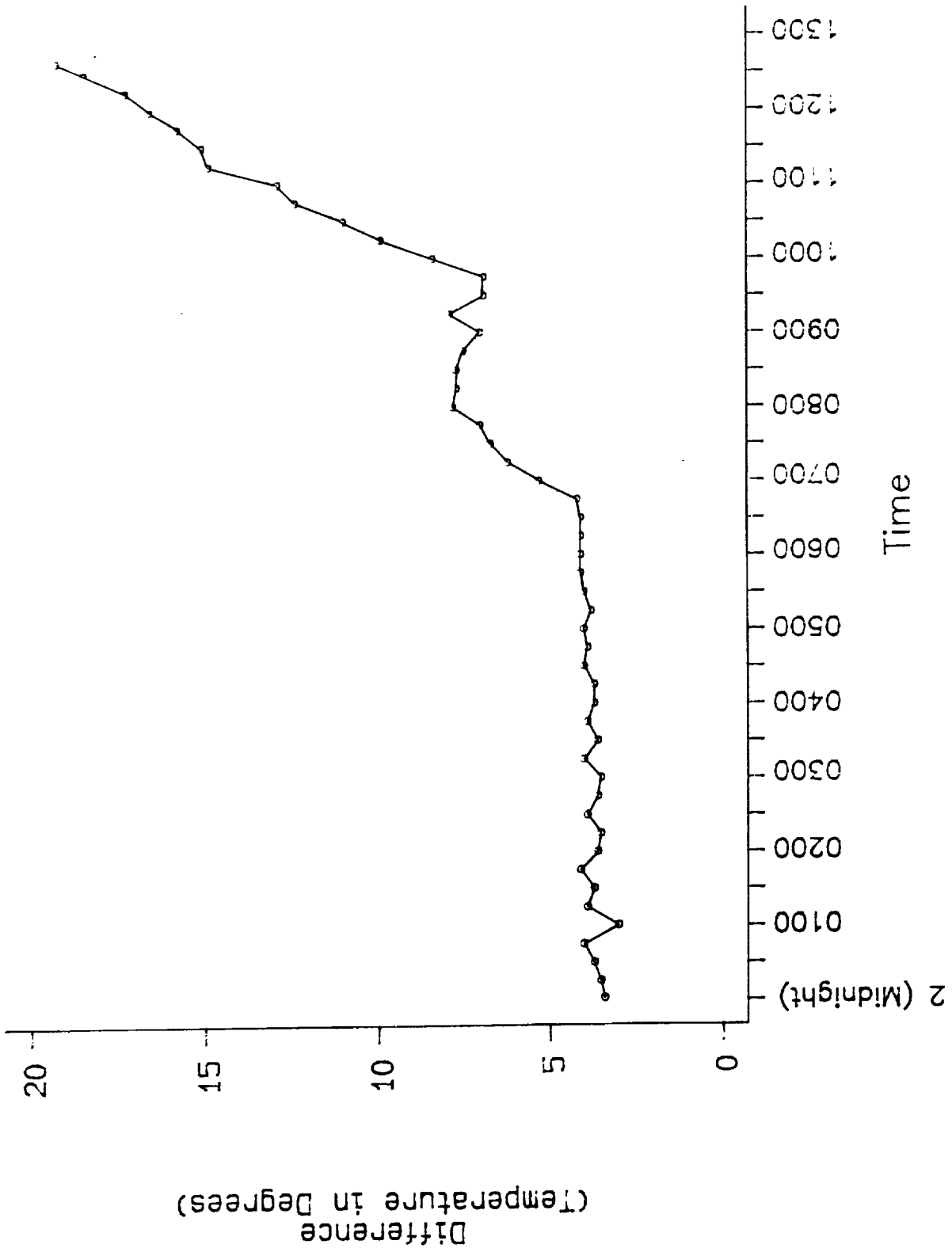


Figure 3.1.6.1-3. Minimum Differential Temperature of Joints 1, 2, and 3

on the performance of the motor. The new forward segment transition block could not be linked with abnormal gas flow or pressure disturbances. Ignition interval and pressure rise rate limits were met. Impulse gates were met. The PV-1 ballistic performance compared closely with QM-7, QM-6, DM-9, and DM-8 performance and HPM historical data. Table 3.1.11-1 lists the predicted and reconstructed values for the performance of PV-1 against the CPW1-3600 specification Table 2 values. All the values were within the limits. Figures 3.1.11-1 and 3.1.11-2 shows the predicted values versus the measured head end pressure and vacuum thrust values, respectively.

I_{sp} continues to be higher than the original HPM baseline value. I_{sp} as well as the thrust time envelope baselines need to be updated with measured increase in specific impulse (I_{sp}). PV-1 slag accumulation theory associated with the AP particle size distribution needs to be further investigated. The modified igniter performed successfully and as predicted.

The PV-1 motor exhibited chamber pressure oscillation similar to previously tested Space Shuttle RSRMs, particularly the QM-7 motor. The first longitudinal (1-L) mode oscillations experienced by PV-1 were the strongest ever measured by an ac coupled transducer in a Space Shuttle motor. The data from the dynamic pressure gage which provided oscillatory head end chamber pressure is displayed in waterfall plot format in Figure 3.1.11-3. A possible cause for the increased oscillations from HPM to RSRM is the change in the joint insulation. The clevis-side base thickness of the insulation has decreased, and late in burn time the NBR inhibitor is supported by this insulation. This would allow more flexibility in the inhibitor and cause increased pressure oscillation. Investigation into this theory is being conducted.

TWR-17592, Volume XI contains a complete discussion of the performance results from PV-1.

3.1.12 Aero/Thermal

The main objective of the flow/thermal/erosion analysis was to compare the predictions to the test results. Full details of the predictions for PV-1 are presented in TWR-17592, Volume X. Considering the thermal objectives,

Table 3.1.11-1. PV-1 Performance Summary With
CPW1-3600 CEI Specification Limits

	Vacuum Spec Limits (60°F)	PV-1	
		Predicted (60°F)	Delivered (60°F)
Web Time (sec)	106.1 - 117.2	111.8	111.4
Action Time (sec)	115.4 - 131.4	123.6	122.1
MOP Head End (psia)	858.7 - 978.1	911.8	908.1
Max Sea Level Thrust (Mlbf)	2.87 - 3.25	3.04	3.06
Web Time Avg Head End Pressure (psia)	625.8 - 695.8	659.4	664.4
Web Time Avg Vacuum Thrust (Mlbf)	2.45 - 2.72	2.59	2.595
Web Time Total Impulse (Mlbf-sec)	286.1 - 291.8	289.1	289.2
Action Time Impulse (Mlbf-sec)	293.3 - 299.2	296.8	296.4
I _{sp} Avg Delivered (lbf-sec/lbm)	265.3 - 269.0	268.6	268.1
Ignition Interval (sec), Time 563.5 psia	0.202 - 0.262	0.232	0.234
Max Pressure Rise Rate (psi/10-msec)	X < 115.9	91.8	92.8
Loaded Propellant Weight of 1,106,190 lb			

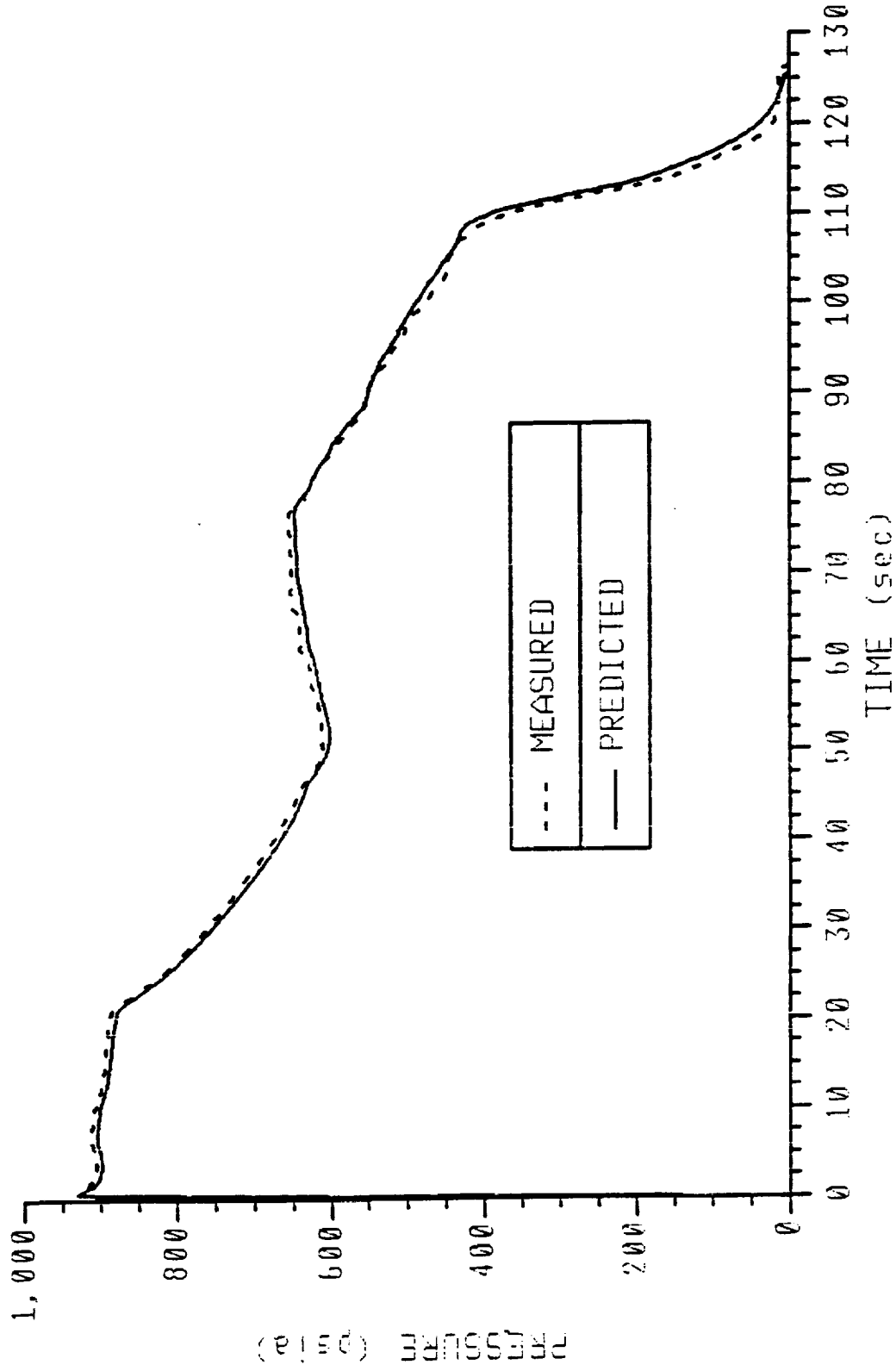


Figure 3.1.11-1. PV-1 Predicted and Measured Pressure at 79°F

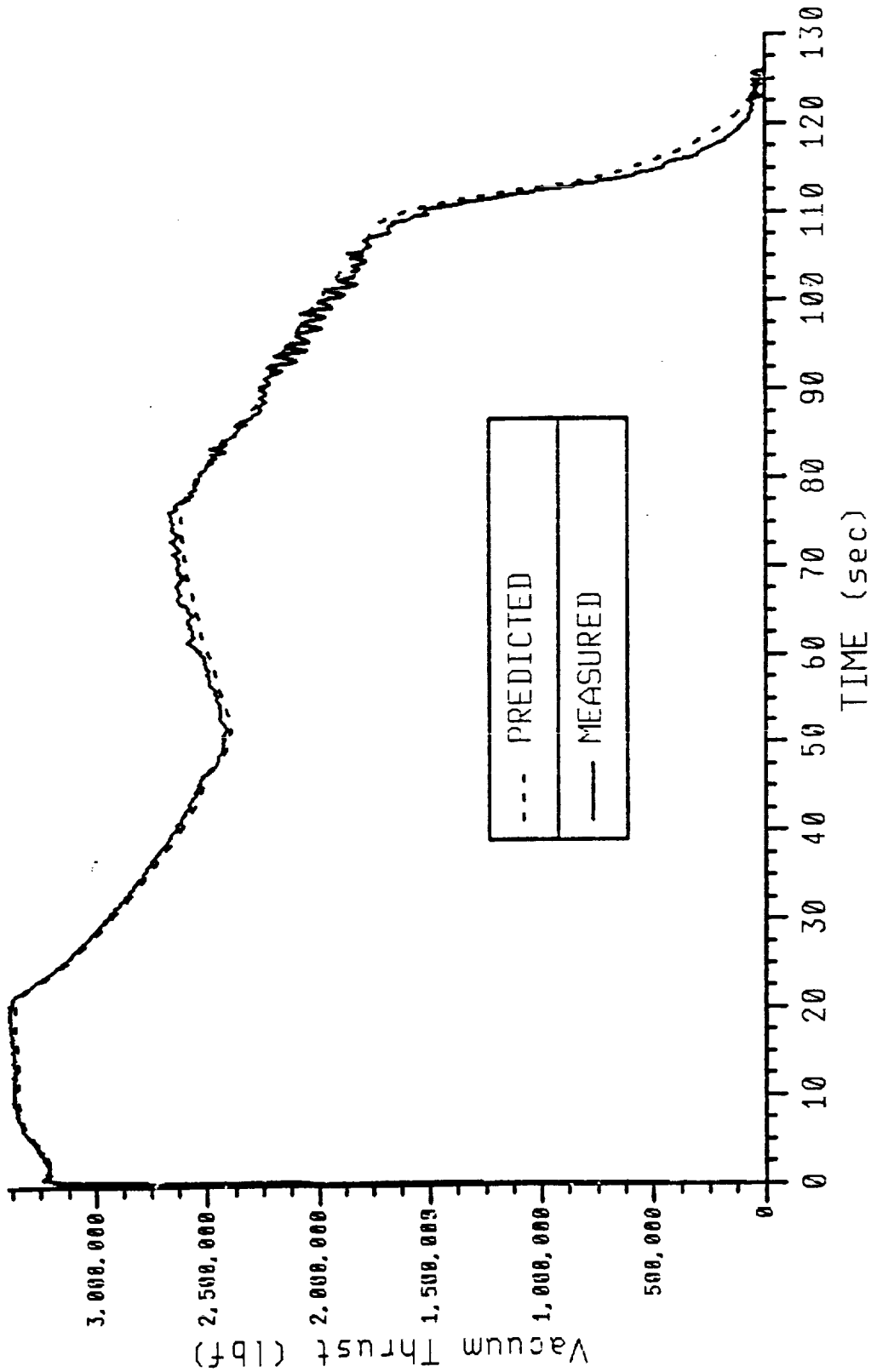


Figure 3.1.11-2. PV-1 Predicted and Measured Thrust at 79°F

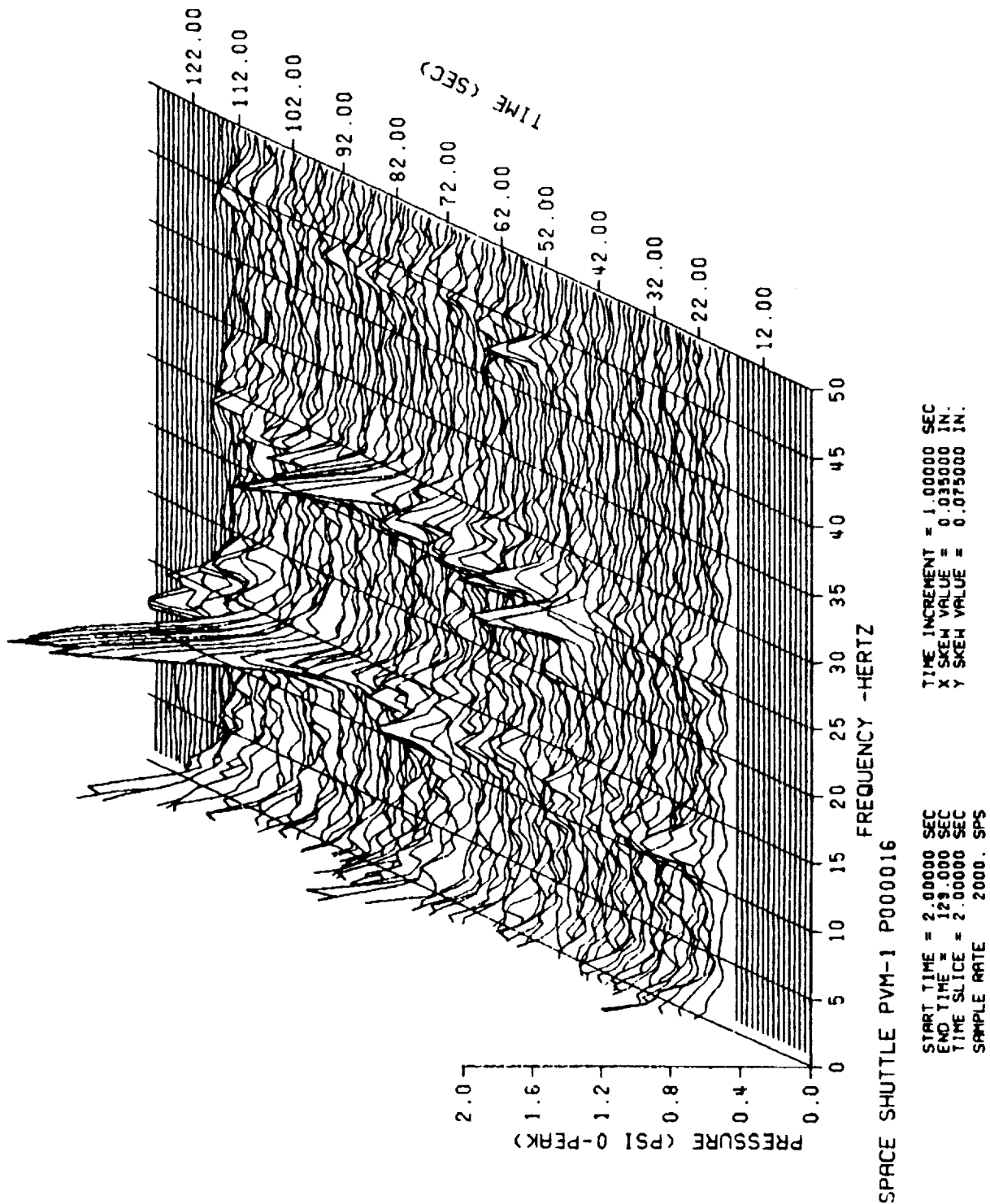


Figure 3.1.11-3. Waterfall Plot of PV-1 Dynamic Pressure, P016

the test was a success. Qualitatively, the test shows the motor can tolerate insulation, capture feature, and wiper O-ring flaws. The V_2 pressurization and temperature in the aft field joint and the V_1 , V_2 , and V_3 volume pressurization and temperature in the nozzle-to-case joint appear reliable. Post-test insulation and O-ring erosion physical measurements provide a good source of quantitative data.

3.1.12.1 Temperature Data. Temperature data were nominal. Ambient temperature at the time of ignition was 87°F and PMBT was 79°F.

3.1.13 Dynamics

Accelerometers only were used on PV-1 to monitor the RSRM dynamic behavior. Most of the displacement gages and accelerometers were removed due to the time constraint, leaving only accelerometers A401 through A403. A brief discussion of these accelerometers is included in this section. Detailed discussions will be in TWR-17592, Volume IX.

Dynamic-related data from PV-1 was used to certify the structural integrity of the case and to verify finite element models.

3.1.13.1 Results/Discussions. Accelerometers A401 through A403 were located in the forward dome area. The time history plots are presented in Figures 3.1.13.1-1 through 3.1.13.1-3, which show that the vibration levels are well below 2 g during the firing, except a few seconds after ignition.

The power spectrum density for each channel was compared to NASA random vibration criteria SE-019-049-2H shown in Figures 3.1.13.1-4 through 3.1.13.1-6 for selected time intervals. These figures show that the random vibration level easily met the criteria. A detailed discussion on the random vibration and spectrum analysis, emphasizing the cross correlation between each channel, will be included in TWR-17592, Volume IX.

The auto-spectrum waterfall plots, which were obtained by Fourier-transforming selected intervals of time history data and plotting them in a stacking manner, are shown in Figures 3.1.13.1-7 through 3.1.13.1-9. The purpose of waterfall plots is to track the modes of vibration when the excitation sources are white-type random vibration. Channel A401 is studied briefly here.

SDRC I-DEAS 4.0: Test Data Analysis 7-SEP-88 17:16:09
 DATABASE: NONE UNITS: IN
 VIEW: No stored VIEW DISPLAY: No stored OPTION

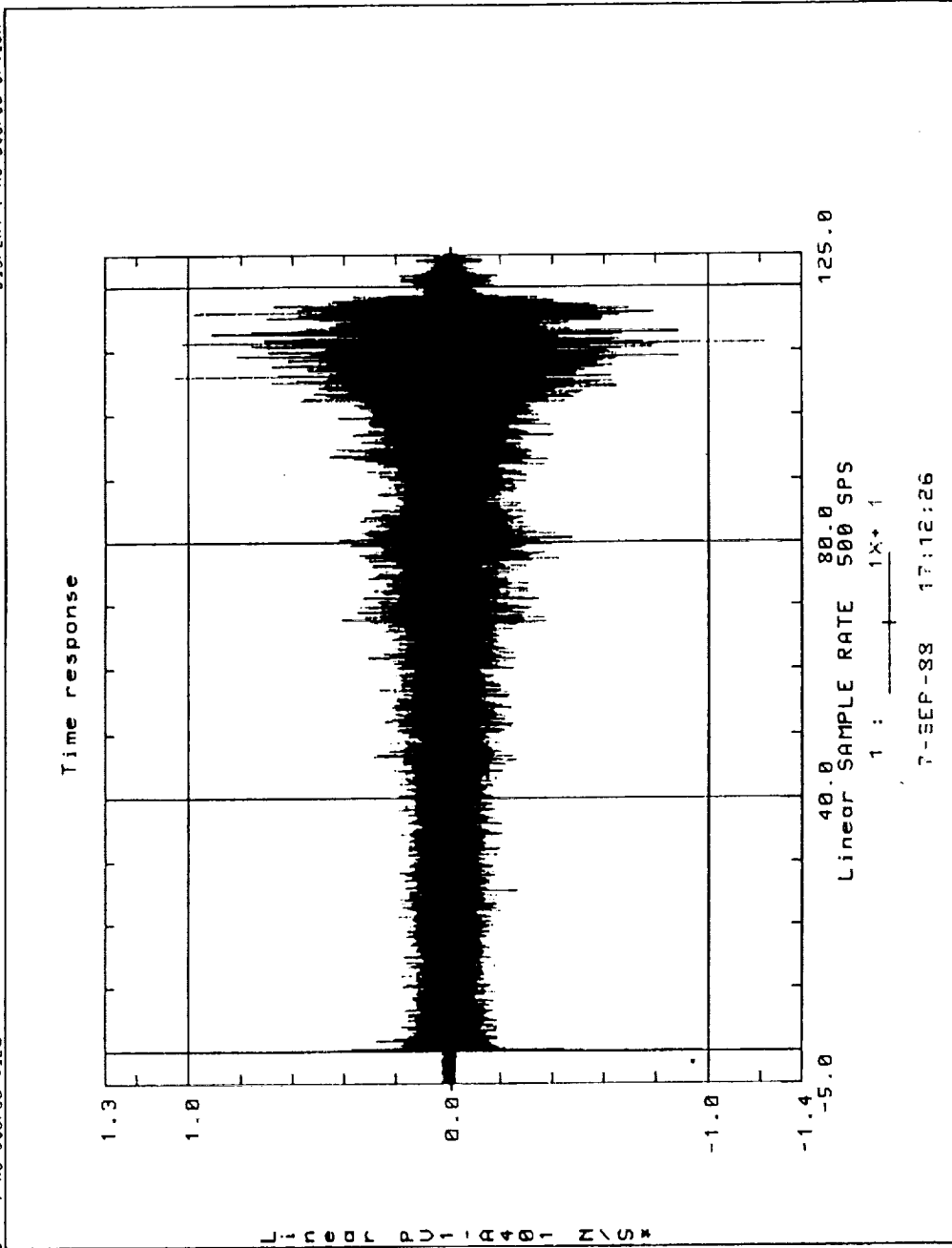


Figure 3.1.13.1-1. A401 Time Response

SDRC I-DEAS 4.0: Test Data Analysis 7-SEP-88 17:27:59
 DATABASE: NONE UNITS: IN
 VIEW: NO STORED VIEW DISPLAY: NO STORED OPTION

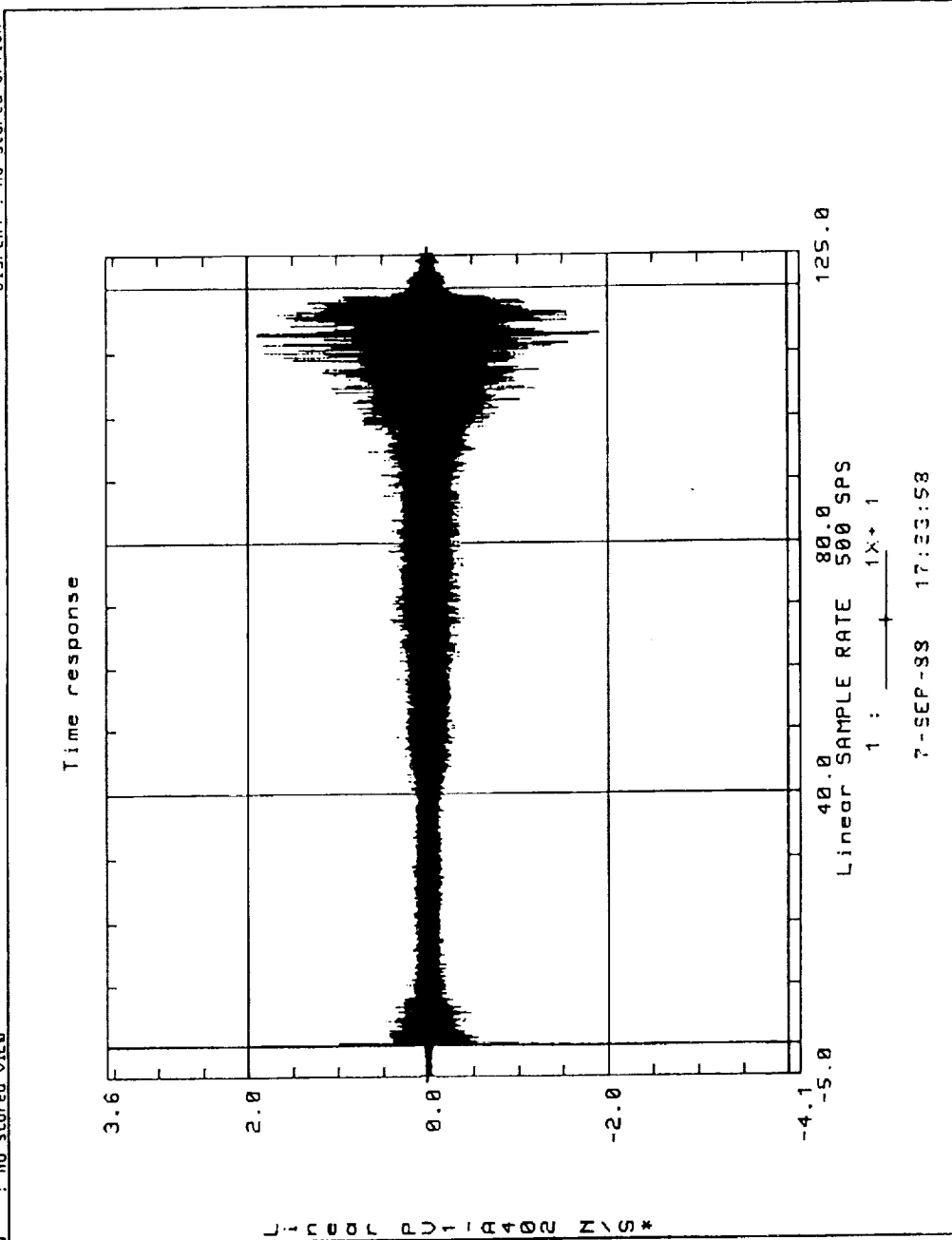


Figure 3.1.13.1-2. A402 Time Response

SORC I-DEAS 4.0: Test Data Analysis 19-SEP-88 20:40:44
 DATABASE: TIME UNITS: IN
 VIEW: NO STORED VIEW DISPLAY: NO STORED OPTION

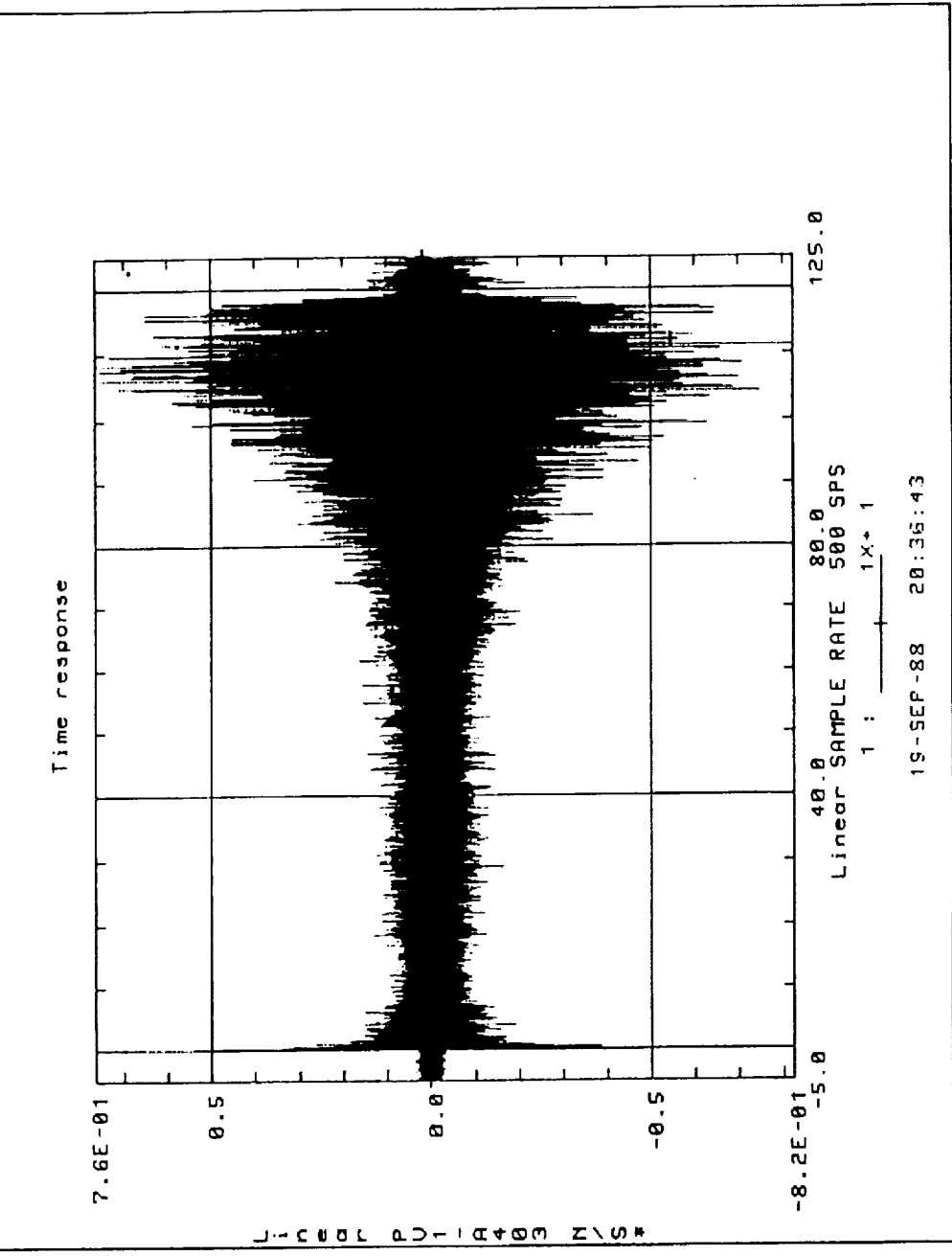


Figure 3.1.13.1-3. A403 Time Response

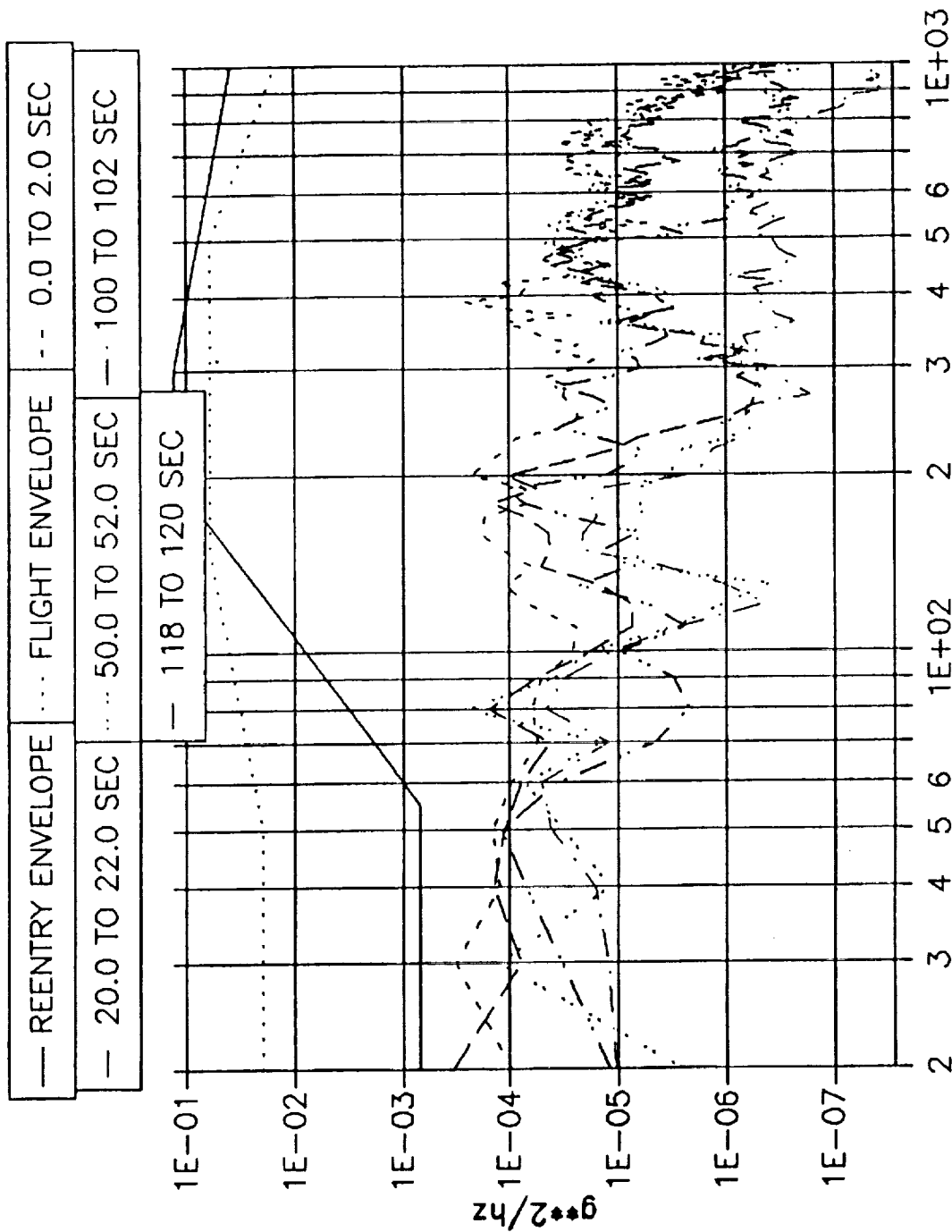


Figure 3.1.13.1-4. PV-1-A401 PSD Compared With NASA Criteria

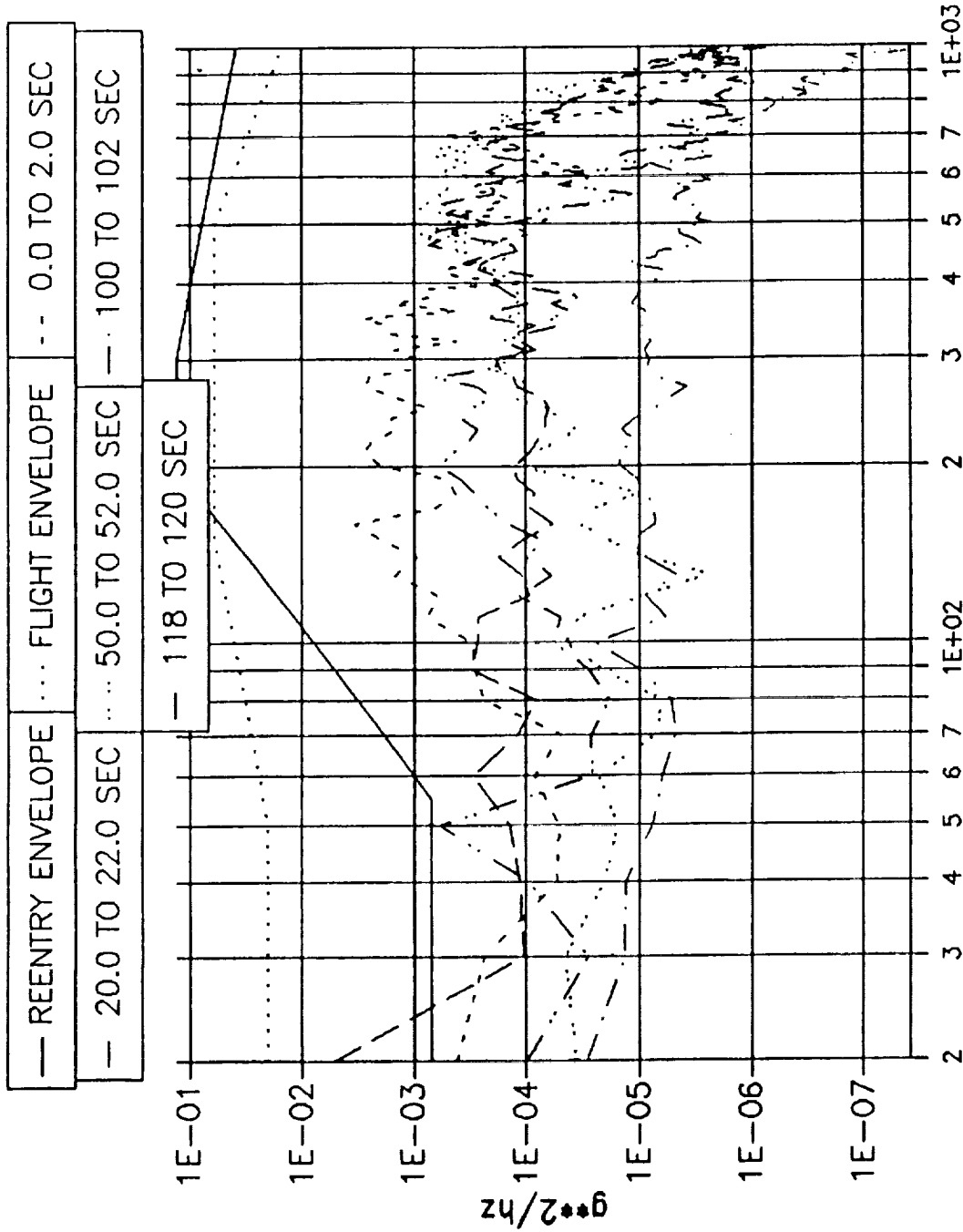


Figure 3.1.13.1-5. PV-1-A402 PSD Compared With NASA Criteria

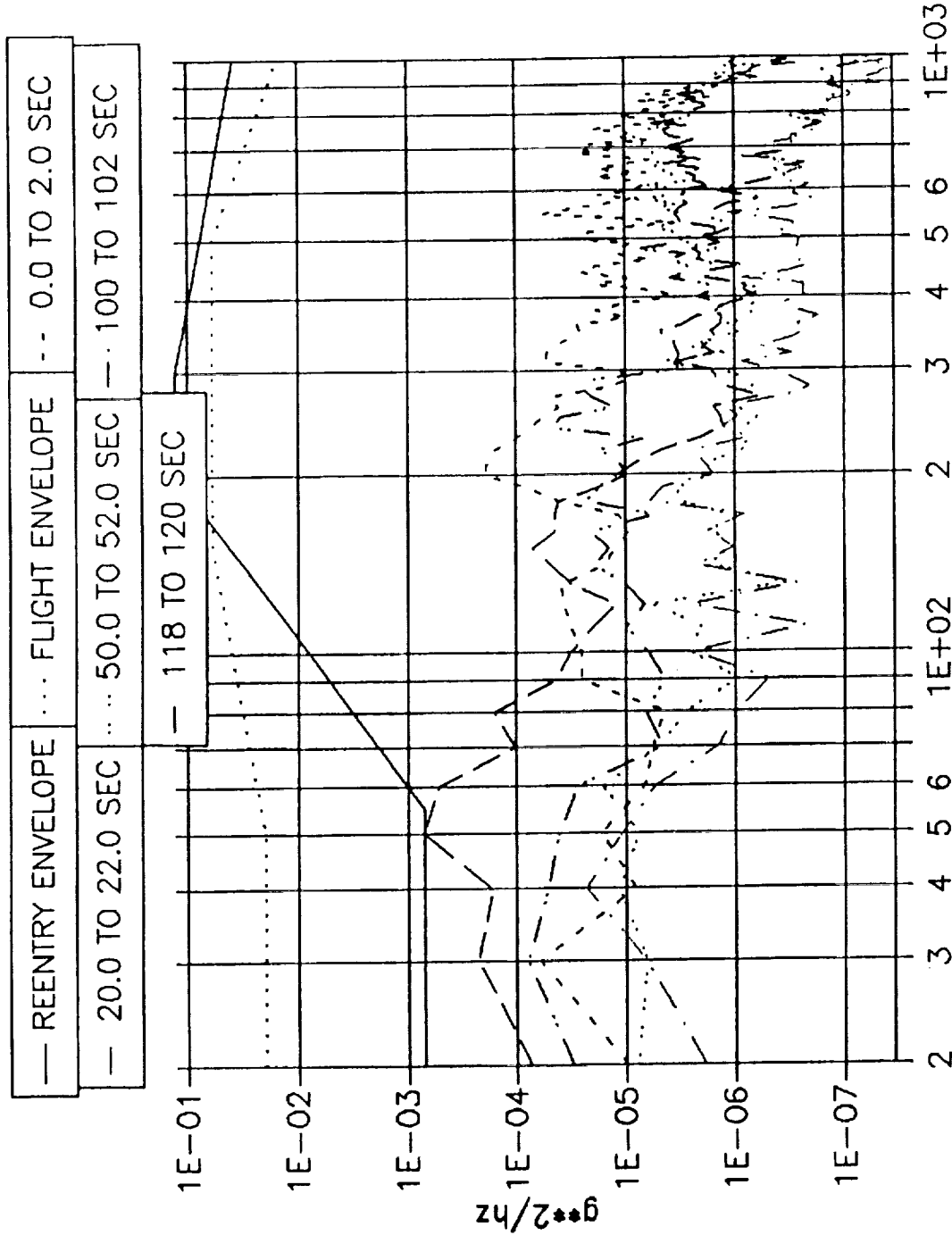


Figure 3.1.13.1-6. PV-1-A403 PSD Compared With NASA Criteria

SDRC I-DEAS 4.0: Test Data Analysis 19-SEP-88 15:42:29
 DATABASE: TDA TDA UNITS : IN
 VIEW : No stored VIEW DISPLAY : No stored OPTION

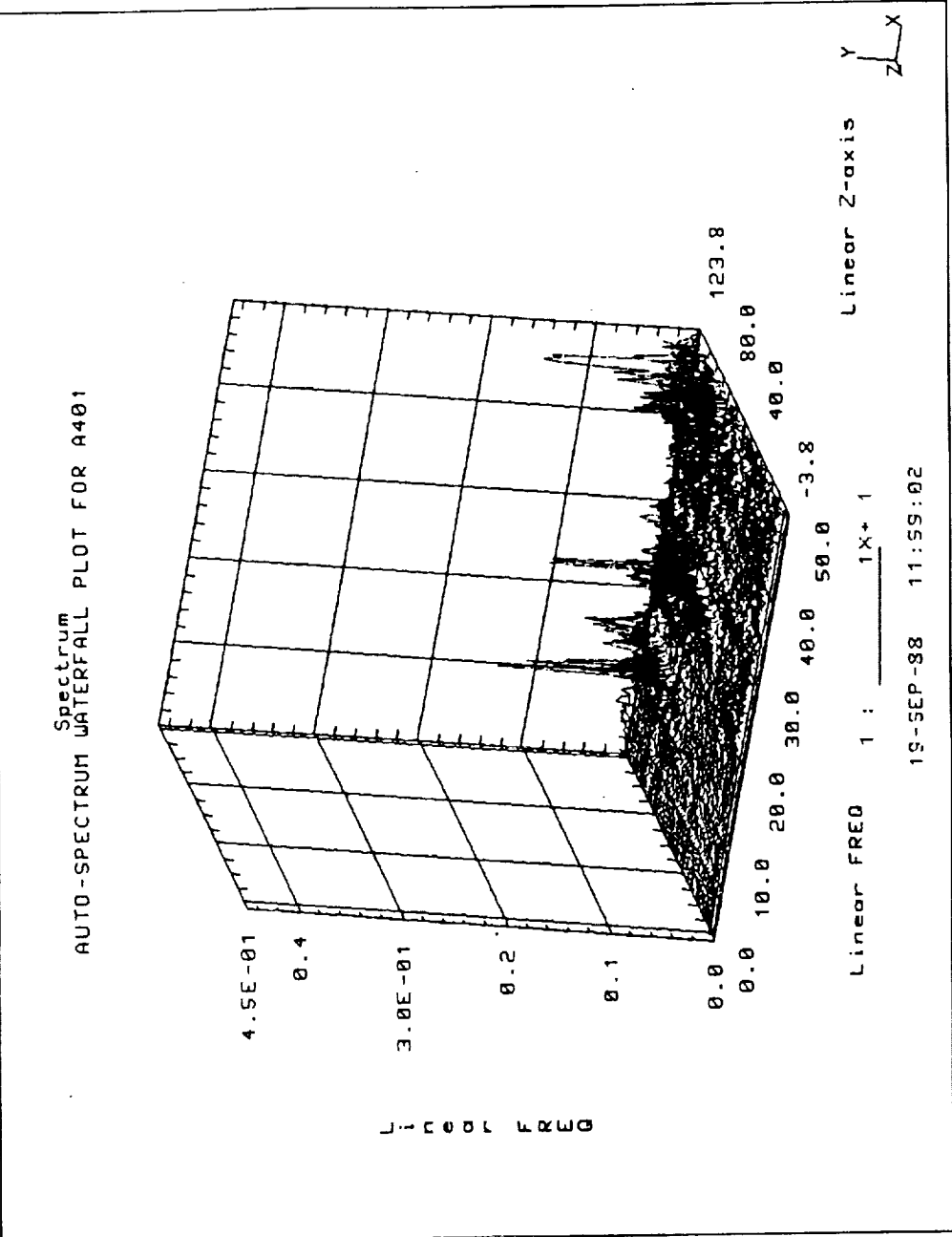


Figure 3.1.13.1-7. Auto-Spectrum Waterfall Plot for A401

C-2

SORC I-DEAS 4.0: Test Data Analysis 19-SEP-88 16:16:46
 DATABASE: TDA TDA UNITS : IN
 VIEW : No stored VIEW DISPLAY : No stored OPTION

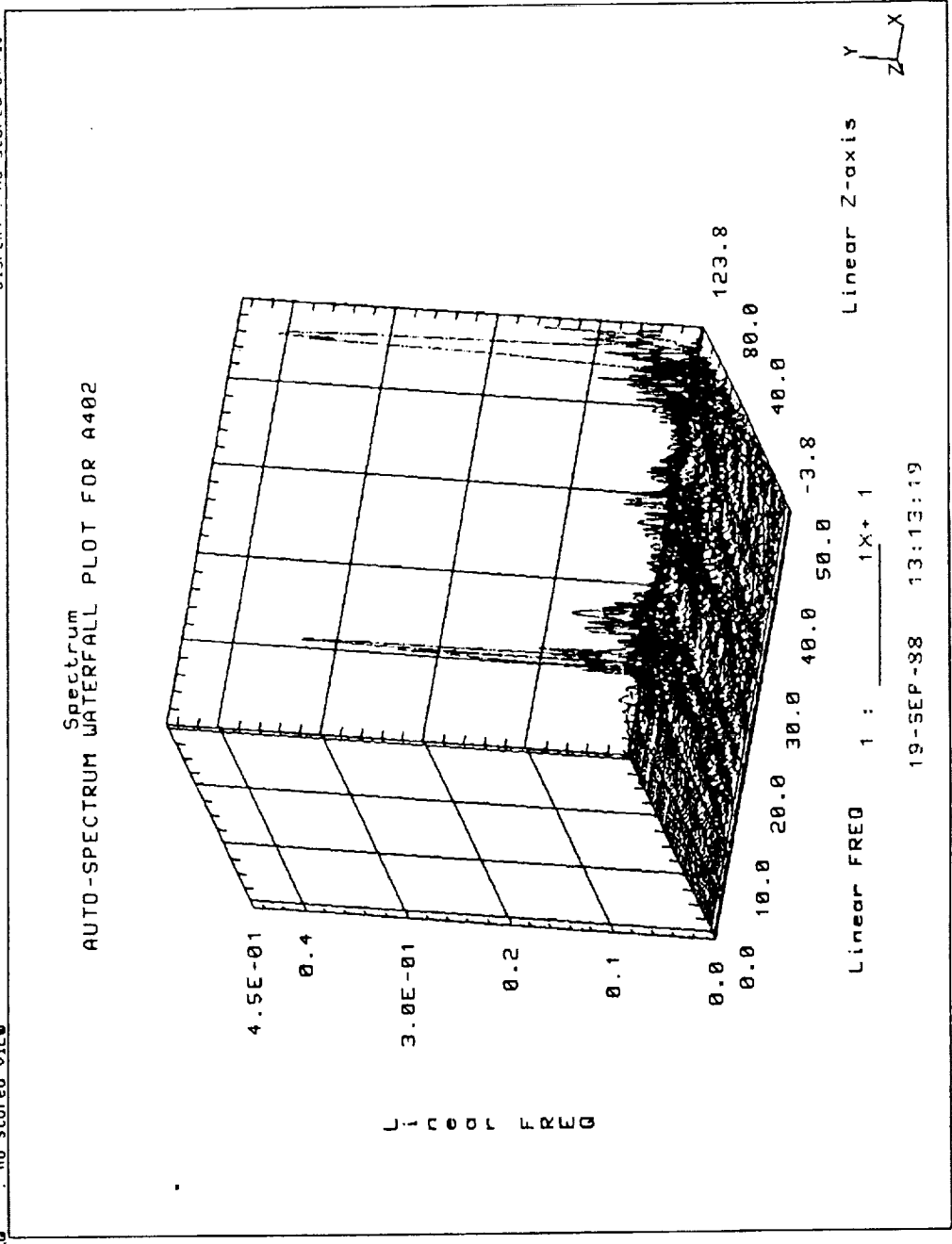


Figure 3.1.13.1-8. Auto-Spectrum Waterfall Plot for A402

SDRC I-DEAS 4.0: Test Data Analysis 19-SEP-88 16:44:41
 DATABASE: TDA TDA UNITS : IN
 VIEW : No stored VIEW DISPLAY : No stored OPTION

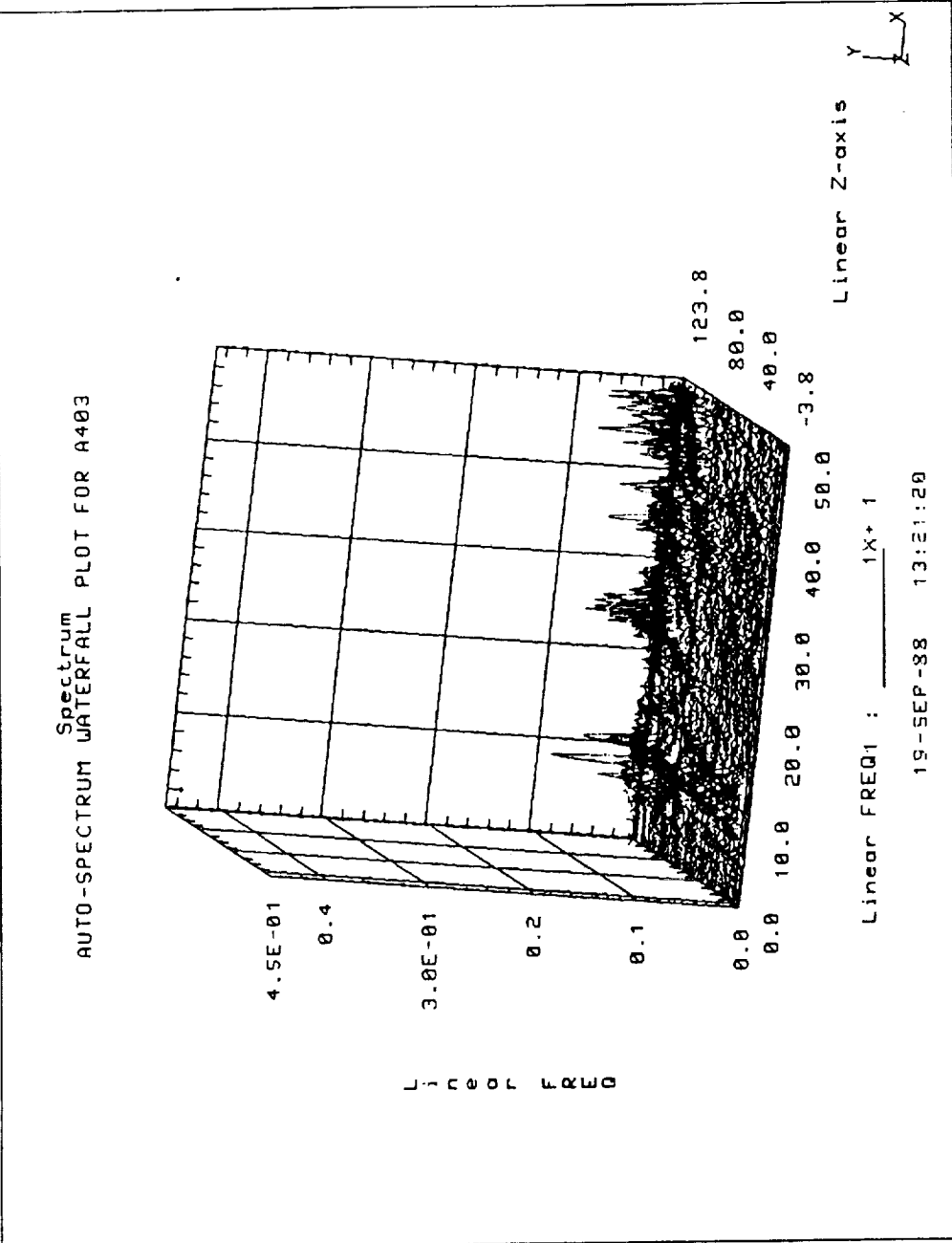


Figure 3.1.13.1-9. Auto-Spectrum Waterfall Plot for A403

Channel A401 is measured in the axial direction. Figure 3.1.13.1-7 shows that the third axial mode, which started at about 21 Hz, dominated the low frequency vibration in the axial direction from after ignition until mid-burn. The first axial mode ended at about 16 to 17 Hz, which was consistent with previous motors fired in the T-24 test stand. When approaching the end of burn, the 1-L acoustic mode has great influence on the motor, which can be seen from the irregular spectrum in the waterfall plots in Figures 3.1.13.1-7 through 3.1.13.1-9.

3.2 RECOMMENDATIONS

3.2.1 Slag Prediction

The slag accumulation theory associated with the AP particle size distribution should be further investigated.

3.2.2 Chamber Pressure Oscillation

The magnitude of chamber pressure oscillations should be observed on future motors.

3.2.3 Nozzle Composite Structure

Fine-tuning nozzle analytical techniques, material properties, and loads continue to be a priority.

3.2.4 Motor Pressure Measurement (Aft Dome)

Direct measurement of motor pressure in the aft dome region has never been made and is recommended for the TEM-2 motor.

3.2.5 Nozzle Instrumentation

Continued instrumentation of nozzle components is important to adequately monitor nozzle response. Development of methods to more directly monitor the thermostructural response of the phenolic parts should be pursued.

3.2.6 TASS Finite Element Model Results

Differences in measured strain results between coarse- and fine-grid Thiokol automated stress system (TASS) finite element model (especially in the forward end ring locations 6 and 8 and the aft exit cone region) should be investigated.

CEI SPECIFICATIONS

This section shows PV-1 static test compliance with Specification CPW1-3600, Addendum D, dated 3 Aug 1987. The following comments are drawn from the test with a one-to-one correlation to the test objectives listed in Section 2.

Qualification Objectives (CEI paragraph number)	Pass/Fail Criteria	Results (Reference Section)
A Certify the motor performance at ambient temperature. (3.2.1)	The motor must meet the performance requirements of the CEI specification when PMBT is calculated and performance extrapolated to a +60°F thermal environment.	Motor performance was extrapolated to +60°F and all performance requirements were met. (Table 3.1.11-1).
B Certify the ignition interval. (3.2.1.1.1.1)	The ignition interval (time to reach head end pressure of 563.5 psia) must be between 0.202 and 0.262 sec after ignition command to the SRM ignition initiators.	The ignition interval was 0.234 sec.
C Certify the pressure rise rate. (3.2.1.1.1.2)	The maximum pressure rise rate must not exceed 115.9 psi for any 10 ms time period.	The maximum pressure rise rate was 92.8 psi/10 ms.
D Determine the thrust-time curve for PV-1 and apply the data to the nominal thrust-time curve for certification of the RSRM design. (3.2.1.1.2.1)	The nominal (arithmetic average) vacuum thrust versus time curve (corrected to 60-deg PMBT) for all appropriate RSRM motors must fall between the upper and lower bounds of Table I in the redesign CEI specification.	The nominal vacuum thrust-time curve lies within the values of Table I of the CEI specification.
E Certify the performance tolerances and limits. (3.2.1.1.2.2)	The individual motor performance parameters must fall within the limits specified in Table II of the redesign CEI specification.	Individual motor performance values are listed in Table 3.1.11-1.
F Determine the impulse attained by PV-1 and apply the data to the nominal thrust-time curve for certification of the RSRM design. (3.2.1.1.2.4)	The nominal thrust versus time curve must comply with the impulse requirements in the redesign CEI specification.	Impulse requirements in the redesign CEI specification were met (Table 3.1.11-1).
G Certify that all RSRM seals, except the center and aft field joints and nozzle-to-case joints, and igniter-to-case joints but including adjustable vent port plug seals in the forward field joint, experience no erosion or blowby throughout the static test, if pressurized. (3.2.1.2)	There must be no evidence of erosion or blowby detected for the specified seals (acceptable erosion is allowed on factory joint insulation acting as the primary seal).	No evidence of erosion or blowby past the RSRM seals.

89265-12.1

REVISION B

DOC NO. TWR-17592	VOL
SEC	PAGE 88

H	Certify the sealing performance of the center and aft field joints and the nozzle-to-case and igniter-to-case joints. (3.2.1.2)	There must be no evidence of gas leakage past the center and aft field joints or nozzle-to-case and igniter-to-case joints.	No evidence of gas leakage past the seals.
I	Certify the verifiability of the RSRM seals (except for the case-to-nozzle joint primary seal, the factory joint primary seal, the fixed housing-to-aft end ring primary seal, the igniter dual seal plugs (5 places), and the OPT primary and secondary seals). (3.2.1.2)	The leak check for these seals must be successfully completed.	Leak check performance of all joints was acceptable.
J	Certify that the forward field joint seals, if pressurized, accommodate static test motor structural deflections. (3.2.1.2.1.a)	There must be no evidence of blowby detected past the field joint seals due to structural deflections.	No evidence of blowby detected due to structural deflections.
K	Certify that the center and aft field joint and the nozzle-to-case joint accommodate static test motor structural deflections. (3.2.1.2.1.a)	There must be no evidence of gas leakage past the center or aft field joint or nozzle-to-case joint due to structural deflections.	No evidence of blowby detected due to structural deflections.
L	Certify that the forward field joint seals, if pressurized, operate at ambient temperature. (3.2.1.2.1.b)	There must be no evidence of erosion or gas leakage past the field joint seals.	No evidence of hot gas past the field joint seals.
M	Certify that the center and aft field joint and nozzle-to-case joint operate at ambient temperature. (3.2.1.2.1.b)	There must be no evidence of gas leakage past the center, aft, or nozzle-to-case field joint.	No evidence of gas leakage past the center, aft, or nozzle-to-case field joint.
N	Certify that the case field joint and case-to-nozzle joint seal verification does not degrade the performance or integrity of the sealing system. (3.2.1.2.1.c)	There must be no evidence of damage to insulation, adhesives, or seals due to leak check procedures.	No evidence of leak check-related damage to joint insulation, adhesives, or O-ring seals.
O	Certify that the bore seals for the forward and center field joint are verifiable in the proper direction. (3.2.1.2.1.d)	The leak check must be successfully completed.	Field joint leak check performance was acceptable: forward - 3.438 psig, center - 3.140 psig, aft - 4.3 psig.
P	Certify that the case-to-nozzle joint O-ring temperature is maintained prior to static firing. (3.2.1.2.1.f)	Pretest data must show that the case-to-nozzle joint temperature was 75°F or higher until time of motor ignition.	Aft skirt conditioning raised the case-to-nozzle joint temperature to greater than 90°F at T-0.
Q	Certify that the factory joint insulation as a seal accomodates static test motor structural deflections and erosion. (3.2.1.2.2.a)	There must be no evidence of hot gas to the primary or secondary O-rings due to structural deflections.	Disassembly of factory joints has not been completed. Initial inspection indicates no anomalous conditions.

89265-12.2

Thiokol CORPORATION
SPACE OPERATIONS

R	Certify that the factory joint insulation as a seal operates at ambient temperature. (3.2.1.2.2.b)	There must be no evidence of hot gas to the primary or secondary O-rings.	Disassembly of factory joints has not been completed. Initial inspection indicates no anomalous conditions.
S	Certify that the insulation performs the seal function for the factory joint. (3.2.1.2.2.d)	At least one virgin ply of insulation must remain over the factory joint with no evidence of hot gas to the primary or secondary O-rings.	Disassembly of factory joints has not been completed. Initial inspection indicates no anomalous conditions.
T	Certify that the factory joint insulation is adequate to preclude leaks. (3.2.1.2.2.e)	There must be no evidence of hot gas to the primary or secondary O-rings.	Disassembly of factory joints has not been completed. Initial inspection indicates no anomalous conditions.
U	Certify that the flex bearing accommodates static test motor structural deflections. (3.2.1.2.3.a)	There must be no evidence of erosion or gas leakage between the flex bearing internal components due to structural deflections.	The flex bearing will be fully inspected and tested during completion of post-test acceptance testing. Visual inspection indicated no obvious problems.
V	Certify that the flex bearing operates as a seal at ambient temperature. (3.2.1.2.3.b)	There must be no evidence of erosion or gas leakage between the flex bearing internal components.	The flex bearing will be fully inspected and tested during completion of post-test acceptance testing. Visual inspection indicated no obvious problems.
W	Certify that the flex bearing seal verification does not degrade the performance or integrity of the sealing system. (3.2.1.2.3.c)	There must be no evidence of damage to the flex bearing due to leak check procedures.	The flex bearing will be fully inspected and tested during completion of post-test acceptance testing. Visual inspection indicated no obvious problems.
X	Certify that the flex bearing maintains a positive gas seal between its internal components. (3.2.1.2.3.d)	There must be no evidence of gas leakage between the flex bearing internal components.	The flex bearing will be fully inspected and tested during completion of post-test acceptance testing. Visual inspection indicated no obvious problems.
Y	Certify that the ignition seals, if pressurized, except for the igniter-to-case joint, accommodate static test motor structural deflections. (3.2.1.2.4.a)	There must be no evidence of erosion or gas leakage past the ignition system seals due to structural deflections.	Soot was found up to, but not past, the S&A primary seal on the aft face. No evidence of hot gas to the inner or outer igniter seals.
Z	Certify that the igniter-to-case joint accommodates static test motor structural deflection. (3.2.1.2.4.a)	There must be no evidence of gas leakage past the igniter-to-case joint.	No evidence of gas leakage past the igniter-to-case joint.
AA	Certify that the ignition seals, if pressurized, except for the igniter-to-case joint, operate at ambient temperature. (3.2.1.2.4.b)	There must be no evidence of erosion or gas leakage past the ignition system seals (except the igniter-to-case joint).	There was no evidence of hot gas to the primary seals and no evidence of blowby, erosion, or heat effect. No evidence of hot gas to the inner, outer, or S&A seals.

89265-12.3

REVISION B

DOC NO.	TWR-17592	VOL
SEC	PAGE	90

Thiokol CORPORATION
SPACE OPERATIONS

AB	Certify that the igniter-to-case joint operates at ambient temperature. (3.2.1.2.4.b)	There must be no evidence of gas leakage past the igniter-to-case joint.	No evidence of gas leakage past the igniter-to-case joint.
AC	Certify that the ignition system seal verification does not degrade the performance or integrity of the sealing system. (3.2.1.2.4.c)	There must be no evidence of damage to the ignition system seals due to leak check procedures.	No evidence of leak check-related damage to ignition system seals.
AD	Certify that the nozzle internal seals, except for Joint 5, and the aft exit cone field joint seals, if pressurized, can accommodate static test motor structural deflections. (3.2.1.2.5.a)	There must be no evidence of erosion, or gas leakage past the nozzle internal seals (excluding Joint 5) or the aft exit cone joint seals due to structural deflections.	No evidence of damage, blowby, or erosion on the aft exit cone joint seals or nozzle internal seals.
AE	Certify that nozzle internal Joint 5 can accommodate static test motor structural deflections. (3.2.1.2.5.a)	There must be no evidence of gas leakage past nozzle Joint 5.	No evidence of gas leakage past nozzle Joint 5.
AF	Certify that the nozzle internal seals, except Joint 5, and the aft exit cone field joint seals, if pressurized, operate at ambient temperature. (3.2.1.2.5.b)	There must be no evidence of erosion or gas leakage past the nozzle internal seals, except Joint 5, or the aft exit cone joint seals.	No evidence of blowby or erosion on the aft exit cone joint seals or the nozzle internal seals.
AG	Certify that nozzle internal Joint 5 operates at ambient temperature. (3.2.1.2.5.b)	There must be no evidence of gas leakage past nozzle Joint 5.	No evidence of gas leakage past nozzle Joint 5.
AH	Certify that the nozzle internal seals and the aft exit cone field joint seals verification does not degrade the performance or integrity of the sealing system. (3.2.1.2.5.c,d)	There must be no evidence of damage to the nozzle internal seals or the aft exit cone field joint seals due to leak check procedures.	No evidence of leak check-related damage to nozzle internal seals or aft exit cone field joint seals.
AI	Certify that the bore seals for the nozzle are verifiable in the proper direction. (3.2.1.2.5.e)	The leak check must be successfully completed.	Nozzle leak check performance was acceptable.
AJ	Certify that the case is capable of containing the static test internal pressure. (3.2.1.3.a)	There must be no evidence of damage to the case due to internal pressure.	No evidence that the case allowed leakage of internal pressures or local yielding.
AK	Certify that the case ETA risers do not degrade the integrity of the case. (3.2.1.3.c)	The case must show no evidence of case damage due to the ETA risers.	No evidence of damage or local yielding of the case at the ETA risers.
AL	Certify by demonstrating horizontal assembly that the case segment mating joints have provisions to ensure proper segment orientation and alignment. (3.2.1.3.f)	Horizontal assembly with proper alignment must be demonstrated.	No GSE was used on PV-1.

89265-12.4

REVISION B

DOC NO.	TWR-17592	VOL
SEC	PAGE	91

Thiokol CORPORATION
SPACE OPERATIONS

AM	Certify that the nozzle assembly and exit cone design are compatible with the system performance requirements. (3.2.1.4, Morton Thiokol-imposed)	The nozzle assembly and exit cone design must be compatible with the specified Morton Thiokol-imposed system performance requirements.	Morton Thiokol-imposed system performance requirements were met.
AN	Certify that the nozzle assembly is capable of vectoring through the planned duty cycle. (3.2.1.4.1)	The nozzle assembly must follow the planned duty cycle within the expected range as determined by engineering from the historical performance data base.	The nozzle assembly followed the planned duty cycle within the expected range.
AO	Certify the geometric nozzle alignment. (3.2.1.4.2)	With the nozzle and motor centerlines within 0.5 deg of each other, the radial offset of the nozzle centerline at the nozzle throat plane must not exceed 0.25 in. from the motor centerline.	With the nozzle and motor centerlines within 0.5 deg of each other, the radial offset of the nozzle centerline at the nozzle throat plane was a maximum of 0.046 in. from the motor centerline.
AP	Certify the misalignment of the dynamic thrust vector with respect to the nozzle centerline. (3.2.1.4.3 and 3.2.1.4.3.a)	Misalignment of the dynamic thrust vector with respect to the nozzle centerline must not deviate more than 1 deg during nozzle vectoring between null and 8 deg.	Misalignment of the dynamic thrust vector with respect to the nozzle centerline deviated a maximum of 0.189 deg during nozzle vectoring.
AQ	Certify the radial offset between the dynamic thrust vector and the nozzle centerline. (3.2.1.4.3 and 3.2.1.4.3.b)	The radial offset between the dynamic thrust vector and the nozzle centerline at the nozzle throat plane must not exceed 1.13 in. during nozzle vectoring between null and 8 deg.	The radial offset between the dynamic thrust vector and the nozzle centerline at the nozzle throat plane was a maximum of 0.046 in. during nozzle vectoring.
AR	Certify the null offset angle at 0 psi nozzle stagnation pressure. (3.2.1.4.4.a)	The nozzle null offset angle with respect to zero actuator command must not exceed +0.96 deg at 0 psi nozzle stagnation pressure.	The nozzle null offset angle with respect to zero actuator command was a maximum of 0.90 deg at 0 psi nozzle stagnation pressure.
AS	Certify the null offset angle at 615 psi nozzle stagnation pressure. (3.2.1.4.4.b)	The nozzle null offset angle with respect to zero actuator command must not exceed ± 0.30 deg at 615 psi nozzle stagnation pressure.	The nozzle null offset angle with respect to zero actuator command was a maximum of -0.2 deg at 615 psi nozzle stagnation pressure.
AT	Certify the null offset angle at 915 psi nozzle stagnation pressure. (3.2.1.4.4.c)	The nozzle null offset angle with respect to zero actuator command must not exceed -0.50 deg at 915 psi nozzle stagnation pressure.	The nozzle null offset angle with respect to zero actuator command was a maximum of -0.30 deg at 915 psi nozzle stagnation pressure.
AU	Certify the nozzle assembly TVC actuator attach points. (3.2.1.4.8)	The nozzle assembly TVC actuator attach points must be compatible with the TVC actuators.	The nozzle assembly TVC actuator attach points were compatible with the TVC actuators.
AV	Certify the nozzle flame front liner design and fabrication. (3.2.1.4.13)	There must be no pockets greater than 0.250 in. deep, no wedgeouts greater than 0.250 in. deep, and no prefire anomalies except as allowed by TWR-16340.	The nozzle flame front liner met the requirements of TWR-16340 and there were no pockets or wedgeouts occurring during motor operation observed as a result of design or fabrication.

89265-12.5

REVISION B

DOC NO. TWR-17592

VOL

SEC

PAGE

92

Thiokol CORPORATION
SPACE OPERATIONS

AW	Certify that the ignition system precludes hot gas leakage during and subsequent to motor ignition. (3.2.1.5.a)	There must be no evidence of hot gas leakage.	No evidence of hot gas leakage past the ignition system.
AX	Certify by demonstration that the igniter and the S&A are separable from each other. (3.2.1.5.b)	Separation of the igniter and S&A must be demonstrated.	The igniter and S&A are separable from each other.
AY	Certify the enable function of the S&A device. (3.2.1.5.1.a)	The S&A device barrier-booster assembly must provide the energy flow required to achieve igniter initiation upon command.	The S&A device both enabled and inhibited ignition upon command.
AZ	Certify the S&A change of position from safe to arm. (3.2.1.5.1.d)	The S&A must change position from safe to arm.	The S&A changed position from safe to arm upon command.
BA	Certify that the S&A device will provide simplex remote position indication. (3.2.1.5.1.e)	The S&A device must provide remote indication of position in both the safe and armed positions.	The S&A device provided remote indication of position.
BB	Certify the igniter design. (3.2.1.5.2)	There must be no debris formed which is capable of damaging any other component which is attributable to the igniter, and the igniter must be installed in only one predetermined rotational position into the igniter port from the outside of the forward segment.	No igniter-related debris formed capable of damaging any other component. The igniter was installed in the predetermined rotational position into the igniter port from the outside of the forward segment.
BC	Certify that the RSRM design meets the electromagnetic compatibility requirements. (3.2.1.6.e)	The electrical bonding resistance measurements must not exceed 2.5 milliohms.	The electrical bonding resistance measurement did not exceed 2.5 milliohms.
BD	Certify the operation of the motor chamber pressure transducer and its installation. (3.2.1.6.2.1)	The motor chamber pressure pressure transducer must be installed and function correctly.	The motor chamber pressure transducer remained positively locked and accurately monitored the motor chamber pressure.
BE	Certify the installation and function of the ground environmental instrumentation (GEI). (3.2.1.6.2.3, Morton Thiokol-proposed SCN 3)	The GEI must be installed and function correctly.	GEI was installed and functioned correctly prior to T-0.
BF	Certify the installation and operation of the strain gages, (steel) and (aluminum) in the nozzle area. (3.2.1.6.2.3, Morton Thiokol-proposed SCN 3)	Strain gages must be installed and function correctly.	Strain gages were installed and mandatory data were collected.
BG	Certify the installation and operation of the girth gages. (3.2.1.6.2.3, Morton Thiokol-proposed SCN 3)	Girth gages must be installed and function correctly.	Girth gages were installed and mandatory data were collected.

89265-12.6

REVISION B

DOC NO.	TWR-17592	VOL
SEC	PAGE	93

BH	Certify the installation and operation of the temperature devices. (3.2.1.6.2.3, Morton Thiokol-proposed SCN 3)	Temperature-sensing devices must be installed and function correctly.	Temperature-sensing devices were installed and mandatory data were collected.
BI	Certify the installation and operation of the igniter chamber pressure transducer. (3.2.1.6.2.4.a, Addendum G)	The igniter chamber transducer must be installed and function correctly.	The igniter chamber transducer was installed and data were collected.
BJ	Certify the calibration of the motor chamber pressure transducer. (3.2.1.6.2.4.b, Addendum G; ICD 3-44005, 4.3.4)	The electrical output must be 75 ± 0.50 percent of the full-scale output.	The electrical output was 75 percent of the full-scale output. The motor chamber pressure transducer was properly calibrated.
BK	Certify the forward field joint insulation temperature control. (3.2.1.8.1.1.a)	There must be no damage to the forward field joint metal structural integrity or sealing integrity due to temperature effects.	No evidence of damage to the forward field joint metal structural integrity or sealing integrity.
BL	Certify the compatibility of the leak tests of seals of field joints, nozzle-to-case joint, and igniter-to-case joint with joints insulations. (3.2.1.8.1.1.b)	There must be no damage to the field joint, nozzle-to-case joint, or igniter-to-case joint metal structural integrity or sealing integrity due to leak check procedures.	No leak check-related damage found at field joints, nozzle-to-case joint, or igniter-to-case joint.
BL-1	The insulation shall ensure that system performance and structural integrity is maintained during the assembly process and operation. (3.2.1.8.1.1.c)	System performance and structural integrity during the assembly process and operation shall not be compromised due to insulation.	The insulation ensured that system performance and structural integrity was maintained during the assembly process and operation. For a complete insulation performance discussion, see TWR-17592, Volume III, Revision A.
BM	Certify that the forward field joint insulation provides seal protection. (3.2.1.8.1.1.d)	There must be no evidence of erosion, blowby, or hot gas jetting on the forward field joint primary and secondary seals.	No evidence of thermal damage to the forward field joint seals.
BN	Certify the ability of the insulation to protect the forward case joint from thermal degradation during an ambient temperature full-duration motor burn. (3.2.1.8.1.1.e)	There must be no thermal degradation to the forward field joint.	No evidence of thermal damage to the forward field joint.
BO	Certify by inspection that the forward field joint insulation will withstand slag accumulation during motor operation. (3.2.1.8.1.1.g)	Slag accumulation in joint must not degrade the case or the sealing capability of the joint.	No evidence of measurable slag damage to joint insulation or case occurring during motor burn.
BP	Certify that the ballistic performance is not affected by the field joint, case-to-nozzle joint, and igniter-to-case joint insulation. (3.2.1.8.1.1.i)	There must be no anomaly in the ballistics trace attributable to the field joint and igniter-to-case joint insulation design.	Changes in insulation design did not measurably alter ballistic performance (Table 3.1.11-1).
BQ	Certify that the igniter insulation provides adequate thermal protection for the main igniter chamber and adapter metal parts. (3.2.1.8.3)	There must be no damage to the main igniter chamber or adapter metal parts due to temperature effects.	No evidence of thermal damage to the main igniter chamber or adapter metal parts.

Thiokol CORPORATION
SPACE OPERATIONS

BR	Certify the ability of the field joint heater assembly to maintain the temperature of the field joints. (3.2.1.11.a)	The field joint temperature must be maintained between 75° and 120°F prior to motor ignition.	Minimum recorded joint heater sensor temperature was 86°F at T-0, ensuring 76°F minimum at the O-rings.
BS	Certify the inert weight by inspection. (3.2.2.2.1)	The inert weight must not exceed 150,847 lb.	The inert weight was 147,318 lb.
BT	Certify the propellant weight by inspection. (3.2.2.2.2)	The propellant weight must be at least 1,104,714 lb.	The propellant weight was 1,106,190 lb.
BU	Deleted.		
BV	Provide data for certification of the reliability of the RSRM design. (3.2.3)	The postfire engineering evaluation limits (TWR-17198) must be met.	Certification and reliability data were collected for evaluation.
BW	Certify that the primary structure, thermal protection, and pressure vessels meet design safety factors. (3.2.3.1)	The primary structure, thermal protection, and pressure vessel subsystems must preclude motor failure.	The minimum measured primary structure, thermal protection, and pressure vessel safety factor was 3.8 for yield strength and 4.1 for ultimate strength, which are well within the design safety factors of 1.1 for yield strength and 1.4 for ultimate strength.
BX	Certify that the RSRM segments are capable of horizontal assembly/disassembly. (3.2.5.1)	Successful assembly and disassembly in the horizontal position must be demonstrated.	Horizontal assembly and disassembly was demonstrated.
BY	Certify that the electrical bonding meets the requirements of MIL-B-5087B. (3.3.5.2)	The pretest electrical bonding resistance measurements must not exceed 2.5 milliohms.	Pretest bonding requirements did not exceed 2.5 milliohms.
BZ	Certify the installation of low pressure transducer fairings (nonmetallic) and the triaxial accelerometer assembly mounting block (metallic) on the forward dome. (3.3.6.1.1, MSFC-HDBK-505A)	There must be no structural failure of the fairings or bondlines.	There were no failures of the fairings or the bondlines.
CA	Certify the case insulation minimum design thermal safety factor. (3.3.6.1.2.2)	There must be a minimum case insulation thermal safety factor of 1.5 (excluding joints).	Evaluation is not complete, but will be included in TWR-17592, Vol. III.
CB	Certify the thermal design safety factor for the case insulation adjacent to metal part field joints and extending over factory joints. (3.3.6.1.2.3)	There must be a minimum case insulation thermal safety factor of 2.0 for the specified joints.	Evaluation is not complete, but will be included in TWR-17592, Vol. III.
CC	Certify the case insulation sandwich construction region (aft and center segment aft end) design safety factor. (3.3.6.1.2.4)	There must be a minimum safety factor of 1.5.	Evaluation is not complete, but will be included in TWR-17592, Vol. III.

89265-12.8

REVISION B

DOC NO.	TWR-17592	VOL
SEC	PAGE	95

Thiokol CORPORATION
SPACE OPERATIONS

- | | | | |
|----|--|---|---|
| CD | Certify the insulation performance. (3.3.6.1.2.6) | The insulation erosion must not exceed design safety factors when corrected using minimum design thickness. | Evaluation is not complete, but will be included in TWR-17592, Vol. III. |
| CE | Certify the nozzle design safety factors. (3.3.6.1.2.7) | The nozzle ablative components must meet or exceed the design safety factors. | Evaluation is not complete, but will be included in TWR-17592, Vol. VII. |
| CF | Certify by demonstration that the RSRM design minimizes the need for new on-plant logistics facilities, and that existing facilities and facility equipment are used for the storage of spares and maintenance functions to the maximum possible extent. (3.4.3) | The PV-1 motor must be manufactured and tested using a minimum of new on-plant logistics facilities. | A minimum of new on-plant logistics facilities were used to manufacture the PV-1 motor. |
| CG | Certify that the OBR shows:
1) no evidence of hot gas erosion inside the flex boot cavity except that produced by the ventholes, and 2) OBR hoop continuity exists through the beginning of motor pressure to tailoff
--Delamination and wedgeout of 35-deg wrap acceptable
--Need not comply with CEI spec 3.2.1.4.13.b dealing with general wedgeouts | Success criteria will be met. | No evidence of hot gas erosion inside the flex boot cavity except that produced by the ventholes.

OBR hoop continuity was maintained through the beginning of motor pressure to tailoff with no delaminations or wedgeouts or 35 deg wrap. |
| CH | Certify the function of the igniter heater. (3.2.1.5.3, SCN 42) | | |

Development Objectives

- A Acquire engineering data for model validation.
- B Evaluate the use of the 3-in-1 gage for data collection.
- C Evaluate nozzle Joint 2 bonding process change.
- D Measure joint gap opening in the nozzle internal joints.

INSTRUMENTATION

5.1 INTRODUCTION

The PV-1 test article included instrumentation similar to that used on previous static motors and subscale test articles. New instrumentation discussed below includes 3-in-1s, 2-in-1s, and an Endevco® pressure transducer installed to directly measure joint deflection, temperature, and pressure. Instrumentation was installed on the test article per Drawing 7U76264. Figures 5.1-1 through 5.1-6 show instrument locations. Refer to Appendix B for instrumentation list and Appendix C for data plots. Additional instrumentation discussion can be found in TWR-17592, Volume XII.

5.2 OBJECTIVES

PV-1 was instrumented to collect the engineering and motor performance data necessary to evaluate the following objectives from Section 2.

Test Objectives

- BD Certify the operation of the motor chamber pressure transducer, P/N 1U50188-07, and its installation with bolt, P/N 1U76488.
- BE Certify the installation and function of the ground environment instrumentation (GEI).
- BF Certify the installation and operation of the strain gages, P/N 1U51212-02 (steel) and 1U51212-04 (aluminum) in the nozzle area.
- BG Certify the installation and operation of the girth gages.
- BH Certify the installation and operation of the temperature devices, P/N 16A0355-01.
- BJ Certify the calibration of the motor chamber pressure transducer.
- BI Certify the installation and operation of the igniter chamber pressure transducer.
- BZ Certify the installation of low pressure transducer fairings and triaxial accelerometer assemblies on the forward segment.

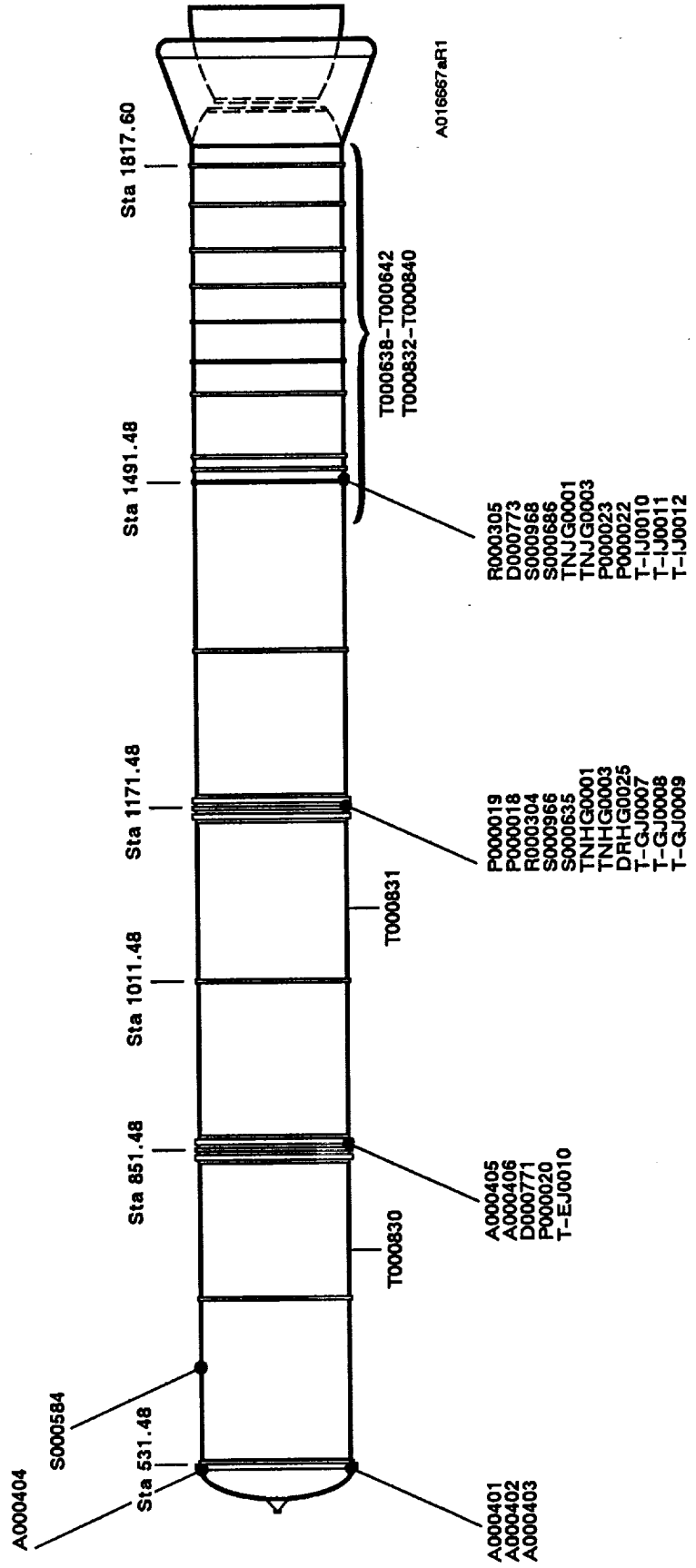


Figure 5.1-1. PV-1 Case Instrumentation

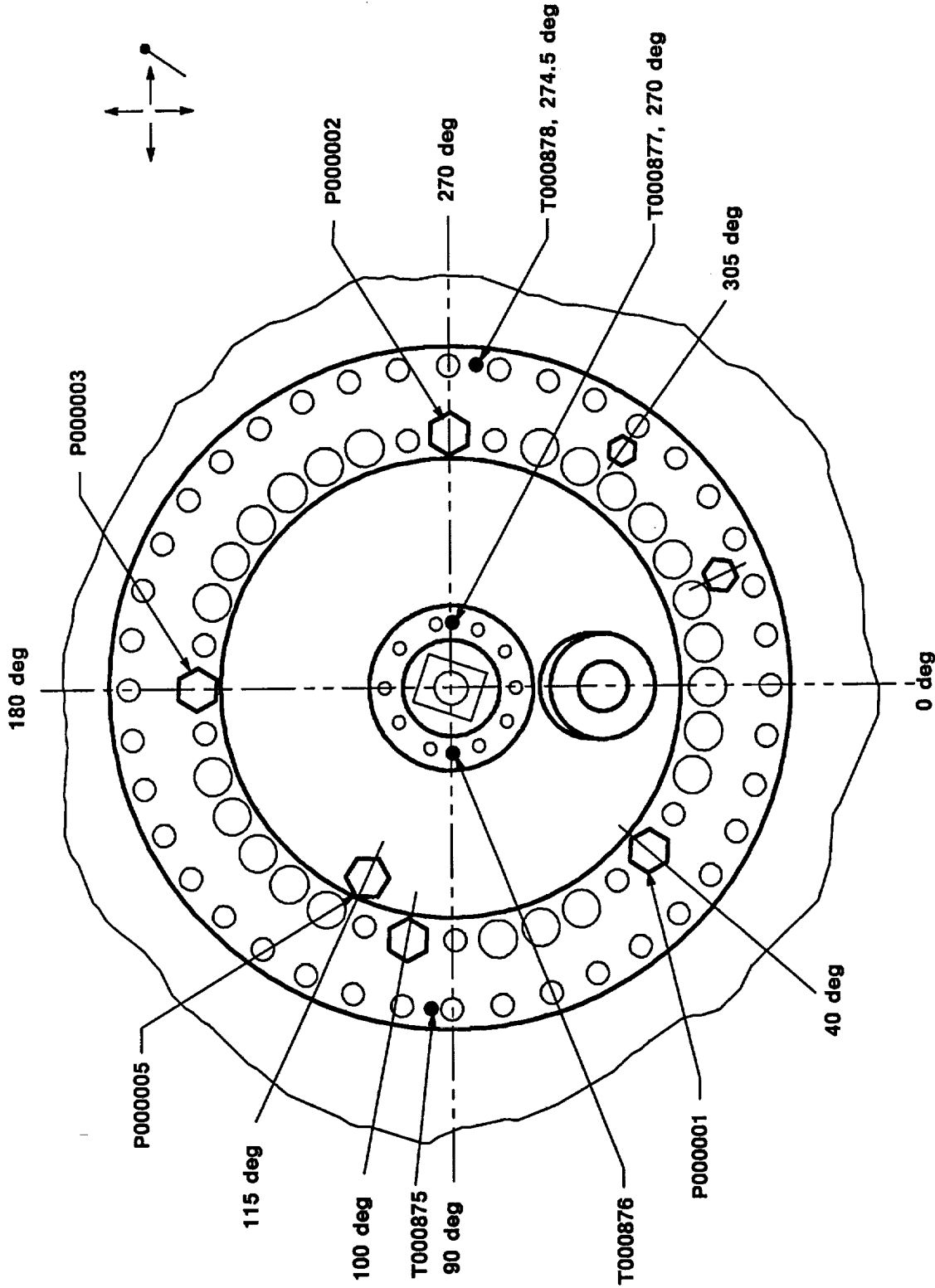
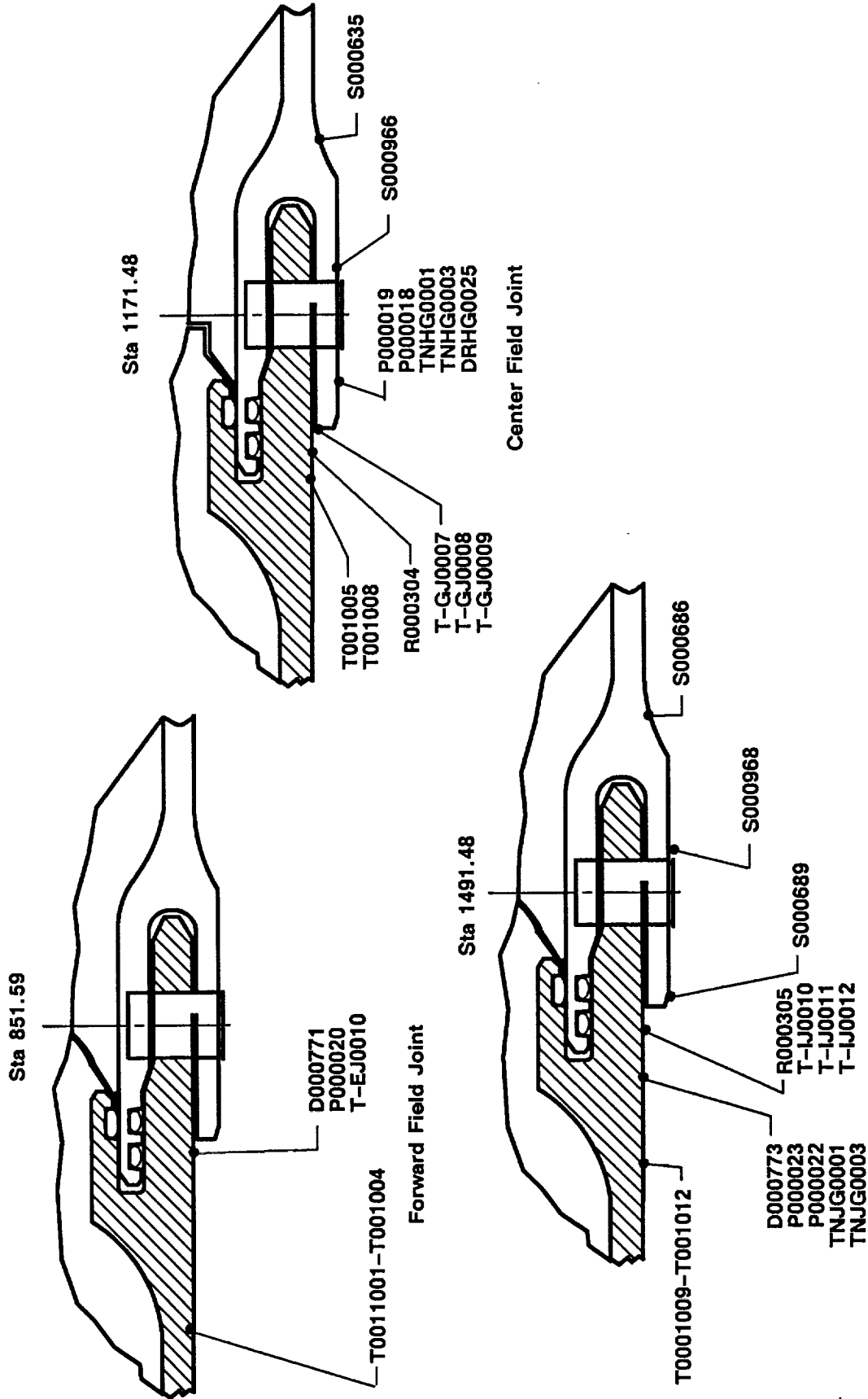


Figure 5.1-2. PV-1 Head End Pressure Transducer Locations

A016669A



A018230a-2

Figure 5.1-3. PV-1 Joint Growth

REVISION B

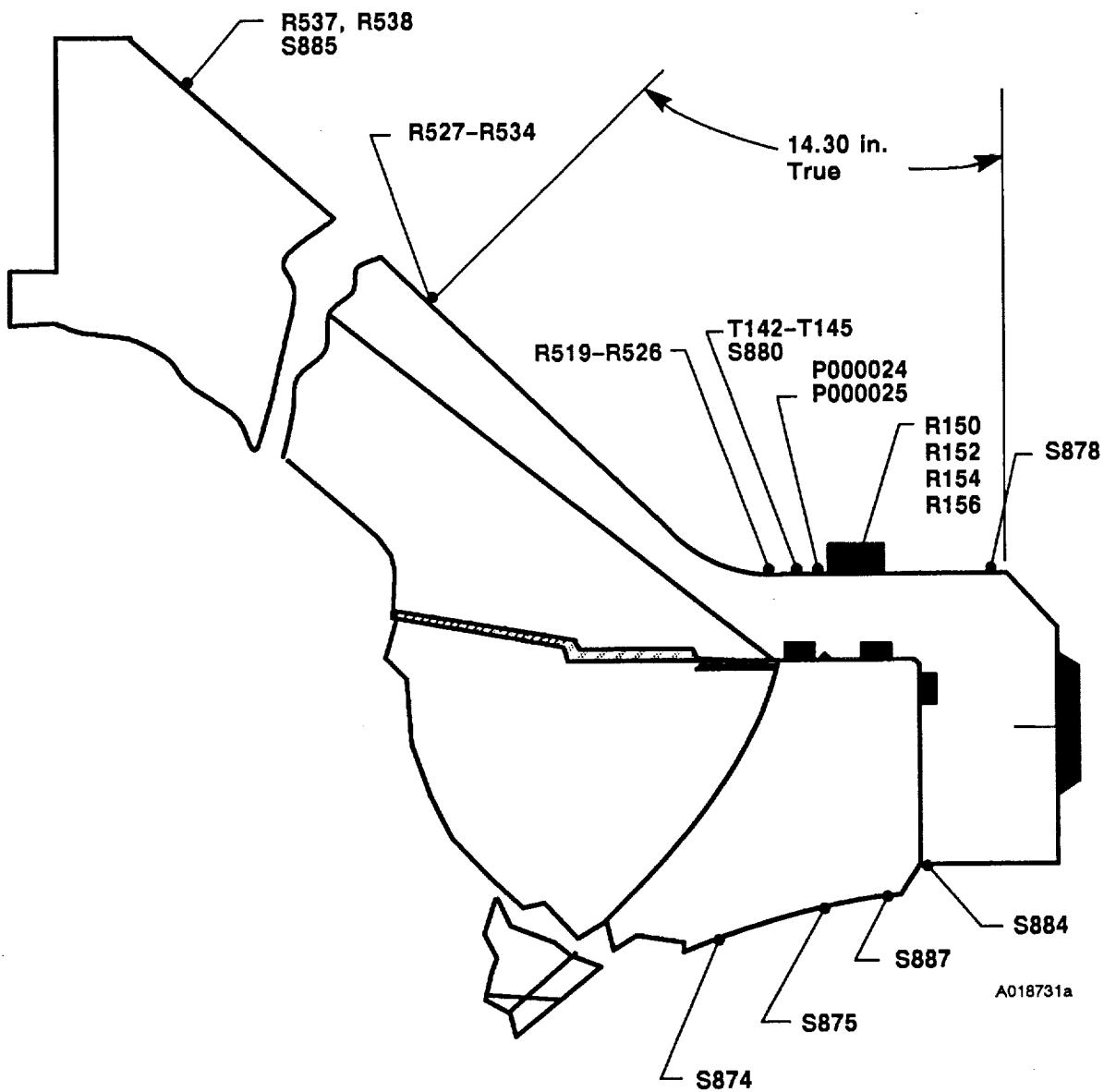


Figure 5.1-4. PV-1 Case-to-Nozzle Joint Instrumentation

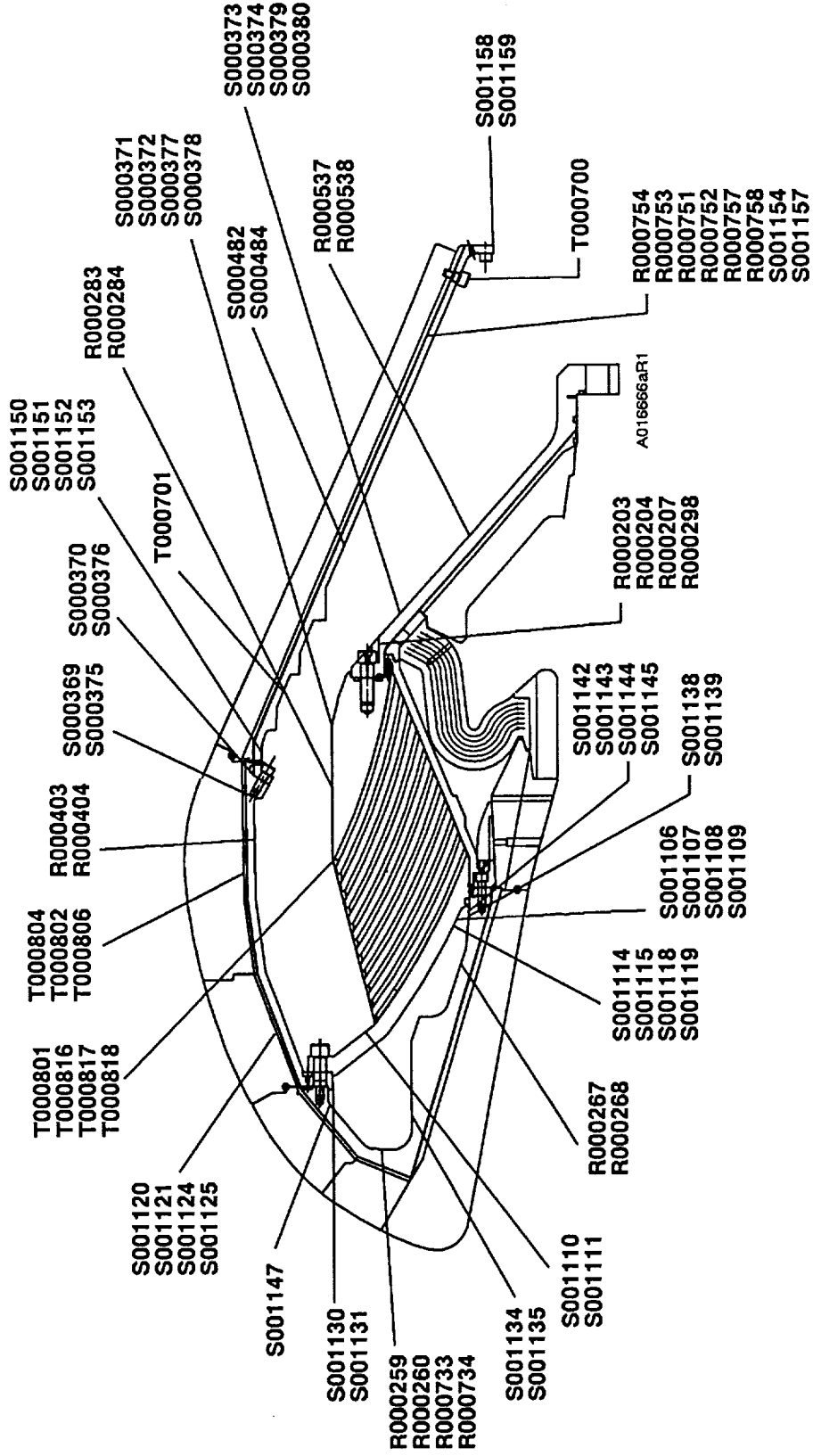
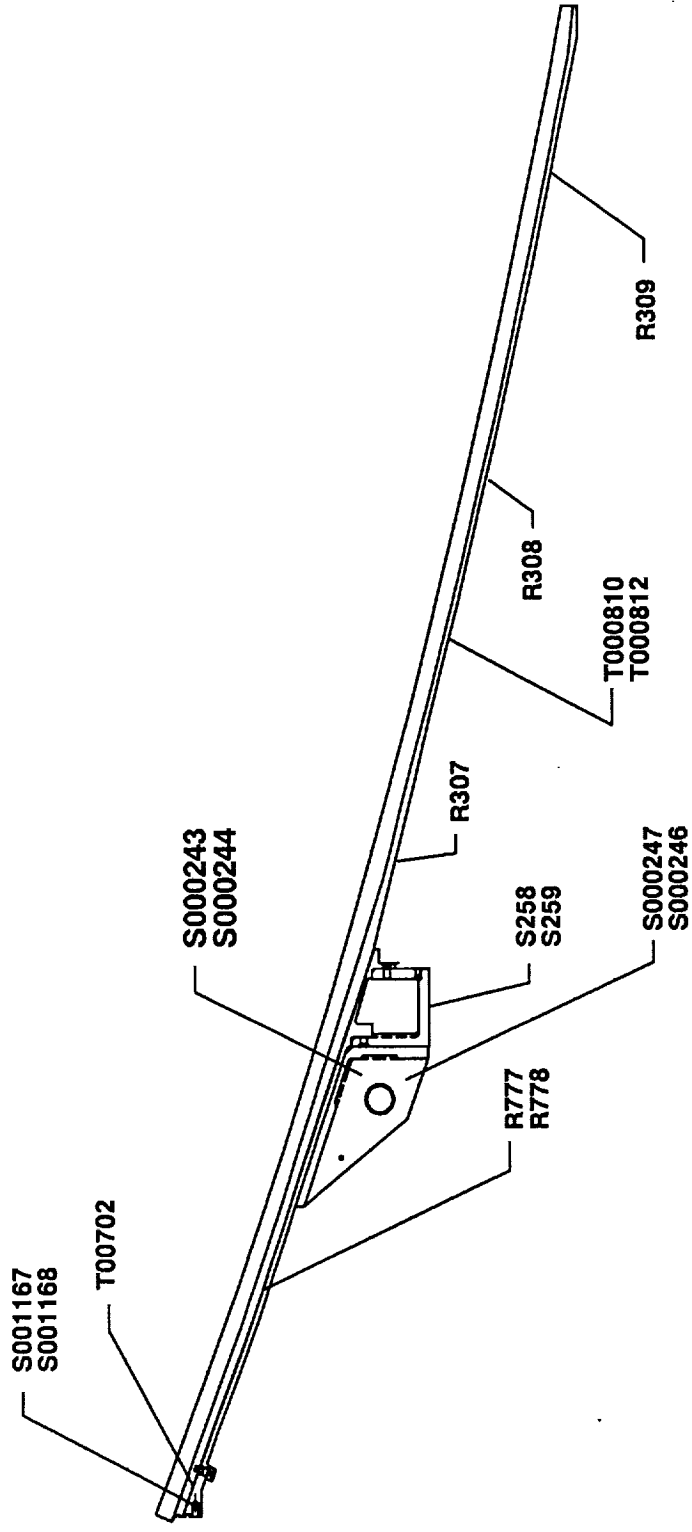


Figure 5.1-5. PV-1 Nozzle Instrumentation



REVISION B

Figure 5.1-6. PV-1 Aft Exit Cone Instrumentation

A017592a-2

Development Objectives

- A Acquire engineering data for joint model validation.
- B Evaluate the use of the 3-in-1 gages for data collection.
- D Measure joint gap opening in nozzle internal joints.

5.3 CONCLUSIONS/RECOMMENDATIONS

Overall, the instrumentation performed well with only a few exceptions. Installation was completed successfully and performance in general was as expected. Valuable performance data were collected. The 3-in-1, 2-in-1, and Endevco pressure transducers in the joints provided valuable data never before measured directly on a full-scale static motor.

All instrumentation-related test objectives were met. Pressure transducer P/N 1U50188-07, was installed with bolt, P/N 1U76488, and performed as expected. GEI performance was good. Table 5.3-1 lists the channels that were nonrecoverable prior to the test firing. Table 5.3-2 is the Test Area official anomaly list after the test firing. Temperature devices, P/N 16A03055-1, were also installed with positive results and the motor chamber pressure transducer was properly calibrated. The unexpected high pressure in nozzle internal Joint 5 was found to be an error in the calibration ranging factors.

Breaking torques were as expected on gages installed with EA 934NA (i.e., 3-in-1s, 2-in-1s, and the Endevco pressure gage).

Additional checks will be made to ensure proper calibration on new gages. Also, inspections of all gages are conducted to ensure that they are located and installed properly. There are changes to the disassembly planning to record breaking torque on gages in joint ports. These changes will help increase the efficiency of gage performance.

5.4 DISCUSSION

Total motor instrumentation was 346 channels, including pressure, force, acceleration, displacement, strain, temperature, propellant mean bulk temperature (PMBT), and GEI gages. There were 327 instrumentation channels that operated correctly.

Table 5.3-1. Nonrecoverable Channels, Prefire

<u>Parameter</u>	<u>Description</u>	<u>Cause</u>
S000399A	Strainert	Broken connection
S000439M	Strain gage	Electrically open
S000370H	Long wire strain	Damaged at gage
S001159C	Long wire strain	Damaged at gage
R000304	Girth gage	Electrically shorted to case
R000305	Girth gage	Electrically shorted to case
S001108	Strain gage	Electrically shorted case
S001142	Long wire strain	Electrically open at gage
S001143	Long wire strain	Electrically open at gage
D000771	3-in-1 displacement	Damaged coil

Table 5.3-2. Instrumentation Anomalies

<u>Parameter</u>	<u>Symptom</u>	<u>Remark</u>
P-NR0001	Saw pressure	Residual pressure in cavity
T000642	No data	Open at thermocouple junction
X000007	Intermittent data	Maintenance problem
P000512	Data after	Cable connection loose +8 sec
P000506	Data shift	Maintenance problem
T000222	Data lost at	Cable connection loose ignition
T000830	No data	Ice point not turned on
D000773	No data	Bad power supply
S001152/	Data shows	Not able to check gages
S001153	Gages switched	Out completely

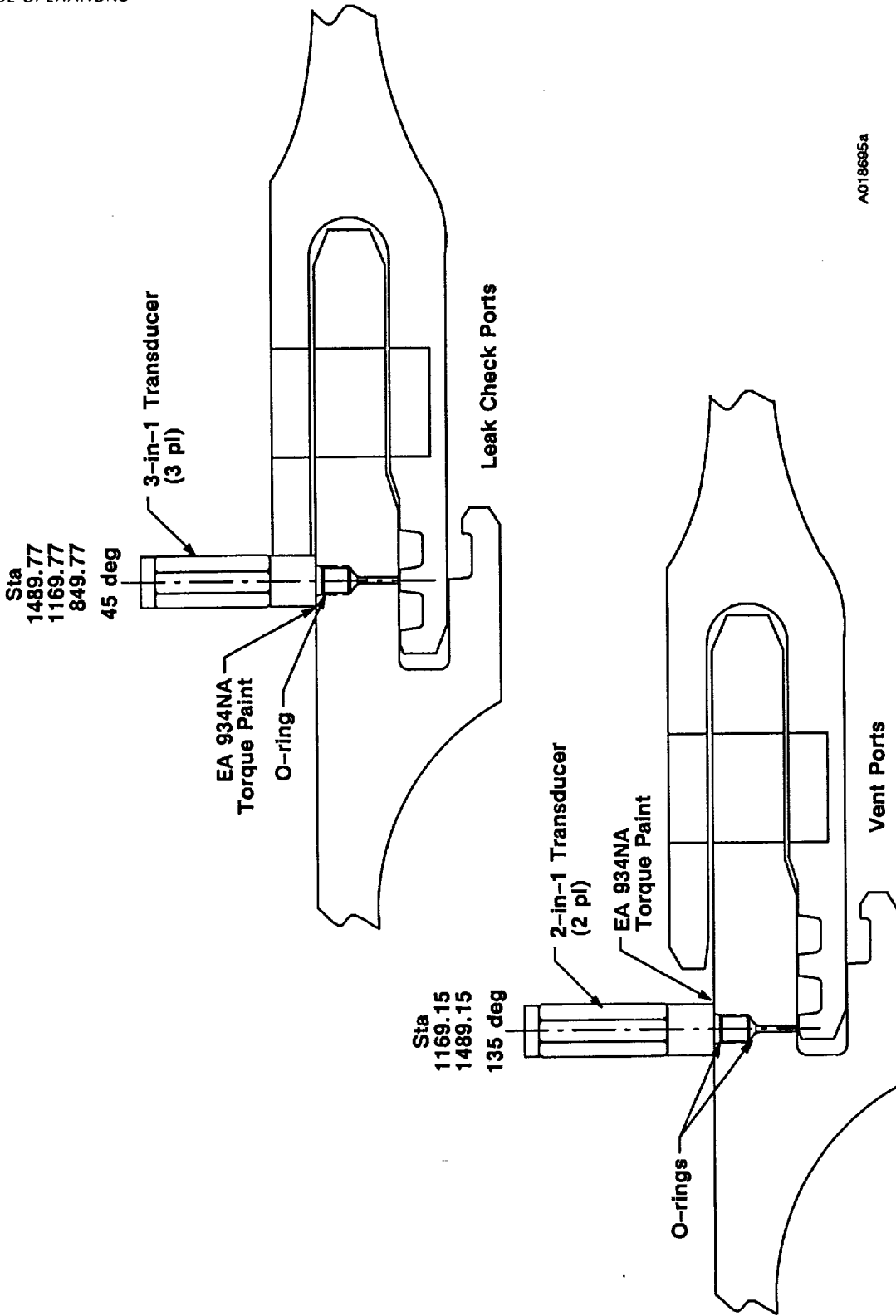
Post-test inspection of PV-1 revealed no missing or loose gages. There were no missing connections or loose wires. There was no evidence of blowby past the transducers in the joint ports.

This was the first use on a full-scale motor of 3-in-1, 2-in-1, and Endevco transducers in the joints. The 3-in-1 transducers were located one each in the forward, center, and aft field joint, and case-to-nozzle leak check ports (Figures 5.4-1 and 5.4-2). The 2-in-1 transducers were located near the flaws in the center, aft field joint, and case-to-nozzle joint vent ports (Figures 5.4-1 and 5.4-2). Performance was similar to that experienced on subscale testing and the data collected proved valuable.

An Endevco 8530B-1000 pressure gage was used for the first time by the flaw in nozzle internal Joint 5 (Figure 5.4-3). This gage recorded a pressure much higher than expected (65.0 psi). It was discovered later that the calibration factors were in error. The actual pressure was 37 psi.

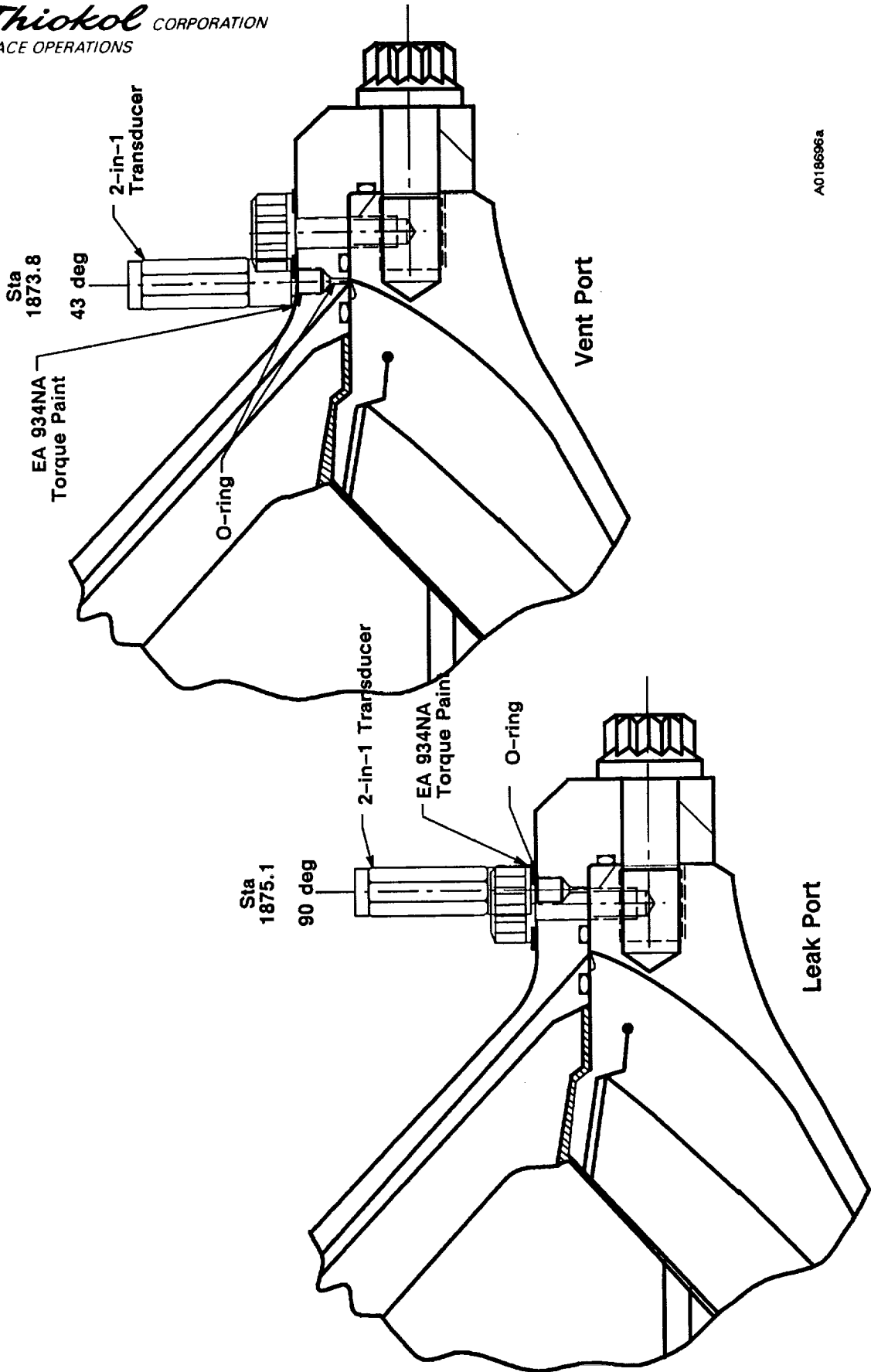
Table 5.4-1 presents a summary of the instrument types used on PV-1. The dual seal feature of the 2-in-1 gages worked as expected. These gages were in ports where flaws assured chamber pressure to the gages. Pressure was recorded at these locations (aft and case-to-nozzle vent ports) with no sign of leakage past any gage seals. The use of EA 934NA for gage retention worked very well. There was no evidence of gage backoff due to vibration or pressure. During gage removal, breaking torques were all in the range of 160-190 in.-lb.

Due to an excess of EA 934NA bonding insulation to the aft exit cone, the wires for the gages on the aft exit cone interfered with thermal curtain installation (DR 152097). The discrepancy report (DR) was dispositioned to shim the gap to protect the wires. In the future, a hole will be provided in the insulation to bring the wires out aft of the compliance ring.



A018695a

Figure 5.4-1. Instrumentation at Flawed Field Joints



A018696a

Figure 5.4-2. Instrumentation at Flawed Nozzle-to-Case Joint

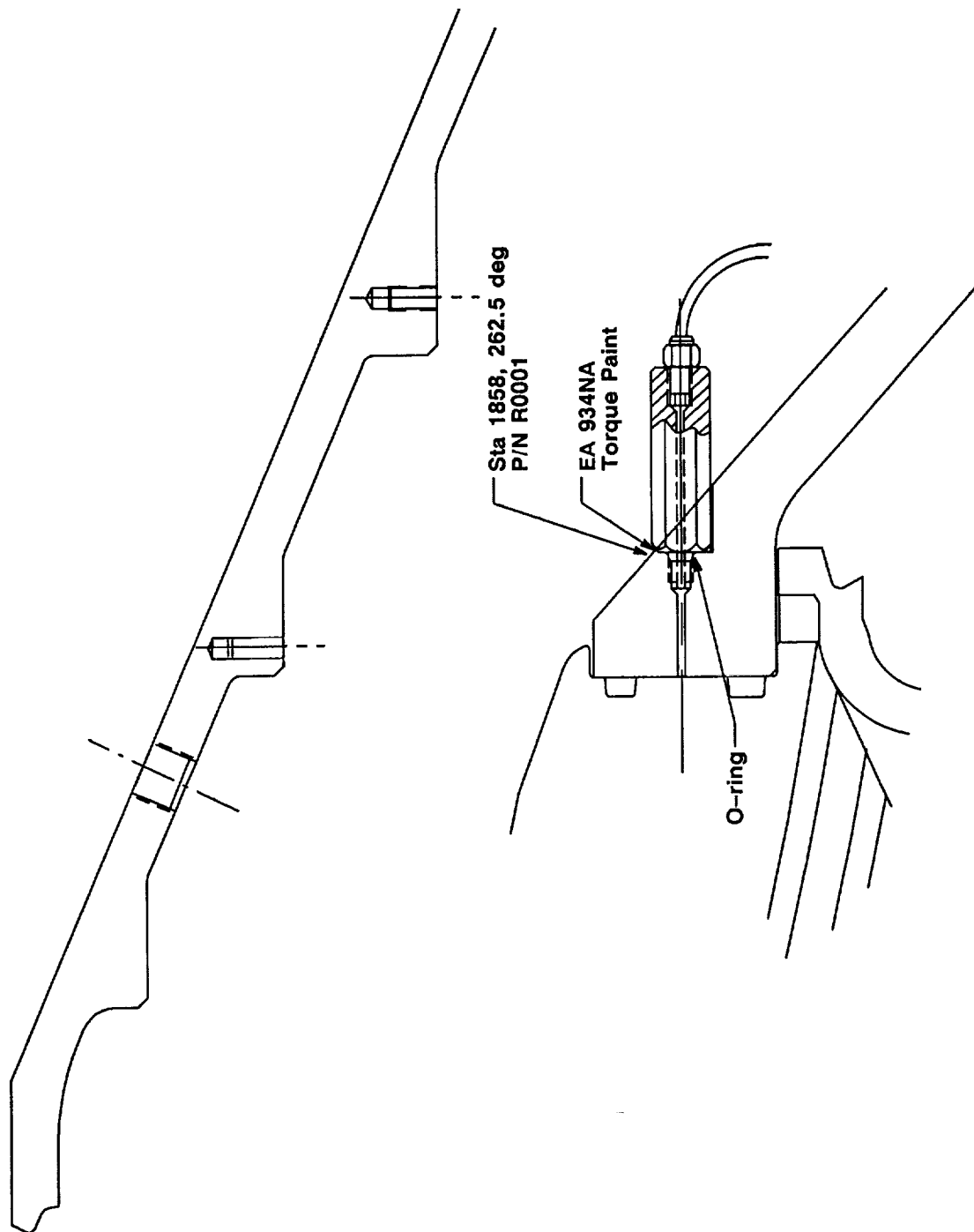


Figure 5.4-3. Nozzle Internal Joint 5

Table 5.4-1. Instrumentation Summary

<u>Type of Instrumentation</u>	<u>Area of Investigation</u>	<u>Number of Recording Channels</u>
Accelerometer (A)	Nozzle and case vibration Actuator flutter	3
Extensometers (D)	Nozzle position	12
Proximity (D)	Exit cone bondline separation Field joint movement	6
Dogbone (D)	Nozzle joint movement	6
Pressure Transducer (P)	Chamber pressure Internal dynamic environment Igniter chamber Aft field Joint Center field joint Fwd field joint Case-to-nozzle joint Nozzle internal Joint 5 Strain Gage	13
Nozzle component stress (S&R)	Aft dome/fixed housing stress	116
Girth (S)	Pressure drop in bore Joint radial growth Aft exit cone growth Aft dome/fixed housing movement Case/nozzle expansion Case-to-nozzle joint skip/rotation Straininserts	15
Nozzle/case joint (S)	Bolt loads	8
Temperature (T)	External joint temperature Slag Exit cone temperature Case-to-nozzle Igniter joint Field joint heaters Test Bay Housekeeping	86
		<u>81</u>
	Total	346

PHOTOGRAPHY

Photographic coverage was required to document the test, test configuration, instrumentation, and anomalous conditions which may have occurred. The PV-1 photographs/video tapes are available from the Thiokol Photo Lab.

6.1 STILL PHOTOGRAPHY

Still color photographs of the test configuration were taken before, during, and after the test. Photographs were taken of joints each 45 deg minimum and at anomalous conditions. A large number of photographs were taken during disassembly.

6.2 MOTION PICTURES

Color motion pictures of the test were taken with 4 video, 14 documentary, 16 high-speed cameras, and 4 still sequence cameras to cover the PV-1 test article. Documentary motion pictures are recorded on Roll No. 7656 and high-speed motion pictures on Roll No. 7657. Photography and video coverage are listed in Tables 6.2-1 and 6.2-2. Camera locations are shown in Figures 6.2-1 through 6.2-3.

Table 6.2-1. Photography and Video Coverage

<u>Camera</u>	<u>Station</u>	<u>Location</u>	<u>Type</u>	<u>Coverage</u>
1	1	Gantry	HS	Motor and plume
2	1	Gantry	SQ	Motor and plume
3	1	Gantry	Doc	Motor and plume
4	2	N. Road	Doc	Motor and plume
5	3	N. Wall	Doc	North side motor joints and plume
5A	3	N. Wall	EHS	Center field joint at 135 deg
6	3	N. Wall	HS	Center fwd joint
6A	3	N. Wall	HS	Center and aft field joints at 135 deg
6B	3	N. Wall	EHS	Aft field joint at 135 deg
7	4	S. Wall	Doc	South side motor joints and plume
7B	4	S. Wall	Doc	Aft case deluge system
8	4	S. Wall	HS	Center joint
9	5	N. Field	HS	North side aft joint and plume
10	5	N. Field	Doc	Aft joint - nozzle and plume
11	6	N. Field	HS	Nozzle and thermal curtain
11A	6	N. Field	HS	Nozzle and 200 ft of plume
12	6	N. Field	HS	North side - all joints
13	6	N. Field	Doc	Motor and plume
13A	6	N. Field	Doc	NASA documentary
13B	6	N. Field	SQ	Motor and plume
14	7	N. Tower	Doc	North side of motor and plume
15	8	S. Field	HS	Aft joint
15A	8	S. Field	HS	Aft case nozzle and plume
15B	9	S. Side	HS	All joints
15C	9	S. Side	HS	Nozzle and thermal curtain
15D	8	S. Field	HS	Nozzle and 200 ft of plume
16	8	S. Field	Doc	Aft case, nozzle and plume
16A	8	S. Field	Vid	Aft case, nozzle and plume
16B	9	S. Side	Doc	Overall of motor/NASA documentary
17	10	S. Tower	HS	Case nozzle and plume
18	10	S. Tower	Doc	Case nozzle and plume
19	11	T-Block	Doc	Motor and plume
19A	11	T-Block	Vid	Motor and plume
19B	11	T-Block	SQ	Motor and plume
20	11	Bay Floor	Doc	Bottom of case

Code: EHS - High speed at 1,000 pps
 HS - High speed at 300 pps
 Doc - Documentary at 24 pps
 SQ - Sequence at 1 pps
 Vid - Video at real time
 Ir - Infrared

Table 6.2-2. Photography and Video Coverage

<u>Camera</u>	<u>Station</u>	<u>Start Time (sec)</u>	<u>Stop Time (sec)</u>	<u>Mandatory (M) or Required (R) Priority</u>
1	1	T-5	T+150	M
2	1	T-2	T+150	R
3	1	T-15	T+180	R
4	2	T-15	T+180	R
5	3	T-15	T+180	R
5A	3	T-2	T+20	M
6	3	T-5	T+150	M
6A	3	T-5	T+150	M
6B	3	T-2	T+20	M
7	4	T-15	T+180	R
7A	4	T-15	T+33 min	M
8	4	T-5	T+150	M
9	5	T-5	T+150	M
10	5	T-15	T+555	M
11	6	T-5	T+150	M
11A	6	T-5	T+150	M
12	6	T-5	T+150	M
13	6	T-25	T+180	R
13A	6	T-25	T+180	R
13B	6	T-2	T+180	R
14	7	T-25	T+180	R
15	8	T-5	T+150	M
15A	8	T-5	T+150	M
15B	9	T-5	T+150	M
15C	9	T-5	T+150	M
15D	9	T-5	T+150	
15E	8	T-5	T+150	
16	8	T-15	T+600	R
16A	8	T-15	T+600	R
16B	9	T-15	T+600	R
17	10	T-5	T+150	M
18	10	T-15	T+180	R
19	11	T-15	T+180	R
19A	11	T-15	T+180	M
19B	11	T-25	T+180	
20	11	T-15	T+150	M

<u>Station</u>	<u>Location</u>
1	Top of gantry crane
2	Northwest of bay
3	North of bay
4	South wall
5	North of nozzle
6	North and aft of nozzle

<u>Station</u>	<u>Location</u>
7	North tower
8	South of nozzle
9	South and aft of nozzle
10	South tower
11	Top of thrust block

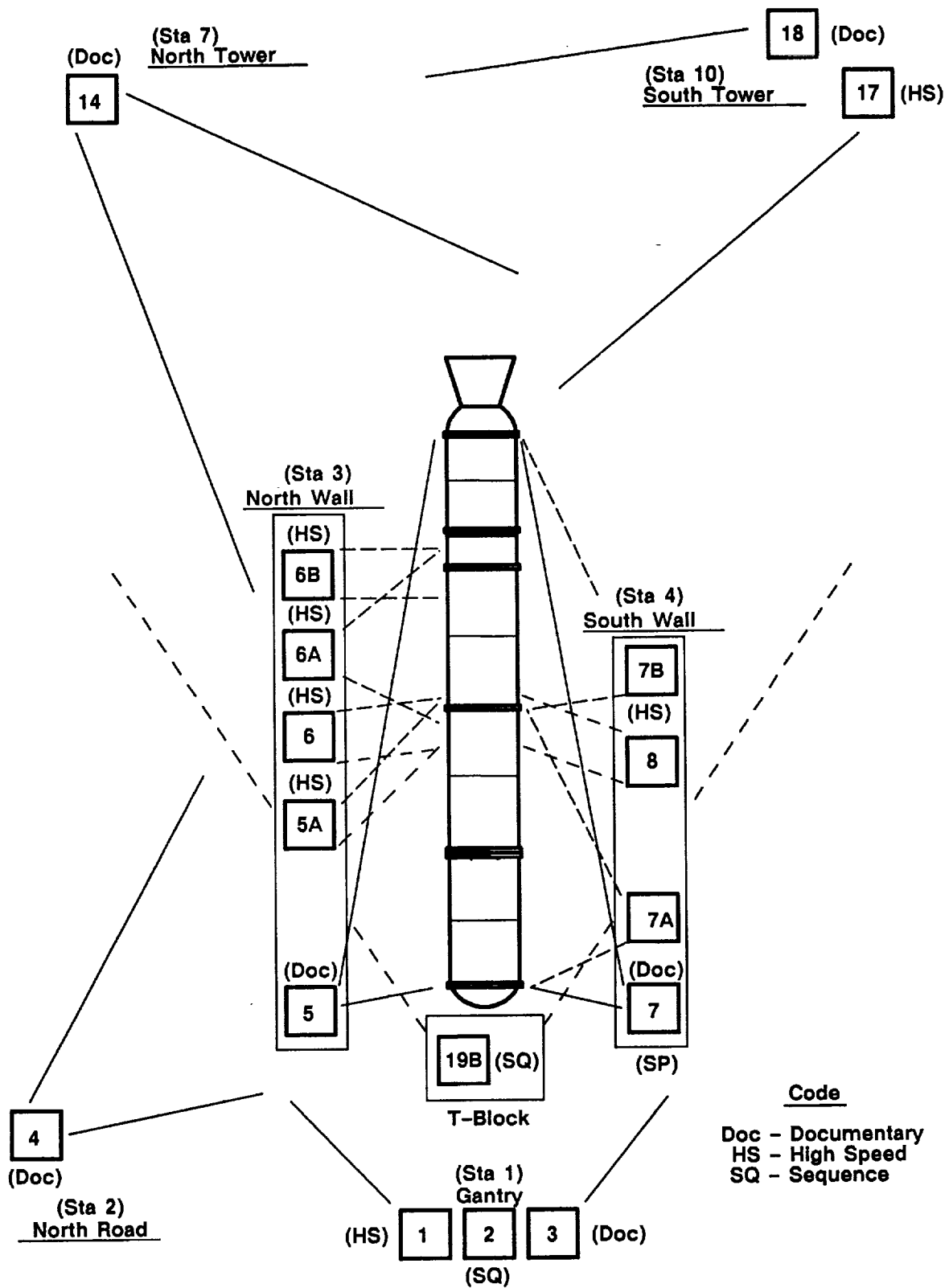


Figure 6.2-1. Photography Coverage

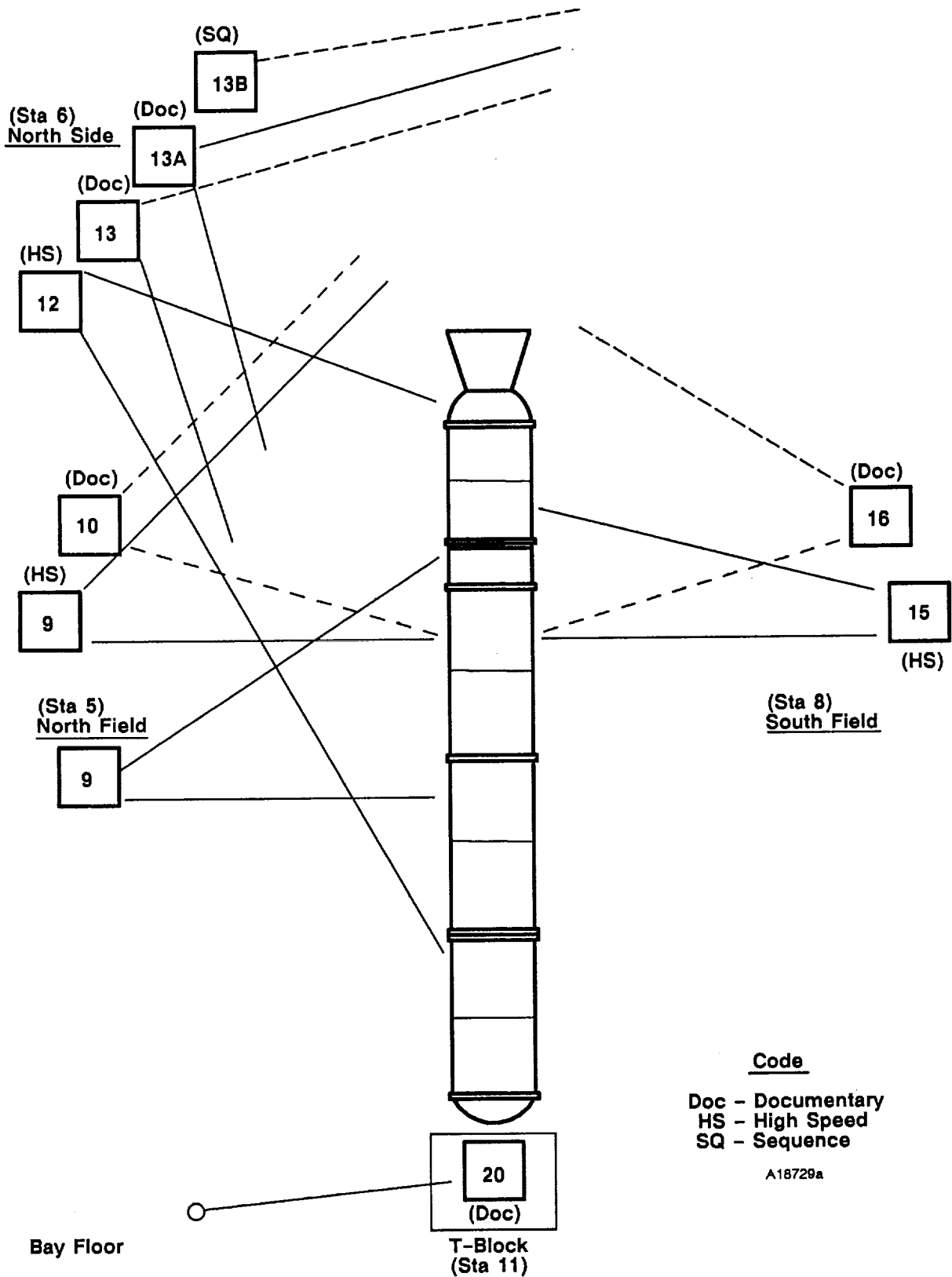


Figure 6.2-2. Photography Coverage

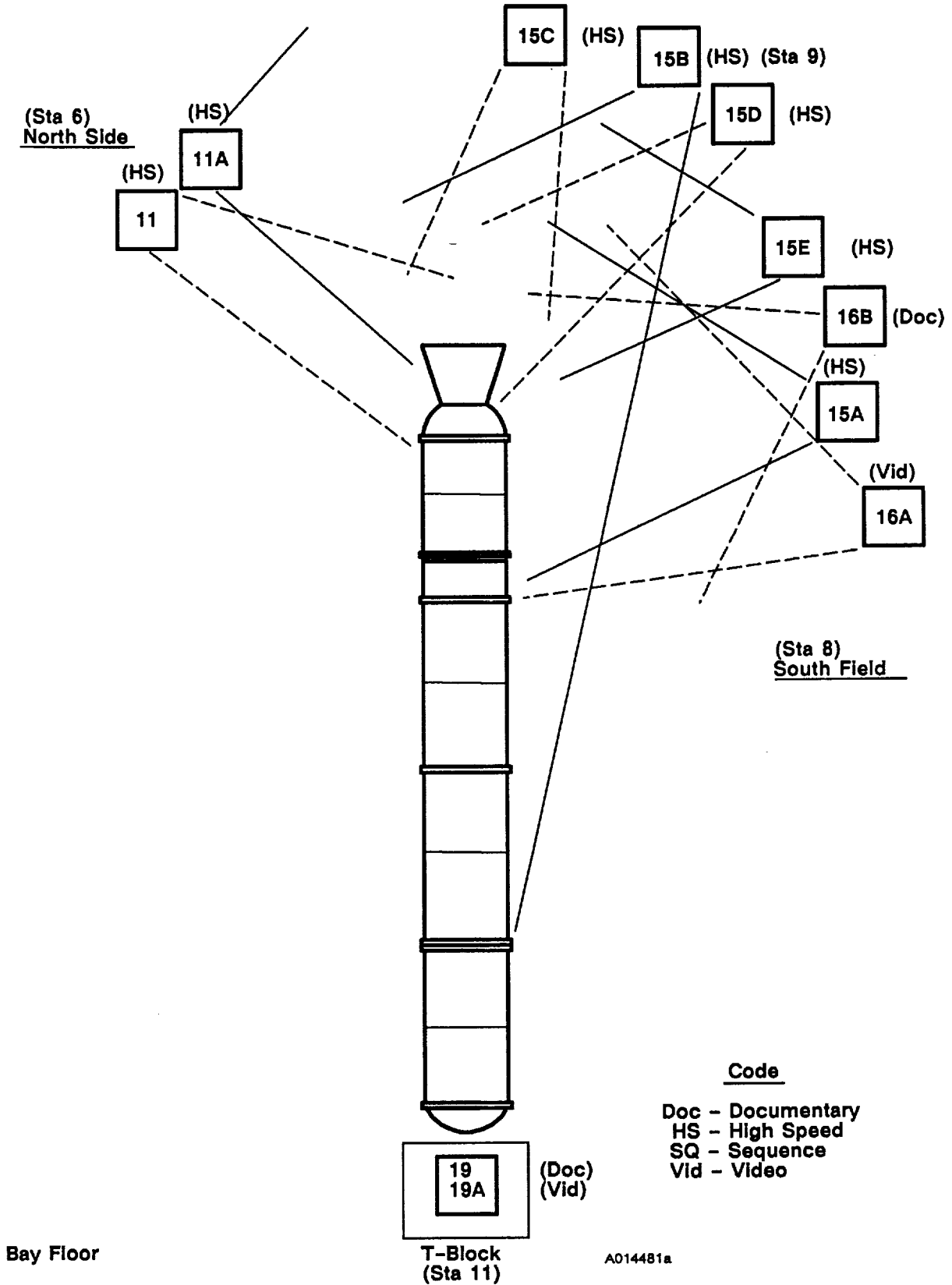


Figure 6.2-3. Photography and Video Coverage

GROUND SUPPORT EQUIPMENT

All GSE used on PV-1 will be discussed in the applicable component volume of TWR-17592.

LOADS AND ENVIRONMENT

8.1 INTRODUCTION

This section is concerned with case line loads and actuator bracket stresses experienced during the PV-1 static test. The maximum case tangential and axial line loads were determined as well as the stresses involved with the TVC nozzle actuator bracket.

8.2 OBJECTIVES

The main test objective from Section 2 with regard to loads and environments is:

BV Certify the reliability of the RSRM design.

While this report does not attempt to certify RSRM reliability, it does provide useful input to that task.

8.3 CONCLUSIONS/RECOMMENDATIONS

The axial line loads that were calculated were well within the design limits stated in CEI specification paragraph 3.2.7.2.2. The nozzle actuator bracket was also analyzed and the stresses induced by the TVC were far below the yield stress for the bracket material.

The line loads due to hoop stress were calculated and can be used for comparison on future tests and flights. The overall case line load envelope could be evaluated if more case strain instrumentation were installed on future tests.

8.4 RESULTS/DISCUSSIONS

The highest tangential line load, i.e., the line load due to the hoop stress, was -43.38 kips/in. (Figure 8.4-1). Since there are no tangential line loads calculated for the RSRM, the values obtained from the PV-1 test can be used for comparison of tangential line loads on future tests and flights. The

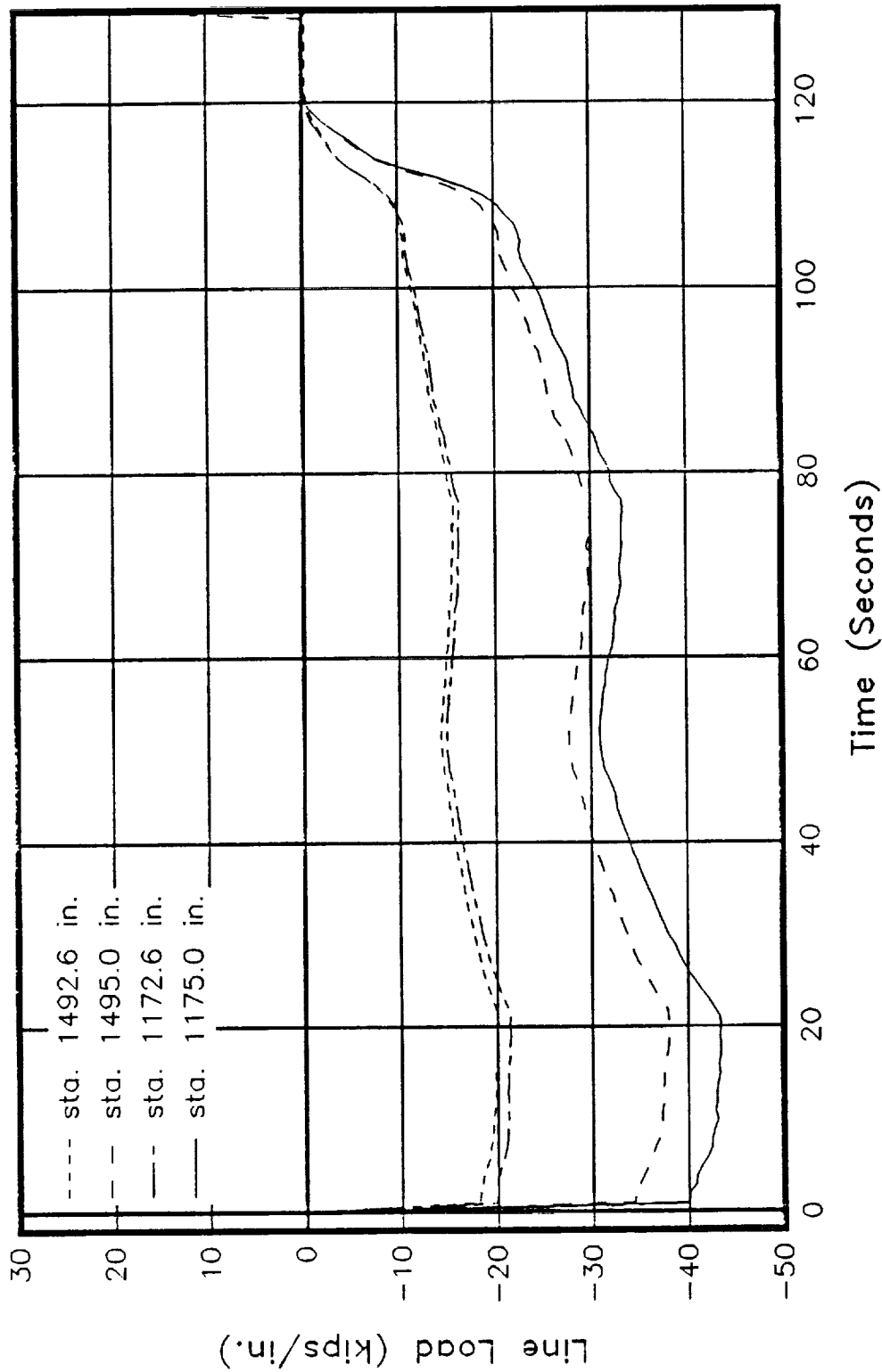


Figure 8.4-1. Tangential Line Loads Versus Time

highest axial line load obtained during the static test was -21.69 kips/inch. (Figure 8.4-2) at Station 1175.0 (Figure 8.4-3). This value is much lower than the -37.5 kips/in. obtained during the lift-off phase at the same station.

Since there was no instrumentation to measure the axial strain directly, Hooke's Law $\sigma = E \cdot \epsilon$, (where ϵ is the strain in μ /in., E is the modulus of elasticity of the material in psi, and σ is the stress in psi) was used to convert the strain into stress. The relation $\sigma_{axial} = \frac{1}{2} \sigma_{hoop}$ was then used to determine the axial stress. The case line load was calculated by multiplying the case stress by the local case thickness.

The axial line loads are negative because of the booster coordinate system sign convention. A positive force is a compressive force in the X direction (Figure 8.4-4). A positive axial stress would signify tension, therefore yielding a negative force. The tangential line loads follow the same convention: a positive stress results in a negative force.

The nozzle actuator bracket was instrumented with two biaxial strain gages to measure the stress transmitted to the bracket during the TVC cycle (Figure 8.4-5). The maximum stress obtained was at the inboard gage location in the axial direction. The stress on the bracket was 11 ksi (Figure 8.4-6), which is much lower than the 43 ksi yield stress of the bracket material. The stress measured at the outboard gage was low and not of significance (Figure 8.4-7).

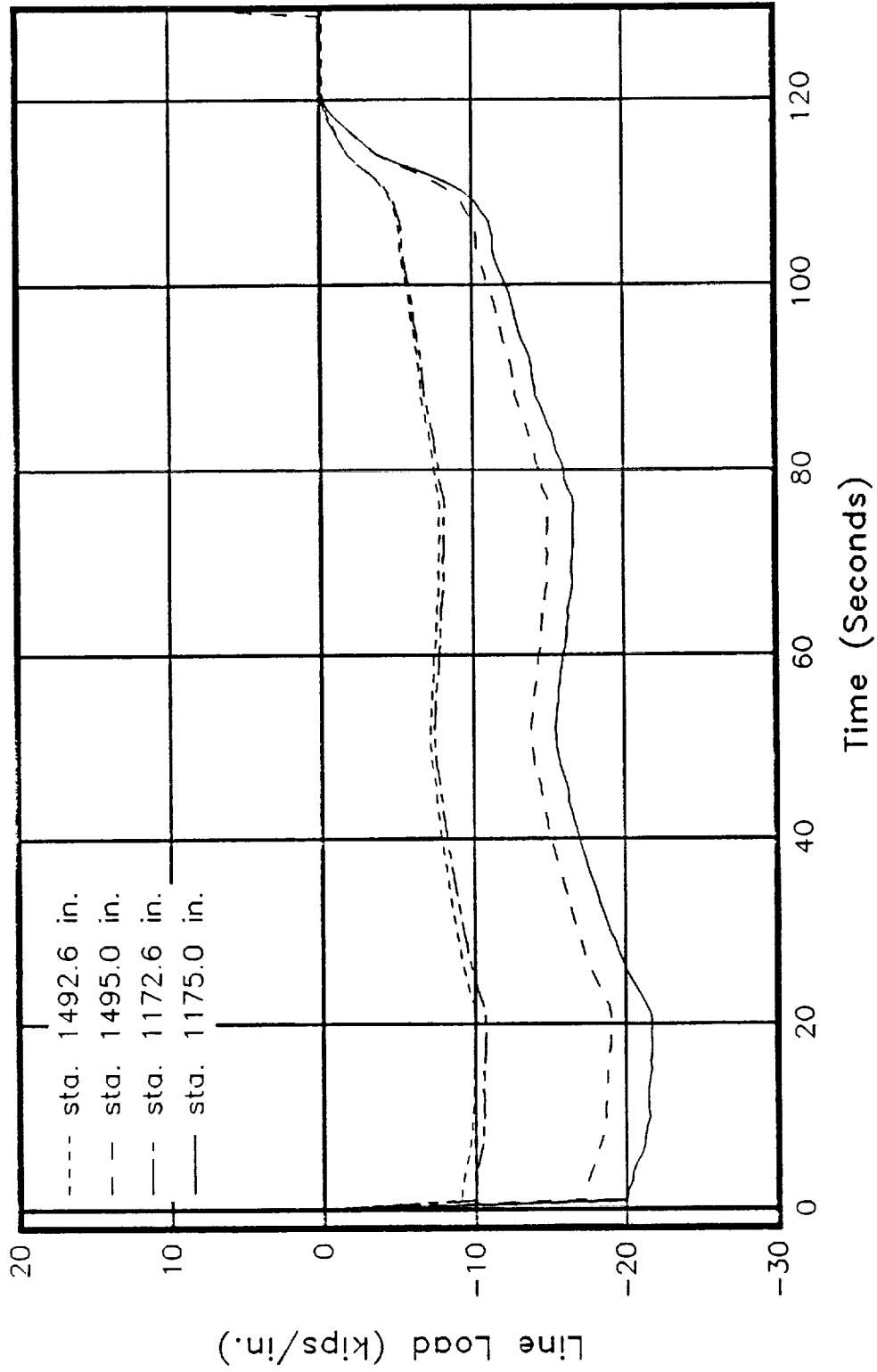


Figure 8.4-2. Axial Line Loads Versus Time

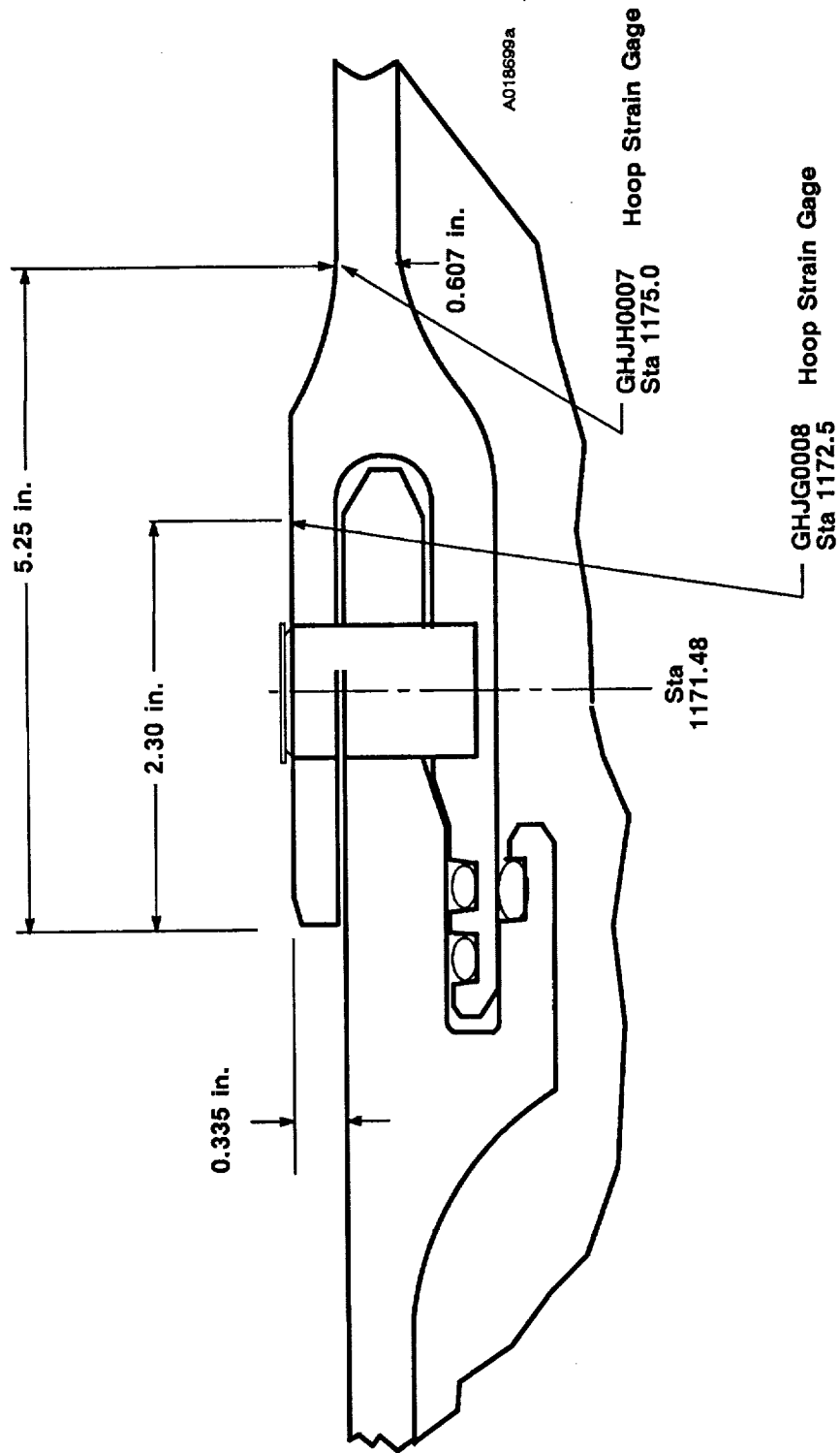


Figure 8.4-3. Strain Gage Locations

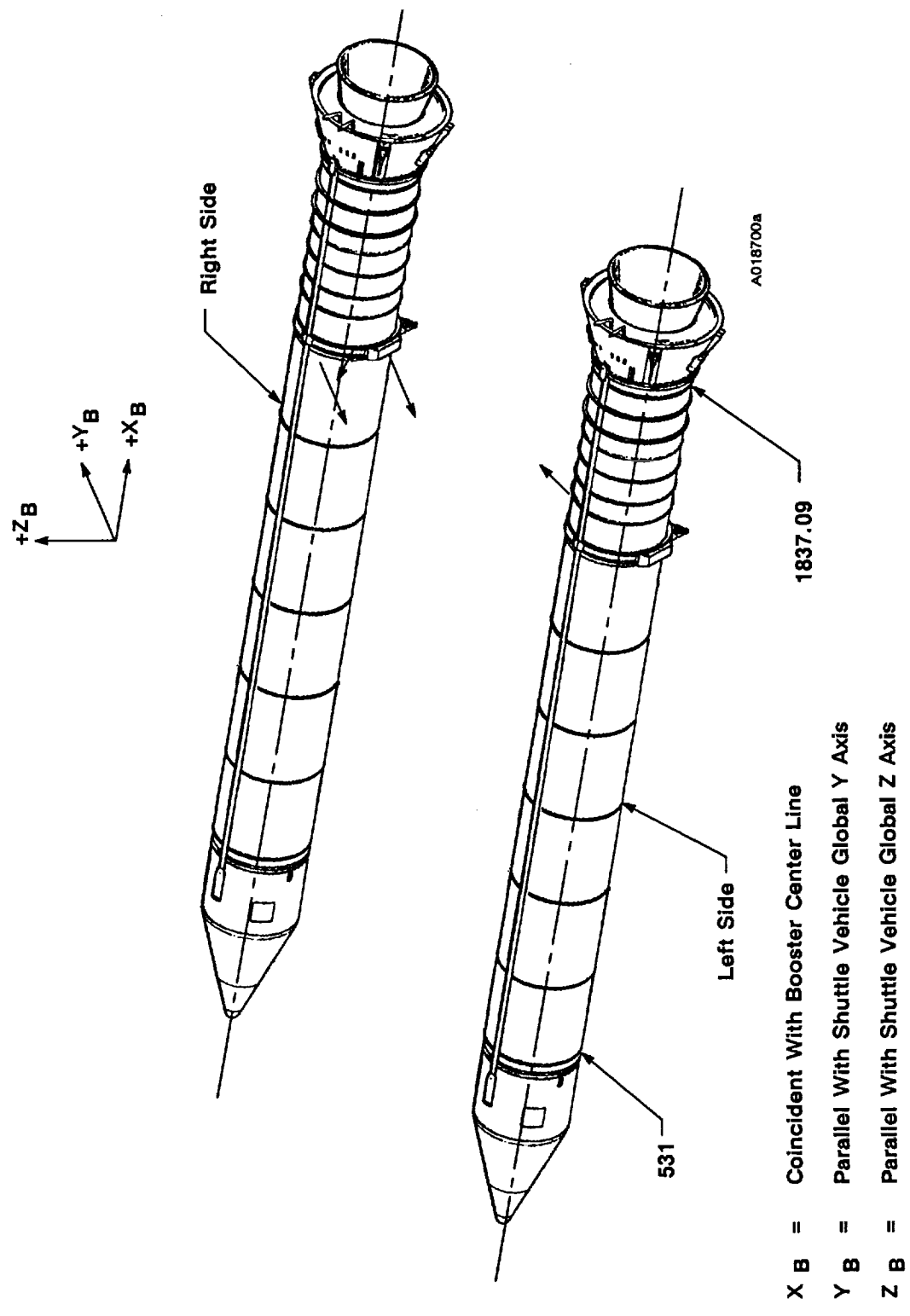


Figure 8.4-4. Booster Local Coordinate System

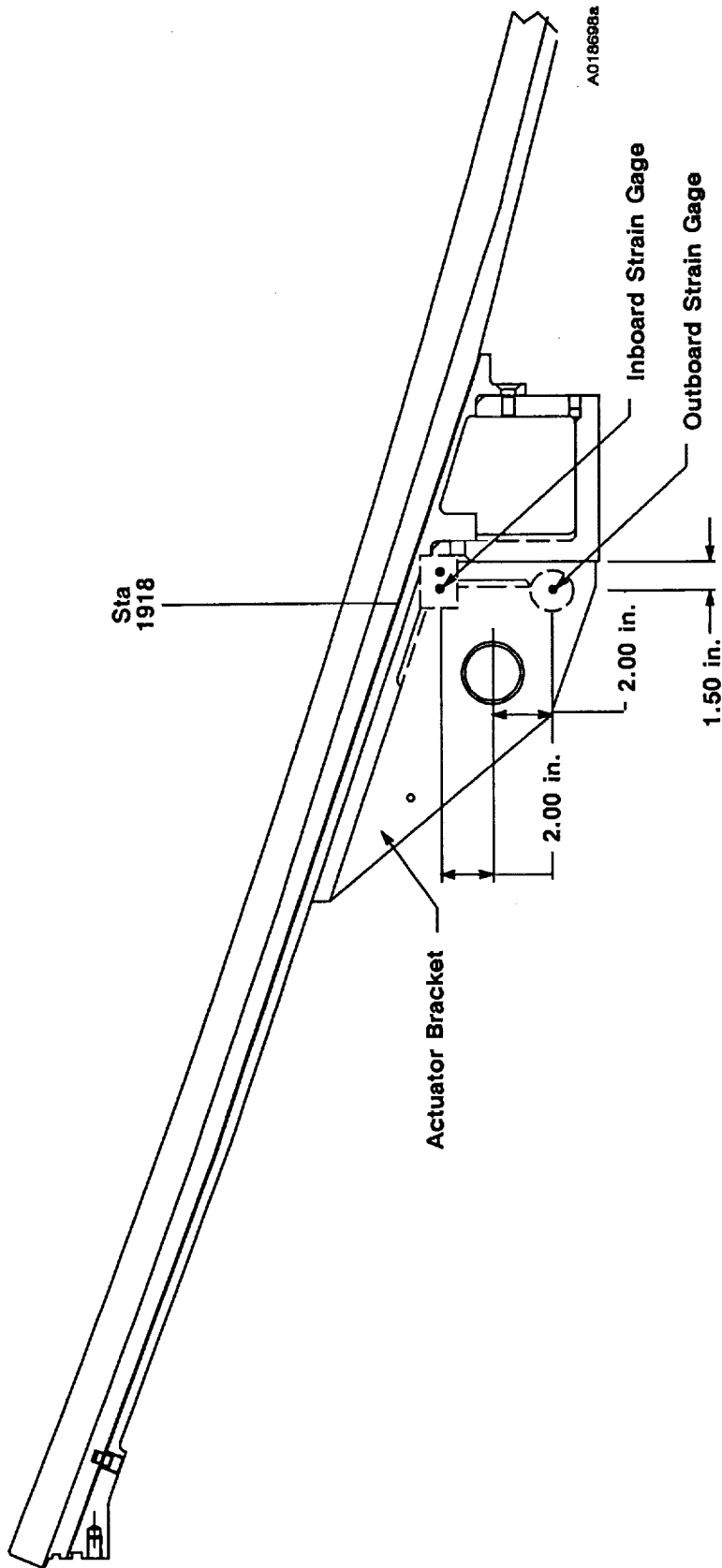


Figure 8.4-5. TVC Actuator Bracket

Station 1918.0 in. @45°
Inboard gage

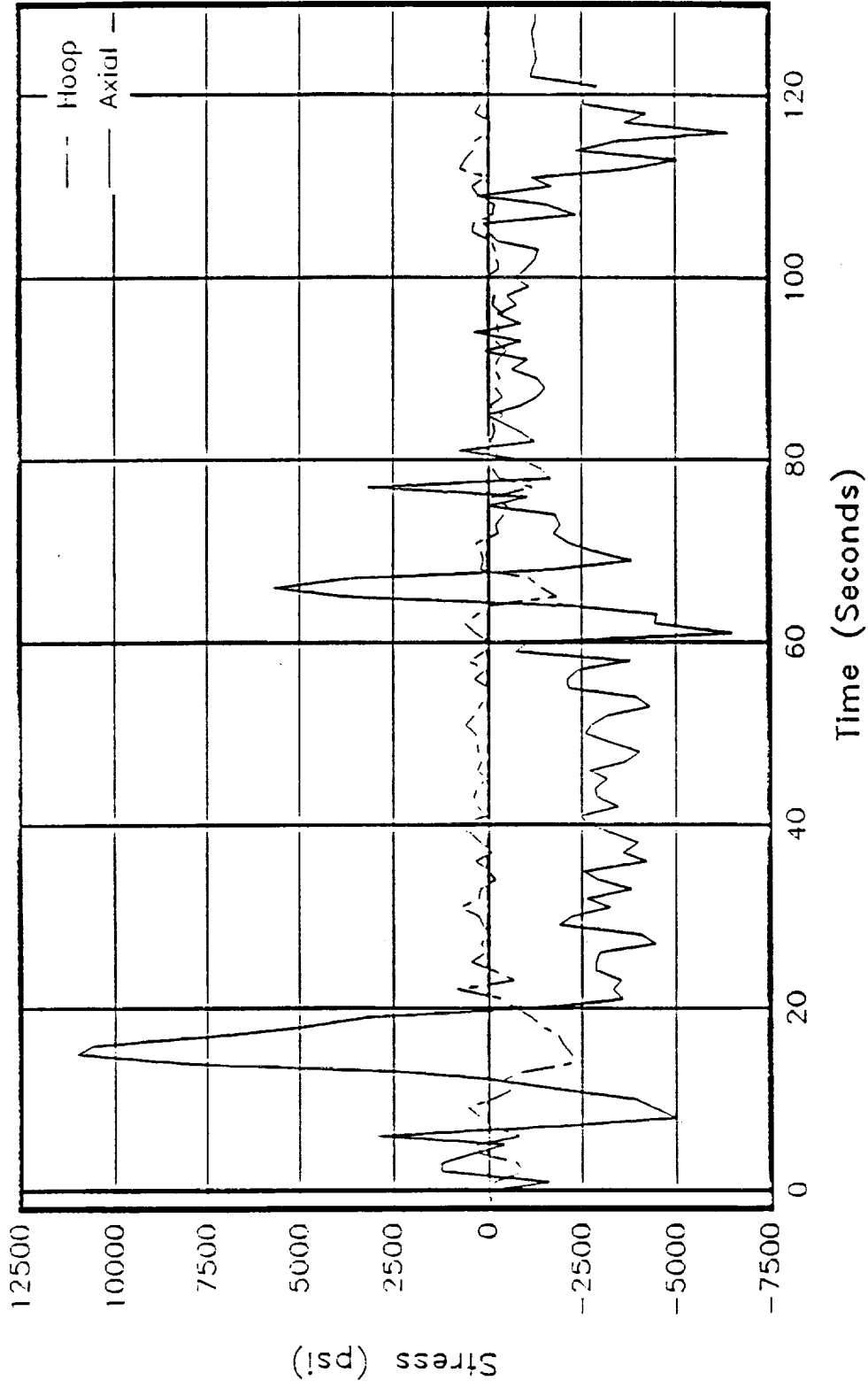


Figure 8.4-6. Actuator Bracket Stress Versus Time

Station 1918.0 In. @45°
Outboard gage

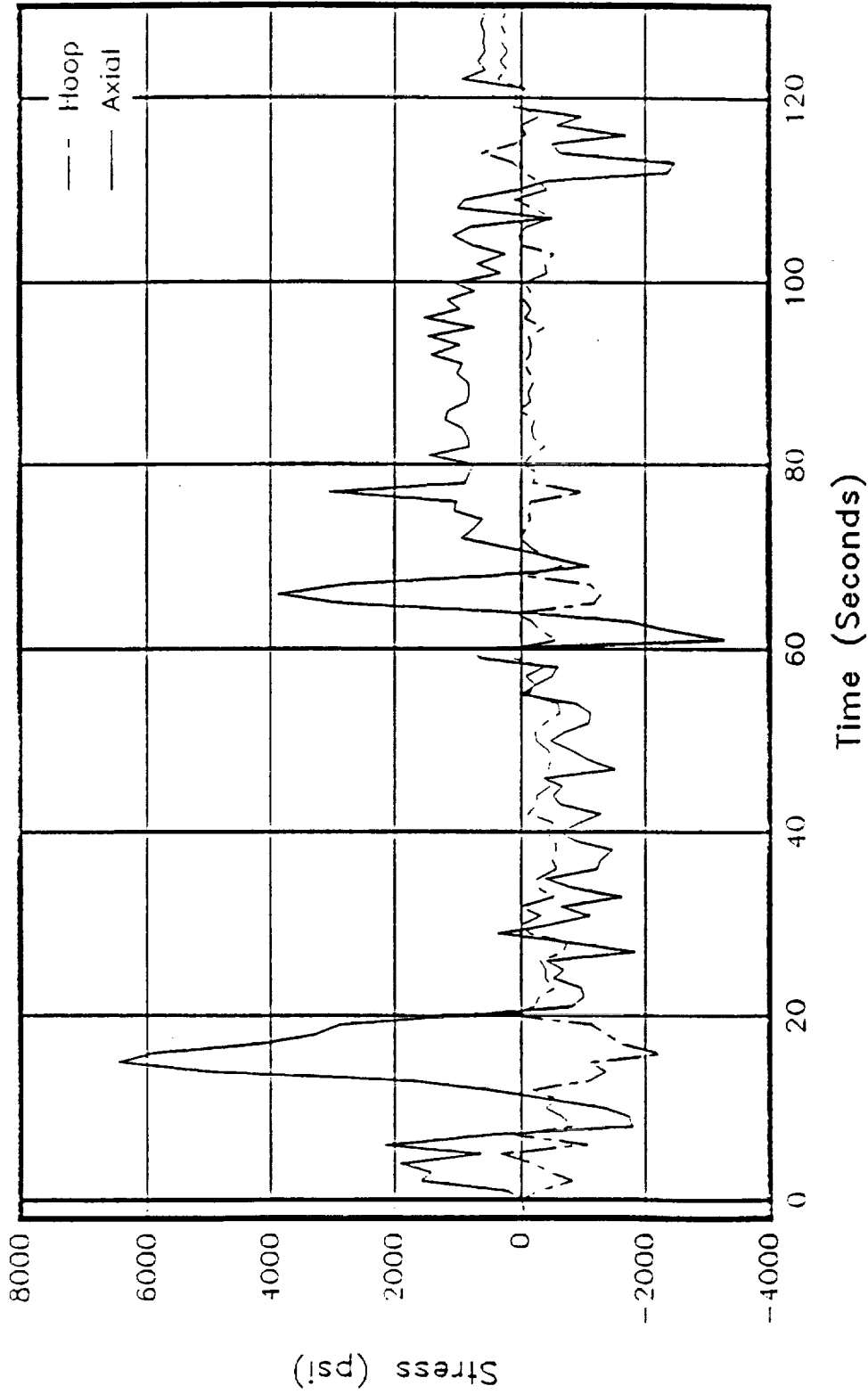


Figure 8.4-7. Actuator Bracket Stress Versus Time

APPLICABLE DOCUMENTS

The latest revisions of the following documents, unless otherwise specified, are applicable to this report.

Specification

CPWI-3600, Addendum D	Prime Equipment Contract End Item Detail Specification (CEI)
CTP-0055	Space Shuttle Process Verification Motor (PV-1) Static Fire Test Plan
TWR-15723	Development and Verification of Nozzle Assembly
TWR-16340	NonDestructive Radiographic Criteria for the Space Shuttle Solid Rocket Motor Nozzle Phenolics
TWR-16416	Pressurization of the Aft End Ring to the Fixed Housing Joint of PVM-1
TWR-16473, Vol. I-IX	Motor Postfire Engineering Evaluation Plan
TWR-17198, Vol. I-IX	Postfire Engineering Evaluation Limits
TWR-17592, Vol. II	Case Component Final Report
TWR-17592, Vol. III	Case Internal Insulation Component Final Report
TWR-17592, Vol. IV	Seals Component/Leak Check Final Report
TWR-17592, Vol. V	Nozzle/Flex Bearing/Composite Structures/TVC Final Report
TWR-17592, Vol. VI	Ignition System Component Final Report
TWR-17592, Vol. VII	Joint Protection System/Factory Joint Weather Seal Final Report
TWR-17592, Vol. IX	Dynamics Final Report
TWR-17592, Vol. X	Aero/Thermal Final Report
TWR-17592, Vol. XI	Ballistics Final Report

DISTRIBUTION

<u>Recipient</u>	<u>No. of Copies</u>	<u>Mail Stop</u>
R. Papasian	45	E05
D. Garecht	1	L36
S. Harris	1	E13
P. Tydeck	1	L23E
S. West	1	411
R. Larsen	1	851
J. Lavery	1	L32
Print Crib	5	282
Data Management	5	L23E